Phase Evolution and Electrical Properties of $Ba_{0.8}Sr_{0.2}TiO_3$ Sol-Gel Thin Films

A Thesis submitted
in partial fulfillment of the requirement
for the Degree of
MASTER OF TECHNOLOGY

By

Aditi Datta

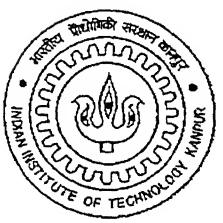

To the

MATERIALS SCIENCE PROGRAMME
INDIAN INSTITUTE OF TECHNOLOGY, KANPUR
December 2002

13 JUN 2003
पुरुषोत्तम
भारतीय
अवाप्ति क्र० A 143521
TH
MSP/2002/M
D262p

CERTIFICATE

It is to certify that the work presented in this thesis entitled *Phase Evolution and Electrical Properties of $Ba_{0.8}Sr_{0.2}TiO_3$ Sol-Gel Thin Films* by Aditi Datta has been carried out under my supervision and this work has not been submitted elsewhere for a degree.

IIT Kanpur

23 December, 2002

(D.C.Agrawal)
Professor
Materials Science Programme
Indian Institute of Technology
Kanpur-208016
India

ACKNOWLEDGEMENT

I gratefully acknowledge my thesis supervisor Professor. D.C Agrawal for his inspiring and constant encouragement throughout the course of this work. His constructive criticisms, positive and methodological approach enabled me to undertake and complete this work.

I express my sincere gratitude to my teachers Prof. S.Kar, Prof. Y. N. Mohapatra, Prof. Jitendra Kumar, and Prof. K. N. Rai whose lectures and guidance helped me in developing the essential capabilities in performing this work.

Heartfelt thanks are due to my present and ex-labmates Sahooji, Sandesh, Shiladitya, Arindam, Sudeep, Lav, Sreya, Animesh, Arpana and Niraj for their constant help and providing a cheerful atmosphere, making the lab an ideal workplace.

I am thankful to Thapaji for his co-operation and help during the tenure of my work

Words cannot do full justice in expressing my thanks to my friends Pooja, Tatha, Gopi, Dulal, Sanjay, Debadi, Santanu, PP, Prateebha, Arpita, Ruchi, Prishati for their splendid company and co-operation. I owe it to them for making my stay in IITK a memorable one.

I am really fortunate to find a caring and understanding friend in Anisia. Her warm association never allowed me to feel away from home whenever I was down and out. Her friendship is one of the greatest gifts that life has offered to me.

I am grateful to Mr. Umashankar (X-ray Lab), Mr.Prabesh Pandey and Mr. K. Rajagopalan (Microanalytical Lab), Agnihotriji and Sharmaji (SEM Lab), Dr. R..S. Anand (Semiconductor Devices Lab), Mr. Karthikeyan (Instrumentation Lab), Mr. Jai Kishan (Machine Shop), Mr. V. P. Sharma (Teaching Lab), Mr. Joshi (MSP Office) for their incredible work, which helped me to finish within time.

During my stay at IIT, I am really pleased to meet Professor Ashoke Mallik, Professor Sabyasachi Sarkar, Professor Amitabha Ghosh, and Professor Utpal Das who accepted me like a member of their family and helped me voluntarily. The list will be incomplete if I do not mention about Tukun da and Boudi. It is indeed a pleasant experience spending time with them. I will miss the delicious homemade dishes of Mrs. Sarkar, Mrs. Rai and Mrs. Agrawal.

Last but not the least, I want to mark this memorable moment by fondly recalling the support of my family members that was always a source of constant inspiration for me.

Aditi Datta

Abstract

Thin films of barium strontium titanate are currently attracting much attention because of their useful properties such as high dielectric constant, low leakage current, low dielectric loss, tunable dielectric constant at microwave frequencies etc. In the sol gel preparation of these films, the formation of the crystalline perovskite phase and the properties are found to markedly depend on parameters such as the additives (chelating agents) and solvents used in the sol, the thickness of the individual coatings, the firing schedule etc. In particular, formation of some intermediate carbonate phase under same conditions is noted. In the present work, the effect of various additives (acetylacetone and DEA) and solvents (2-methoxyethanol and ethylene glycol) on phase formation and dielectric properties of the film was studied. Gel powders prepared from the sol with different additives and solvents and heated to different temperatures were characterized by TGA, FT-IR and XRD in order to get information about the different intermediate phases forming during the course of heating of the BST film. It was observed using FT-IR that when acetylacetone is used as an additive, no intermediate carbonate (CO_3^{2-}) phase forms. XRD data showed that acetylacetone reduced the crystallization temperature of BST. XRD is unable to detect intermediate phases. TGA analysis showed three distinct regions of weight loss and showed that all the organics are not completely removed in the course of heating. Thin films of $Ba_{0.8}Sr_{0.2}TiO_3$ were prepared by the sol-gel processes. The concentration of the starting sol was ~ 0.22M. The films were deposited on Pt substrates at 3000 rpm for 30 seconds. After each coating the film was dried in the furnace at 200^{0}C for 2 minutes. Total number of coatings was 15. After the final coating and drying treatment, the film was annealed at 600^0 - 800^{0}C for one hour in a furnace. The thickness of the films were ~1μm. The films were examined by XRD, optical microscopy and SEM. The films were crack-free and crystallized into tetragonal perovskite phase. SEM pictures showed that the films might be porous in nature. The dielectric measurements show the films have a low dielectric constant (~25) and high loss (at low frequencies). These can be related to the micro porosity and organic residues present in the film. Crystallization of BST thin films by two unconventional methods (microwave radiation and hydrothermal treatment) were also studied but were not successful.

CONTENTS

Chapter 3

Results and Discussions 52

List of Tables

Chapter 1

Introduction

High permittivity perovskite thin films have made an impact on the emerging area of information technology over the last decade. This has been felt mostly in the area of information storage, especially for high density Dynamic Random Access Memories (DRAMs). On the other hand, the drive towards miniaturization has led to the Ultra Large Scale Integration (ULSI) era. In the next generation of ULSI DRAMs memory cells of capacity up to 1 Gbit are being envisaged. The realization of 1 Gbit memory devices exposes many challenges. If we see the road map of DRAM technology (given in Table 1) it can be easily visualized that this advancement is mainly achieved by

i> reducing the thickness of the dielectric layer and

ii> increasing the effective capacitor area of the device.

Table 1: The road map of DRAM technology [1]

Memory capacity	Minimum feature size(μm)	C/A (fF/μm^2)	Capacitor area (μm^2)	Operating Voltage (V)	Year*
16 Mbit	0.60	25	1.10	3.3	1992
64Mbit	0.35	30	0.70	3.3	1995
256 Mbit	0.25	55	0.35	2.2	1998
1 Gbit	0.18	100	0.20	1.6	2001
4Gbit	0.15	140	0.10	1.1	2004

* Year in which 1 million devices were/are projected to be produced.

With the advance of technology, the capacitor dielectric thickness (t_{di}) for traditional insulators/dielectrics (SiO_2/Si_3N_4) has reached their practical limit or the quantum

limitation value. To overcome this problem, the use of high dielectric constant (high-K) material seems to be the only solution. In recent years, thin film perovskite materials with high dielectric constant such as PZT, $SrTiO_3$, and $Ba_xSr_{1-x}TiO_3$ (BST) have been investigated as dielectric materials for future DRAMs. The best-suited dielectric material would have a low leakage current and a high dielectric constant and would also be in paraelectric phase to avoid fatigue from ferroelectric domain switching. Thus BST is the most promising material for DRAM capacitors. The high charge storage density and low leakage current density of BST are attractive for DRAM whereas the voltage tunable dielectric constant with low dielectric loss is attractive for microwave dielectric applications[2]. BST films also find use in phased array antennae[3], phase shifters[4], infrared detectors[5], and sensors[6]. In addition to the beneficial dielectric properties of BST solid, it is well known that appropriate Ba/Sr ratio (Ba/Sr = 0.984/0.016) shows interesting electro-optic effects and is useful for pyroelectric applications that operate in the dielectric bolometric mode [7]. BST films are also used in. In the present chapter after a brief introduction to the need of the hour for the use of BST in ULSI DRAMs, structure and properties of BST are discussed. This is followed by a description of the sol-gel method to prepare thin films. Available literature on sol-gel preparation and other methods are briefly reviewed in six sub-sections. The chapter ends with a statement of problem of the present research.

1.2 What is BST?

Barium Titanate ($BaTiO_3$) was the first piezoelectric ceramic material and is still widely used because its dielectric constant and coupling factor are substantially higher as compared to other materials. It is isostructural with the mineral perovskite ($CaTiO_3$) and so referred to as a perovskite. Below its Curie point, the structure is slightly distorted to the tetragonal form with a dipole moment along c-direction. Above its Curie temperature (~120^0C), the unit cell is cubic with large cations(Ba^{+2}) on the corners, smaller cation(Ti^{+4}) at the center and six oxygen ions(O^{-2}) at the center of faces. The Ti ion is surrounded by six oxygen ions in an octahedral configuration (TiO_6)[8]. At T > 120^0C, the thermal energy is sufficient to allow the Ti-ions to move randomly from one position to another, so there is no net fixed asymmetry. The open octahedral site allows the Ti-atom to develop a large dipole moment in an applied field, but there is no spontaneous alignment of the dipoles. In this symmetric configuration the material is paraelectric, i.e. there is no net dipole moment when E = 0.

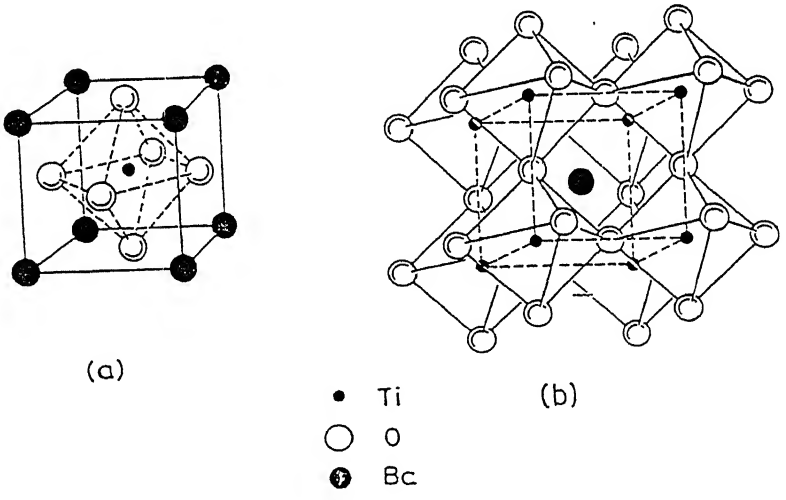

Fig. 1.1: (a) $BaTiO_3$ structure and (b) the oxygen octahedra

BST: Barium Strontium Titanate ($Ba_xSr_{1-x}TiO_3$) is a solid solution of Barium Titanate ($BaTiO_3$) and Strontium Titanate ($SrTiO_3$). $BaTiO_3$ is a ferroelectric material with Curie temperature (T_c) of 120° C, while $SrTiO_3$ is a paraelectric material with no ferroelectric phase transition. Adjusting the ratio of Ba to Sr can suitably control the Curie temperature of BST. The Curie point of $BaTiO_3$ is found to decrease linearly with solid solution of Sr^{2+} in place of Ba^{2+} at the rate of 3.7°C / % of mole[8]. Bulk $Ba_xSr_{1-x}TiO_3$ is ferroelectric and tetragonal at room temperature for x= 0.7 to 1.0 (Ba-content). All other compositions are paraelectric and cubic. The Curie temperature of bulk BST varies from 30 to 400 K depending upon the Ba/Sr ratio. But in thin films the properties seem to change[9].

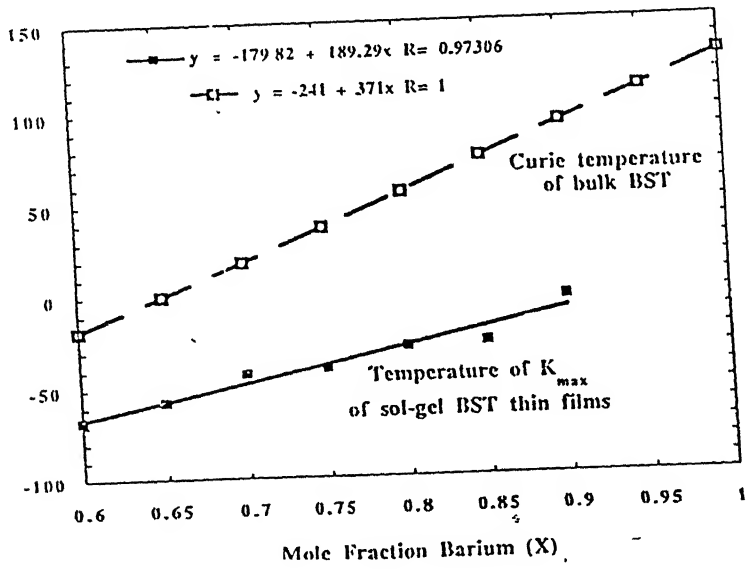

Fig1.2 Curie temperature Vs mole fraction of barium for thin film and bulk BST[9]

1.3 Why BST?

In the first section the necessity of using BST as capacitor dielectric is explained. Here all the strong points of BST as the most suitable material for ULSI DRAMs are listed.

1. High dielectric constant ($\varepsilon_r > 200$).
2. Low leakage current.
3. Low temperature coefficient of electrical properties.
4 Small dielectric loss.
5. Lack of fatigue or aging problem.
6. High compatibility with device processes.
7. Linear relation of electric field and polarization.
8. Low Curie temperature (T_C).

1.4 Material Processing of BST thin films:

BST thin films can be deposited by a variety of techniques. The commonly used techniques for depositing dielectric thin films are rf- sputtering, ion beam sputtering, pulsed laser ablation, metallorganic chemical vapour deposition (MOCVD), metallorganic deposition (MOD), and sol-gel. Each technique has its merits and demerits. For example MOCVD can be used for large-scale production but elevated temperature is required for cracking the metal-organic source[1]. Pulsed laser ablation is suitable for low temperature epitaxial growth but it can only process sample on a limited scale. For device applications, whatever be the method of production of thin films, it must be economical and films of good homogeneity and purity must be prepared. Sol-gel is a novel technique in this regard as it offers some practical advantages over the other processing methods.

1.5 Sol-Gel Processing:

In sol-gel films are processed by a wet chemical method.

Sol: Sol is a suspension of sub-micron particles in a liquid.

Gel: Interconnected solid network with an interspersed continuous liquid phase formed by the aggregation or polymerization of sol particles.

The sol-gel process offers the following **advantages** over the conventional methods:

1. Films of high purity can be obtained.
2. Films have good compositional homogeneity.
3. Processing is carried out at a lower temperature.
4. Dopants can be easily introduced for desired electrical and physical properties.
5. Thickness of the film can be controlled by modifying the solute concentration and by varying the no of coatings.
6. It is easier and low-cost method compared to other methods like CVD, sputtering etc.

However it has some **disadvantages**

1. Long processing time.
2. Residual fine pores after drying and annealing.
3. Large shrinkage in films during heating and annealing, which cause crack formation in the film.

Two types of sol-gel processing are generally used

(a) **Colloidal Processing**: Particles of size 1- 1000 nm are used. They form a gel network and are subsequently sintered to yield a continuous film.

(b) **Polymeric Processing:** Different metal alkoxides $M(OR)_x$ are used as precursors. In the sol-gel synthesis, $M(OR)_x$ is mixed with water and appropriate solvent (usually an alcohol). A small amount of acid or base is added to catalyze the reaction. To avoid or minimize the condensation, some additives like metal salts (chloride, nitrate, acetate), chelating agents (ethylene glycol, acetylacetone), DCCA (drying control chemical additives) (DEA, PVA, PVP) are used. During polymeric gel formation, hydrolysis and condensation reactions take place simultaneously.

i. Hydrolysis reaction: In this an -OH group replaces the alkoxy group.

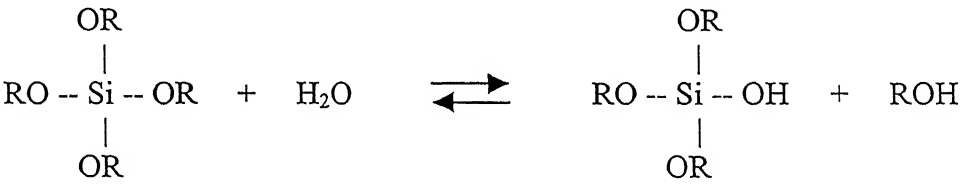

ii. Condensation Mechanism: The -OH group is eliminated and M-O-M linkages form:

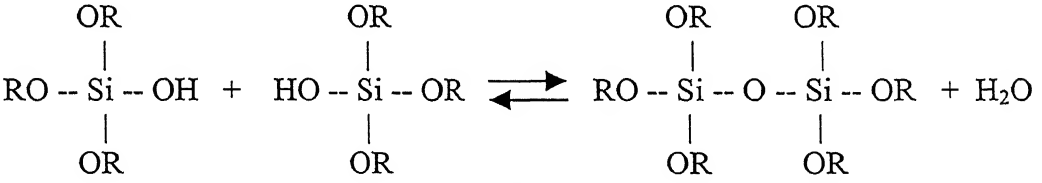

(a)

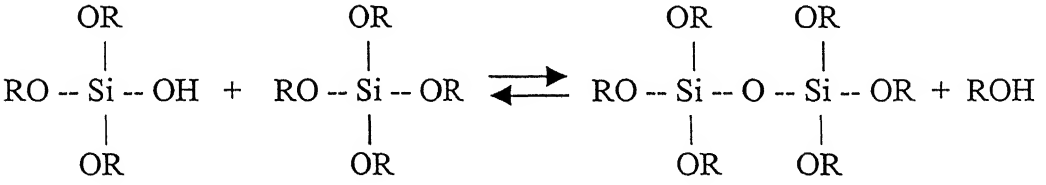

(b)

1.6 BST system:

In the sol-gel processing of BST thin films precursors generally used are barium acetate [$Ba(CH_3COO)_2$], strontium acetate [$Sr(CH_3COO)_2,2H_2O$] dissolved in heated acetic acid, and titanium butoxide [$Ti(OC_4H_9)_4$]. In case of BST, Ti-butoxide hydrolyzes and condenses in the solution to form a 3-d network of $(-Ti-O-Ti-)_n$ bridges[10]. Ba and Sr ions are trapped in the network to form the BST sol complex.

1.7 Thin film formation:

The substrate is coated with the sol, which eventually transform into a 3-d network by the elimination of water or some other group like alcohol. After drying, it forms an amorphous coating which after annealing gives a polycrystalline thin film.

1.8 Literature Review:

The quality of the BST films depends upon a series of interrelated factors like sol concentration, thickness of the films, use of different substrates, microstructures and crystal structure of the film, use of different additives, effect of annealing temperature, annealing atmosphere, and post-annealing treatment to name a few. In the next section evolution of different phases, microstructure, and the effect of different parameters related to the processing of BST thin films is discussed based on the experimental facts described in different journal articles in the following sub-sections.

1. Sol-gel processing of BST films
2. FT-IR study of BST films
3. Ferroelectricity in BST films

4. Effect of additives

5. Intermediate phase

6. Dielectric properties

1.8.1 Sol-gel processing of BST films:

In sol-gel processing of BST different precursors and additives are used by different research groups and depending on different treatments properties of the film vary. In this sub-section different routes to prepare BST sol is discussed. So acetate route is chosen for the present study

Tahan et al[9] used Ba-acetate, Sr-acetate and Ti IV isopropoxide as the precursor materials for the sol of BST. The acetic acid aided in the dissolution of acetates while the ethylene glycol stabilized the solution to precipitation. The optimum ratio of acetic acid and ethylene glycol was found to be 3:1 from the DTA and XRD results [fig 1.3 (a) and (b) and 1.4 (a) and (b)]. DTA shows that the use of R_{ac}/R_{eg} in 3:1 ratio lowers the crystallization peak to 510-580^{0}C compared to 600-680^{0}C for R_{ac}/R_{eg}= 1:0.

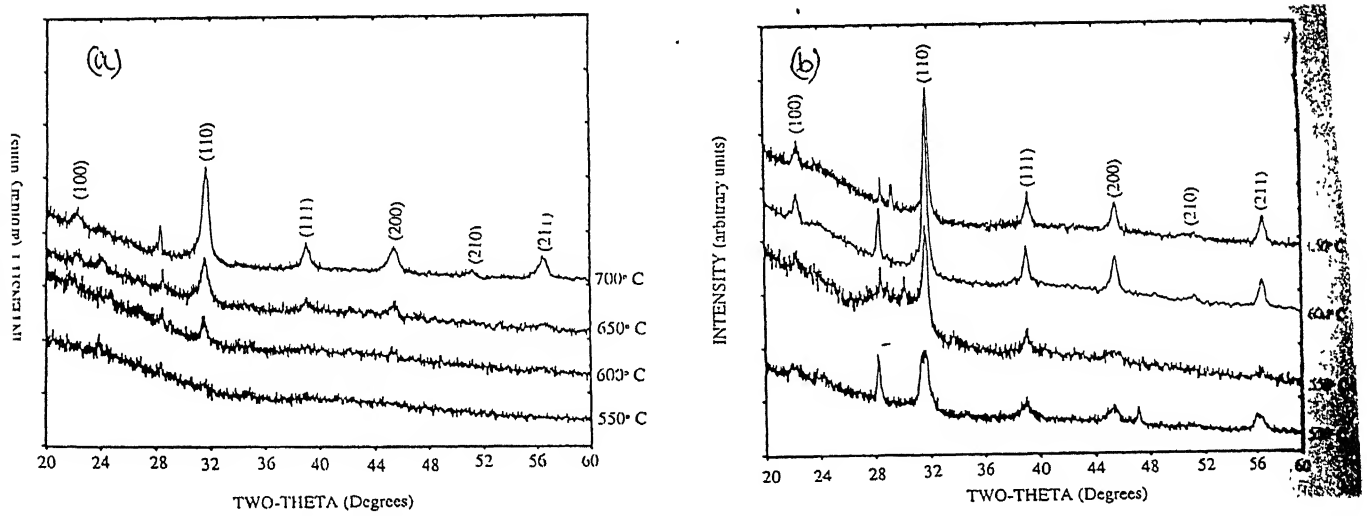

Fig 1.3: XRD patterns of BST(x=0.8) films heated to various temperatures, made from solutions with an acetic acid :ethylene glycol ratio of (a) 1:0 and (b) 3:1. [9]

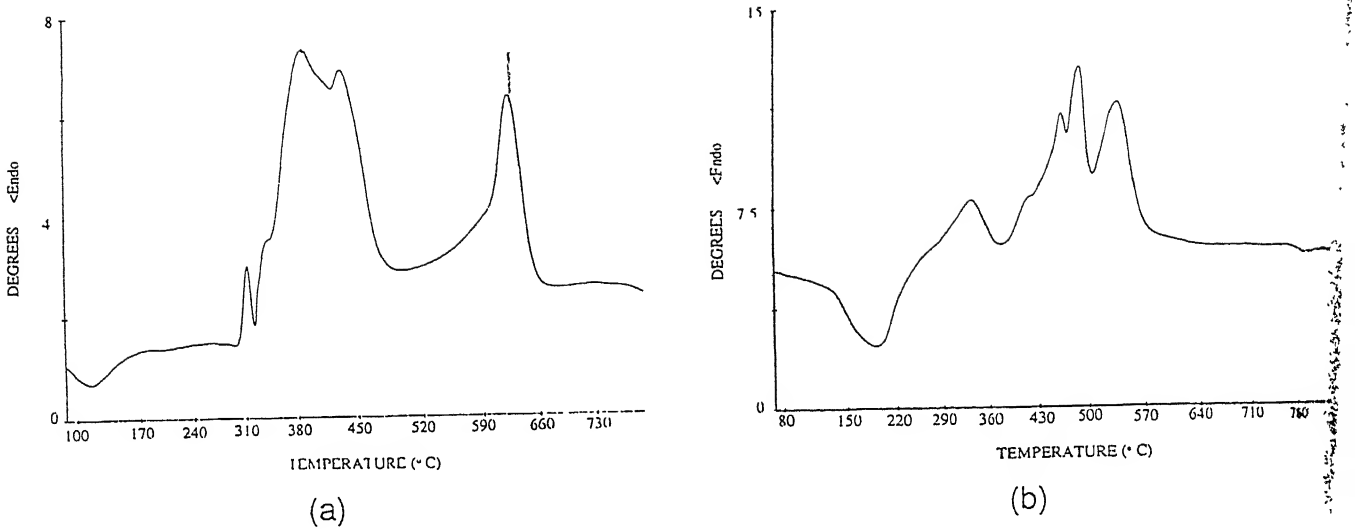

Fig 1.4: DTA patterns of dried BST(0.8) gels of acetic acid :ethylene glycol ratio of (a) 1:0 and (b) 3:1[9].

Jang et al [11] used Ba-, Sr-isopropoxides in isopropanol and Ti-isopropoxide as the starting precursors for the synthesis of sol. Acetyl acetone was used as a chelating agent. Films of thickness 250 nm were prepared on RuO_2(150 nm)/Ru(100nm)/SiO_2(100nm)/Si(100) substrates. Final annealing was carried out at 700^{0}C for 2 h. After that a post-annealing is carried out at a temperature of 600^{0}C for 1 h under O_2 or Ar atmosphere. The BST/RuO_2 interface was studied with the help of AES and RBS. Films annealed in O_2 atmosphere showed a lower value of leakage current than the film annealed under Ar-atmosphere.

Films of $Ba_{0.4}Sr_{0.6}TiO_3$ were prepared by Lahiry et al[12] by a hexanoate route. 0.4 moles of Ba-ethyl hexanoate and 0.6 moles of Sr-ethyl hexanoate were dissolved in ethyl alcohol in a reflux condenser. Ti-IV-isopropoxide was added to Ba and Sr solution to produce a Ba-Sr-Ti complex solution. Acetyl acetone and formamide were used as stabilizers. Films were spin coated at 4000 rpm for 30 seconds, pyrolyzed at 350^{0}C for 5 min on a hot-plate and annealed at 700^{0}C for 1hr to obtain a polycrystalline film.

Tian et al [13] used Ba-acetate, Sr-acetate and tetrabutyl titanate as precursors Acetic acid and ethylene glycol were selected as solvents. Formamide was used as an additive in order to reduce crack formation in the films. DTA/TGA and XRD measurements show that the films were crystallized above 600^{0}C and the perovskite phase forms at 750^{0}C [fig. 1.5(i)]. The powder fired at 950^{0}C for 1 hr shows tetragonal structure [fig. 1.5(ii)].

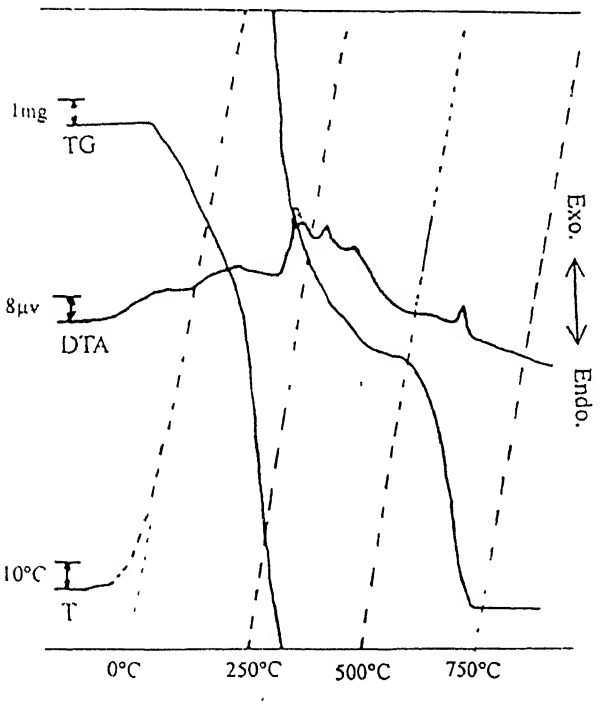

Fig. 1.5(i): TD/DTA curves of dried $Ba_{0.8}Sr_{0.2}TiO_3$ gels at about 70^{0}C[13].

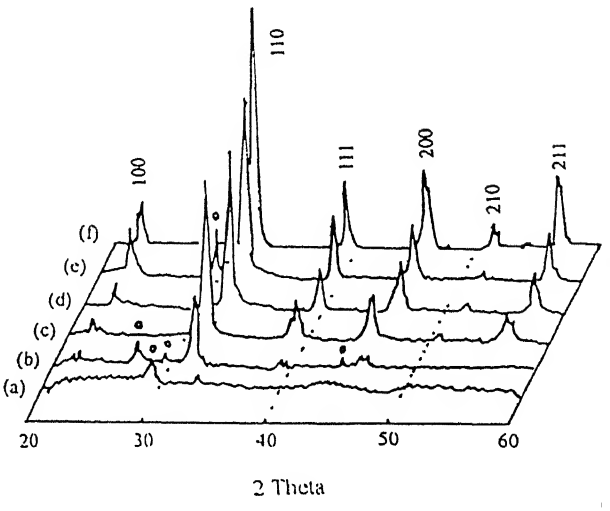

Fig. 1.5(ii): X-ray diffraction patterns of the BST thin films at: (a) 500^{0}C;(b) 600^{0}C;(c) 700^{0}C; (d) 730^{0}C; (e) 750^{0}C; and patterns of BST powder fired at 950^{0}C.Intermediate phase(IP) marked with a hollow circle[13].

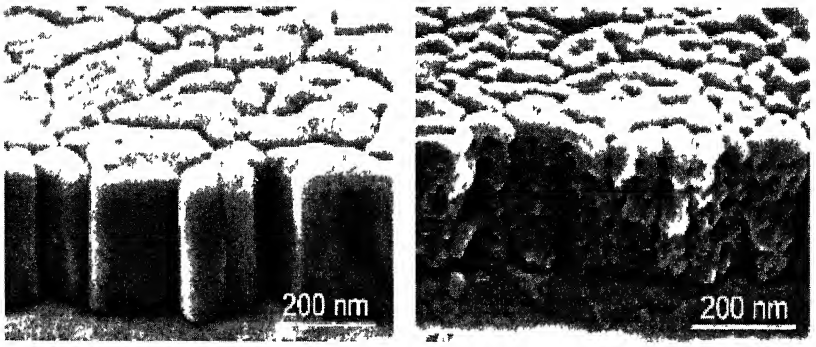

(a)

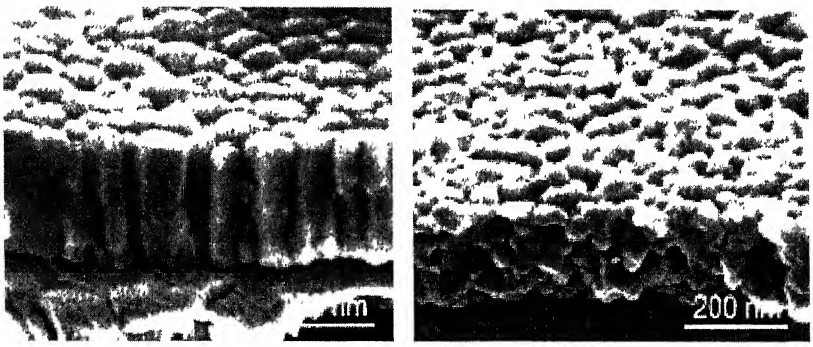

(b)

Fig 1.6(a): SEM micrographs of the cross section and surface of two $SrTiO_3$ thin films prepared from acetate precursors; (left) 22 layers, 0.1 M solution; (right) six layers, 0.3 M solution.

(b): SEM micrographs of the cross section and surface of two $SrTiO_3$ thin films prepared from propionate precursors; (left) 22 layers, 0.1 M solution; (right) six layers, 0.3 M solution[14].

Hoffmann et al [14] in order to differentiate between the influence of the precursor chemistry and the processing conditions on the film formation process, applied different carboxylate routes, varied the concentration of the CSD solutions in the range of 0.1 to 0.3 M, and performed different pyrolysis and annealing temperatures between 250^0C and 800^0C. The carboxylates having different length of the alkyl chain, i.e. acetates, propionates and 2-ethyl hexanoates dissolved in the corresponding caboxylic acid, and diluted with the parent alcohol (2-methoxyethanol in case of acetate solution, 1-butanol in case of propionate solution, and hexanol for 2-ethyl hexanoate solution) were mixed

with the Ti-element (Ti-tetra-n-butoxide). Acetyl acetone was used as a stabilizer. In case of short chain precursors i.e. acetates for a single step heating procedure i.e. crystallization of every deposited layer and a lower solution concentration (0.1 M) resulted into the formation of columnar grains [Fig.1.6]. All other combinations of the precursor, heat treatment and solution concentration led to polycrystalline film with grainy morphology. The evolution of columnar grains in case of acetate based solutions can be attributed to the formation of an intermediate phase that in turn provides the sites for heterogeneous nucleation.

1.8.2 FT-IR study of BST films:

Horng et al[15] made films of BST (Ba/Sr composition 0.7/0.3), deposited on Pt (200nm)/Ti (20nm)/SiO_2 (250nm)/Si by spin on sol-gel process. The films were implanted with Ar^+, N^+, F^+ ions with different doses. The samples were subjected to rapid thermal processing (RTP) in a purified O_2 atmosphere at 650 ± 50 ^{0} C for 3 minutes. For Ar^+ and N^+ samples no drastic change in leakage current characteristics is observed but in case of F^+ implanted samples leakage current is reduced by about 1 order of magnitude. To study F implantation effect the samples with and without implanted ions were measured by FTIR [fig.1.7] It is seen that the width of Ba(Sr)-Ti-O absorption peak at 816 cm^{-1} decreases and its magnitude increases with the increasing dose. On the other hand the -OH region (3600-3000 cm^{-1}) clearly exists in the non-implanted sample. As the ion dose increases the -OH region decreased first ($5X10^{14}$ cm^{-2}) and then increased ($1x10^{15}cm^{-2}$). Ion implantation induces rearrangement and residual evaporation at the same time thus the process tends to increase the density of the material. As the density of the material increases with implantation, the average bond energy of the sample is also

increasing which explains the changes observed in the Ba(Sr)-Ti-O peak. On the other hand many more oxygen vacancies exist in non-implanted BST films as compared to implanted one and they absorb a greater amount of moisture. This moisture absorption may provide the current leakage paths and may be the main reason for the reduced dielectric constant. As the ion-dose increases ($5x10^{14}$ cm^{-2}) the F^+ ions substitute the O vacancies thereby reducing the -OH peak in the FTIR spectra. But for still larger ion doses ($1x10^{15}$ cm^{-2}) excess F^+ ions may form bonds with Sr and Ba and produce Sr-F or Ba-F compounds. Once Sr-F and Ba-F is formed, they readily absorb moisture from air resulting in the increase of the -OH signal.

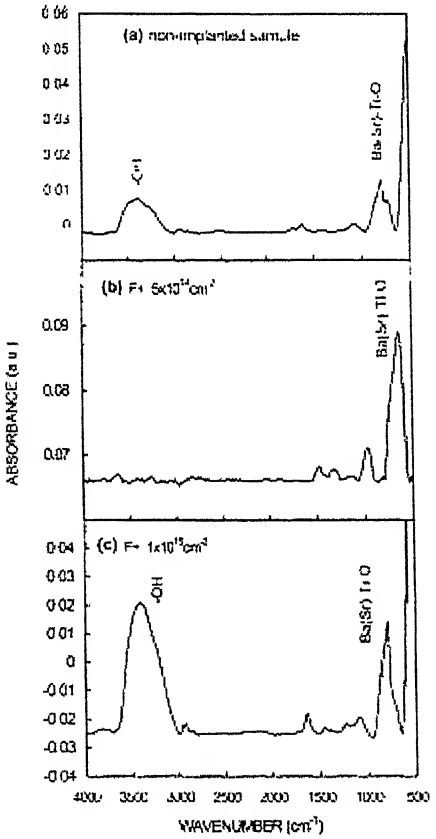

Fig 1.7: FT-IR spectra for non-implanted and implanted BST samples [15]

$Ba_{0.5}Sr_{0.5}TiO_3$ (BST) thin films were grown on Si by an ultraviolet-assisted pulsed laser deposition (UVPLD) technique by Craciun et al [16]. FTIR was used to examine the presence of any additional phase with Ba-atoms in a different chemical state FTIR spectroscopy investigations were performed in the transmission mode. No bands due to carbonate (CO_3^{2-}) groups around 1450cm^{-1}were observed. Ti-O bonds were observed around 600 cm^{-1} and Si-O bond around 1100 cm^{-1}.

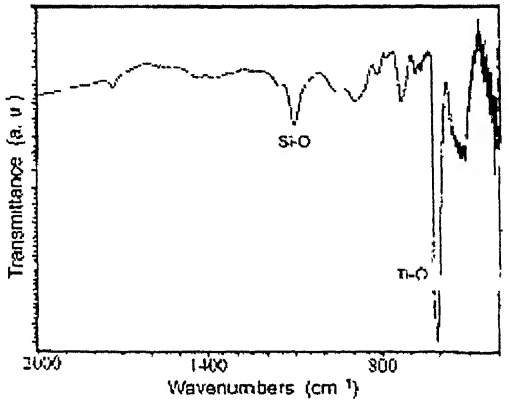

Fig 1.8: FTIR transmittance spectrum of a BST film grown by PLD at 450 °C. [16]

$Ba_{0.7}Sr_{0.3}TiO_3$ (BST) thin films doped with La, Nb, Mg ions were prepared by Chen et al [17] through metal-organic deposition (MOD) method on Pt/Ti/SiO2/Si substrates. Examination of ceramic powders by FTIR revealed the existence of carbonate ions[fig.1.8]. The absorbance peaks at wave no. 1451, 1050, and 857 cm^{-1} belong to CO_3^{2-}, while those at 1090 and 880 cm^{-1} are caused by the vibration of C-O and C-C bonds. An intermediate oxycarbonate phase with chemical formula $(Ba,Sr)_2Ti_2O_5CO_3$ was investigated by this study.

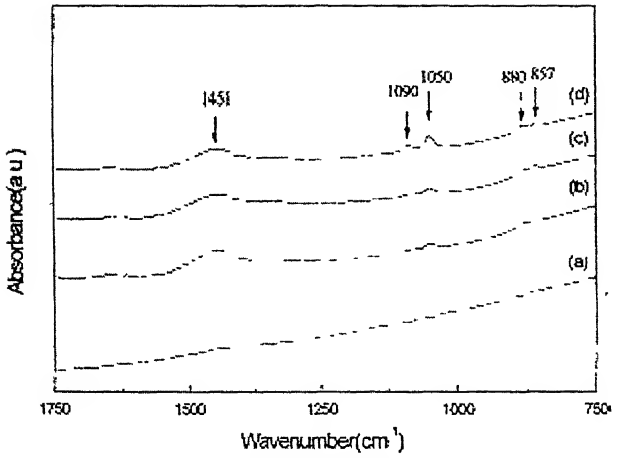

Fig. 1.9: FT-IR for BST powders after calcinations at (a) 500°C/h, (b) 525°C/0.5 h, (c) 525°C/h, and (d) 550°C/0.5 h. [17]

1.8.3 Ferroelectricity in BST films:

$Ba_{0.8}Sr_{0.2}TiO_3$ thin films were prepared by Cheng et al [18] with different individual layer thickness i.e. 60, 20, 8 nm for concentration of the spin on solution of 0.4M, 0.1M, and 0.05M respectively on Pt/Ti/SiO2/Si substrates. Films were pyrolyzed at 350°C for 5 minutes after each coating and annealed at 750°C for 10 minutes for crystallization. The films prepared with an individual thickness of 60 nm showed small equiaxed grains, cubic structure, temperature dependent dielectric constant, and no ferroelectricity. The films prepared with an individual layer thickness of 8 nm showed columnar grains, tetragonal structure, good ferroelectricity and two dielectric peaks in the dielectric constant Vs temperature curve [Fig.1.10, 1.11,1.12 and 1.13]. From the surface and cross sectional FE-SEM micrographs it is concluded that the mechanism of growth within the grain is layer by layer homoepitaxy.

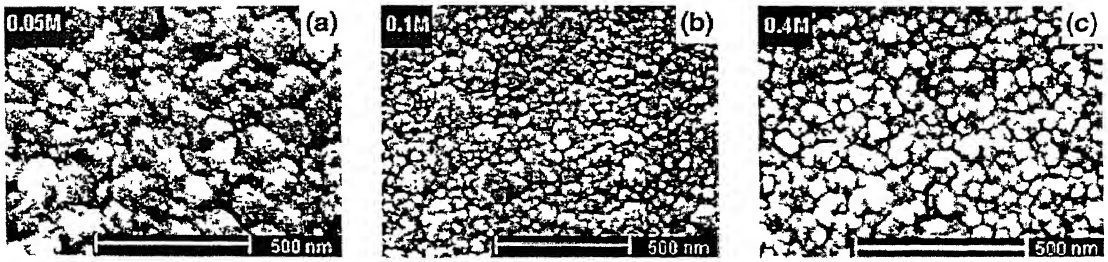

Fig 1.10: Surface FE-SEM micrographs of sol– gel-derived $Ba_{0.8}Sr_{0.2}TiO_3$ thin films from (a) 0.05*M*, (b) 0.1*M*, and (c) 0.4*M* precursor solutions[18].

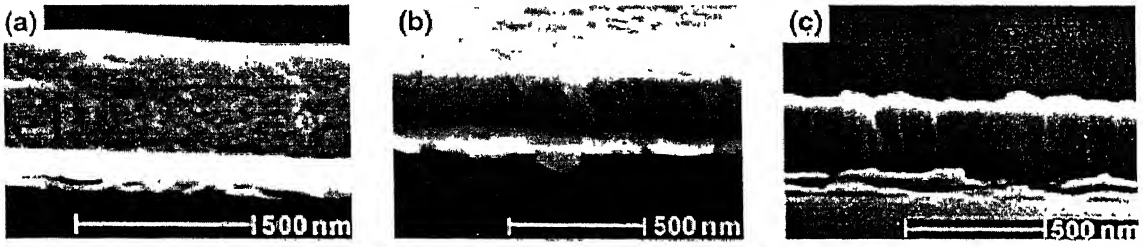

Fig. 1.11: Cross-sectional FE-SEM micrographs of sol– gel-derived Ba0.8Sr0.2TiO3 thin films from (a) 0.4*M*, (b) 0.1*M*, and (c) 0.05*M* precursor solutions[18].

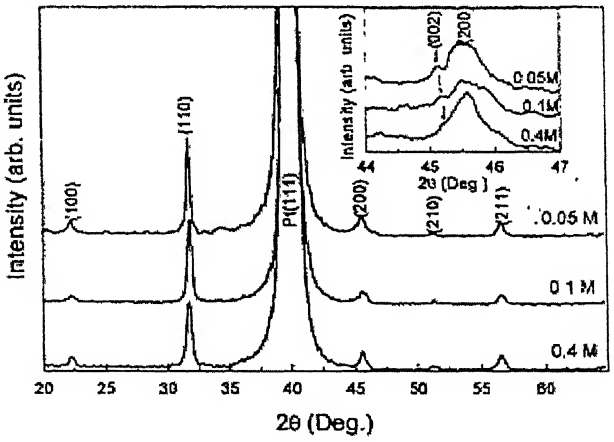

Fig. 1.12: XRD patterns of sol– gel-derived $Ba_{0.8}Sr_{0.2}TiO_3$ thin films from 0.4*M*, 0.1*M*, and 0.05*M* precursor solutions. Inset is {200} reflections for the films[18].

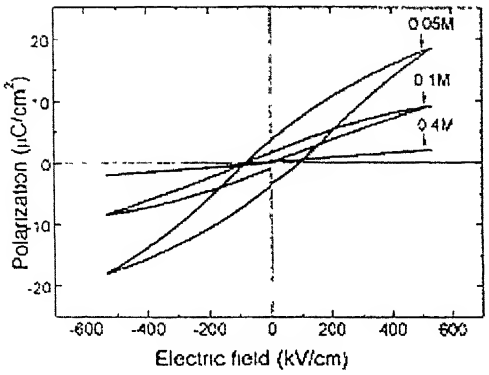

Fig. 1.13(a): P–E hysteresis loops of sol– gel-derived Ba0.8Sr0.2TiO3 thin films from 0.4*M*, 0.1*M*, and 0.05*M* precursor solutions[18].

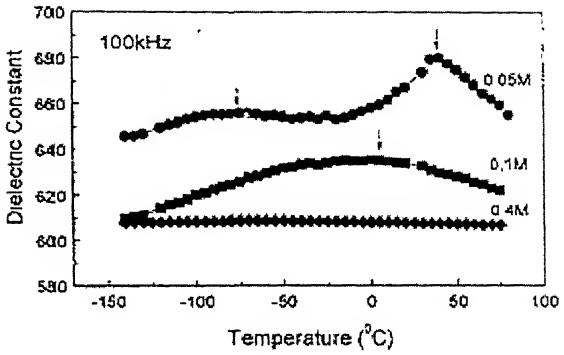

Fig. 1.13(b): Temperature dependence of dielectric constant for sol– gelderived Ba0.8Sr0.2TiO3 thin films from 0.4*M*, 0.1*M*, and 0.05*M* precursor solutions[18].

1.8.4 Effect of additives:

One of the most important factors determining the properties of thin films made by the sol-gel route is the precursor chemistry. Additives used in the sol can control the properties of the films. Here the effects of two different additives are discussed.

Ding et al [10] studied the effect of acetylacetone (HAcAc) as an additive for $Ba_{0.7}Sr_{0.3}TiO_3$ system. Films were given an intermediate heat treatment at 400^{0}C for 20 minutes. Finally annealed at 750^{0}C for 1.5 hours. In the DSC (differential scanning calorimety) of the powders showed two exothermic peaks at 648^{0}C and 681^{0}C for sol without additive; one exothermic peak at 577^{0}C for freshly prepared HAcAc modified sol and all the three peaks in the aged HAcAc modified sol. Conclusion is that, in the freshly prepared sol without HacAc, intermediate phases, probably $(Ba,Sr)CO_3$ form and then BST forms, while in the freshly prepared sol with HAcAc the formation of BST takes place directly. In the unmodified sol the hydrolysis and condensation of the butoxide takes place rapidly and the Ba & Sr are excluded. In the HAcAc modified sol the

hydrolysis and condensation are slowed and the Ba and Sr are uniformly distributed in the gel. This results in the intermediate phase formation in the sol without HAcAc. Use

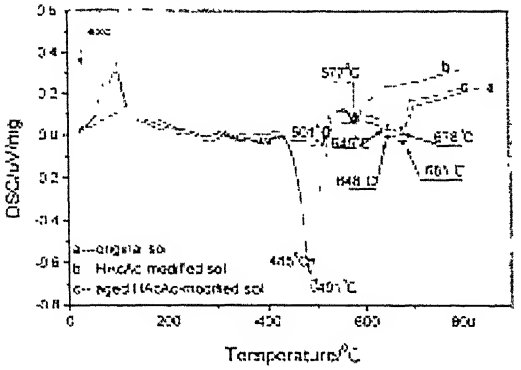

Fig. 1.14 (a): The DSC curves of different sols.[10]

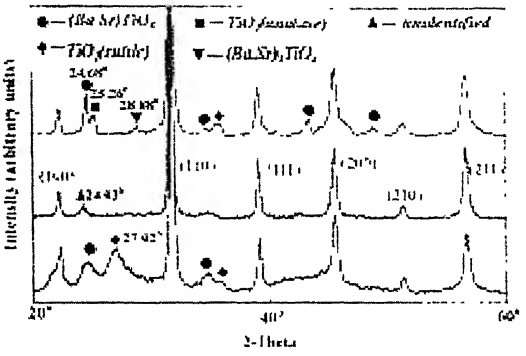

Fig. 1.14 (b): XRD patterns of powder prepared from (a) original sol, 650°C=0.5 h; (b) fresh HAcAc modified sol, 580°C=0.5 h; and (c) aged HAcAc-modified sol, 650°C=0.5 h. [10]

of HAcAc also lowers the crystallization temperature[fig.1.14 (a) and (b)].

Tahan et al [9] prepared 0.75M sol by dissolving Ba, Sr acetates in glacial acetic acid. Ti-butoxide and ethylene glycol are added in acetic acid with acetic acid : ethylene glycol = 0:1, 1:1, 3:1, and 1:0. The solution is heated to promote condensation reaction between acetic acid and ethylene glycol

$$OH\text{-}CH_2\text{-}CH_2\text{-}OH + CH_3\text{-}COOH \longrightarrow OH\text{-}CH_2\text{-}CH_2\text{-}O\text{-}CO\text{-}CH_3 + H_2O$$

Films of composition $Ba_{0.8}Sr_{0.2}TiO_3$ were spun at 7500 rpm for 90 seconds on Si(100) and Pt/Ti/SiO_2/Si, treated at intermediate temperature 250°C, and annealed in air between 500-700°C. The process was repeated to get films of 400-nm thickness. It was found that without ethylene glycol, the sol precipitated after several hours. For acetic acid; ethylene glycol ratio 1:1 the sol was stable but the film obtained was non-uniform as observed by color variation. Optimum acetic acid to ethylene glycol ratio was found to be 3:1. The

crystallization temperature of the film was lowered to 600^0C to about 500^0C when ethylene glycol was used fig. 1.3 and 1.4.

1.8.5 Intermediate phases:

A key issue of the sol-gel process is the chemistry of the precursor solution, which governs the quality of the films. It is believed that the films crystallize by the decomposition of one or several intermediate phase(s). Differential Thermal Analysis (DTA), Thermogravimetric analysis (TGA) and X-ray Diffraction (XRD) studies are the main characterization techniques which give clues about the crystallization and phase formation in BST films. Based on these studies and others like FT-IR, XPS, Raman spectroscopy and electron diffraction patterns the crystallization path and formation of intermediate phases during crystallization of BST films are investigated.

A number of intermediate phases for the BST system have been proposed for different processing route including the sol-gel.

BST sol doped with La, Mg, Nb is prepared with different molar concentrations by Chen et al[17]. They used a metal-organic deposition (MOD) method with Ba-acetate, Sr-acetate, Ti-butoxide, La-acetate, Nb-ethoxide, and Mg-methoxide as precursors. The glacial acetic acid and 2-methoxyethanol are used as solvents. The sol was deposited on platinized Si by two-step spin coating (1000 rpm, 10s and 6000rpm, 30s). The wet coatings were pyrolyzed at 550-800^0C for 10 min. The presence of an intermediate phase $(Ba,Sr)_2Ti_2O_5CO_3$ was investigated for both thin film and powder. The phase development was investigated using X-ray diffraction analysis. Surface morphology and thickness of the films were investigated by FESEM. Grain size was determined by TEM. SADP(selected area diffraction pattern) is used to identify the crystalline phase. Further

examination of the intermediate phase is done by FT-IR and Raman spectroscopy. In pure BST thin films XRD results show the presence of $(Ba,Sr)_2Ti_2O_5CO_3$ that started forming at 600^0C and disappeared at 650^0C. BST crystalline phase forms at 650^0C. In case of doped films it is seen that the addition of dopants extends the stability temperature domain of $(Ba,Sr)_2Ti_2O_5CO_3$ phase and suppresses the formation of BST crystalline phase till 700^0C[fig. 1.15(a) and (b)]. In case of ceramic powder samples the intermediate phases identified as $BaCO_3$(major) and $(Ba,Sr)_2Ti_2O_5CO_3$(minor)[Fig.1.16(a)]. It was inferred that the titanium ions seem more likely stay with Ba-ions in case of the thin film and forms the $(Ba,Sr)_2Ti_2O_5CO_3$ phase which is directly observed by SADP at 2θ = 26.8[Fig.1.16(b)]. This intermediate phase is

believed to be favoured by three factors: i> distortion of perovskite structure, ii> physical constraint in two dimensions, iii> effect of small grain.

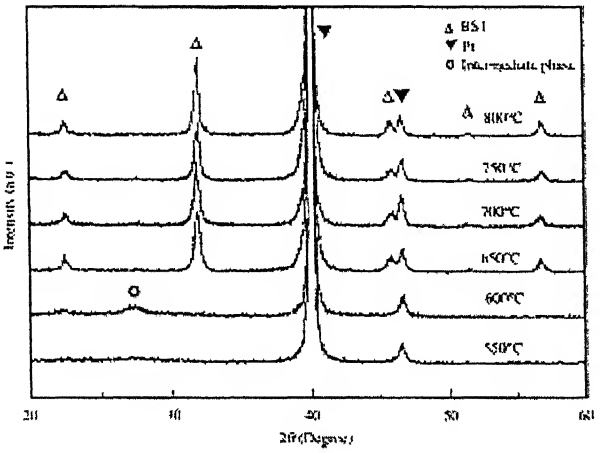

Fig. 1.15(a): XRD diffraction patterns for BST film annealed at 550–800 ^0C for 1 h[17].

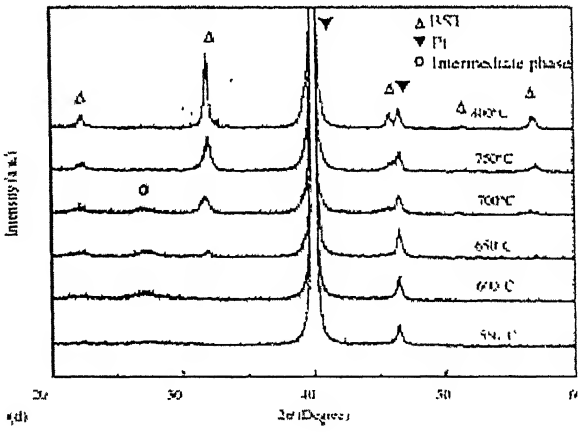

Fig 1.15(b): XRD diffraction patterns for 15 % La-doped BST films annealed at various temperatures for 1 h[17].

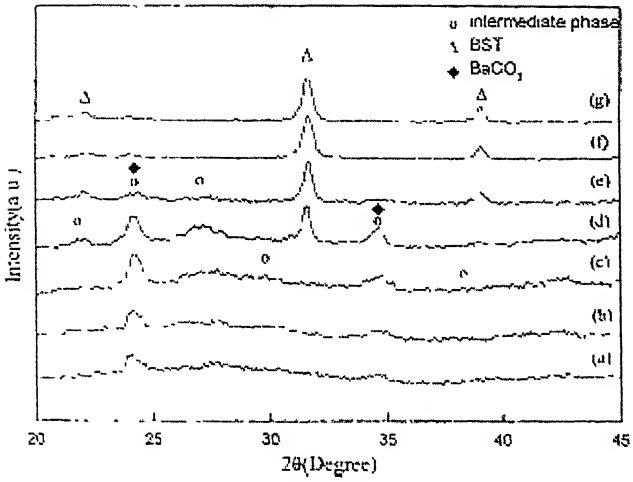

Fig.1.16(a): XRD diffraction patterns for BST powders after calcinations at different temperatures. (a) 500 ^{0}C, (b) 525 ^{0}C, (c) 550 ^{0}C, (d) 575 ^{0}C, (e) 600 ^{0}C, (f) 700 ^{0}C, and (g) 800 ^{0}C.[17]

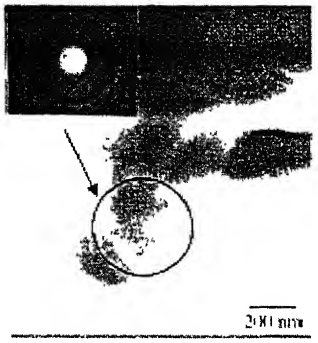

Fig. 1.16(b): TEM image and SADP for the intermediate phase of BST films.The ring distance is correspondent to the $2\theta = 26.8$.[17]

Ding et al[10] have studied the effect of acetyl acetone (HAcAc) on the phase evolution and microstructure of BST thin films by investigating the properties of sol without acetyl acetone, freshly prepared sol with HAcAc and aged sol with HAcAc. DSC of pyrolyzed powders(at 400^{0}C for 20 min) shows two exothermic peaks at 648^{0}C and 681^{0}C for sol without Hacac; one exothermic peak at 577^{0}C for freshly prepared HAcAc modified sol and all the three peaks in the aged HAcAac modified sol [Fig.1.14(a)]. XRD results show (Ba,Sr)CO_3 and rutile peaks at 24.68^0, 25.26^0, and 36.78^0 for unmodified sol. Film was annealed at 650^{0}C for 30 min.For freshly prepared sol with HAcAc a single phase at 24.3^0 belonging to the intermediate phase was found when annealed at 580^{0}C for 30 min. Aged sol XRD pattern looks like the unmodified sol pattern with an extra peak at 28.88^0 [Fig.1.14(b)]. BS-SEM shows that films are much homogeneous in case of HAcAc modified sol. It was concluded that the use of HAcAc changed the crystallization path

from solid diffusion reaction of multi-intermediates to decomposition of a mono intermediate and it was proposed that the single intermediate phase might be an oxycarbonate phase. It was suggested that HAcAc suppresses the condensation growth of Ti-alkoxides and avoids segregation of the Ti from Ba and Sr in the precursor.

Liedtke et al[19] have used a chemical solution deposition (CSD) method in order to deposit the $Ba_{0.7}Sr_{0.3}TiO_3$ thin films on platinized Si ($Pt/TiO_x/SiO_2/Si$) and study their structural and dielectric properties. They have compared the properties of a CSD derived film and a recrystallized film derived from the CSD film amorphized by oxygen ion-implantation. The starting materials were barium propionate [$Ba(CH_3CH_2COO)_2$], strontium propionate [$Sr(CH_3CH_2COO)_2$], and titanium tetra-n-butoxide(TBT) [$Ti(C_4H_9O)_4$]. Propionic acid [CH_3CH_2COOH] and 1-butanol [$CH_3(CH_2)_3OH$] were used as solvents. TBT was stabilized by acetyl acetone (HAcAc) in molar ratio of 1:2. Sol concentration was 1.0M. Films were spun at 4000rpm for 30 seconds. The films were pyrolyzed at 200^{0}C in air and subsequently annealed in a rapid Thermal Annealing System (RTA) for 3min in 1 bar oxygen atmosphere. A film thickness of 130 nm is achieved after 16 coatings. From the XRD data it is seen that for low temperatures (430^{0}C to 650^{0}C) no BST peaks appeared, only the wafer peaks were present. A broad peak was observed at around $2\theta = 27^0$ which is attributed to an intermediate oxycarbonate phase. The peaks of this intermediate phase at 2θ values of 27^0 and 35^0 sharpen up to a temperature of 650 ^{0}C but disappear at 700^{0}C and are replaced by the peaks of the perovskite phase. The composition of the phase is assigned as $Ba_2Ti_2O_5CO_3$. In case of recrystallized thin films clear diffraction peaks of the perovskite phase start appearing from 600^{0}C. The broad peak at $2\theta = 27^0$ reaches its intensity maximum at

550^{0}C [Fig.1.17]. The crystallization temperature can be further reduced to 550^{0}C by post annealing for 2h. The CSD derived films show a columnar microstructure and better

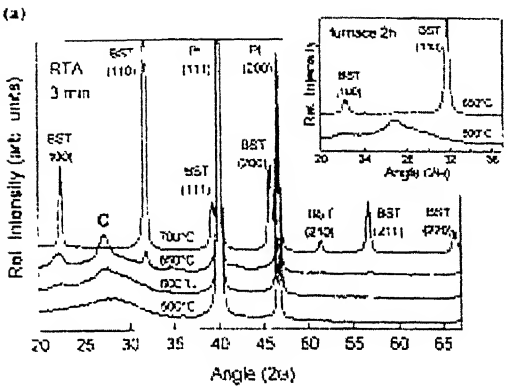

Fig. 1.17: XRD pattern of BST thin films prepared at different temperatures [9]

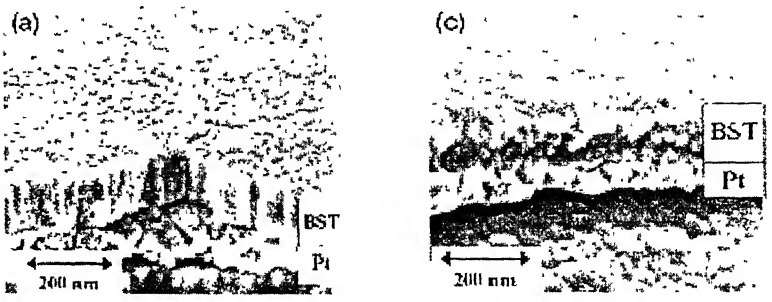

Fig.1.18: SEM micrographs of BST thin films: (a) BST thin film prepared by CSD at T=700°C, (b) recrystallized thin film from the amorphous phase at T=750°C. [9]

electrical properties than the recrystallized films, which exhibit a small grained microstructure [Fig. 1.18].

Hoffmann et al[14] prepared (Ba,Sr)TiO_3 from different alkaline earth carboxylates/titanium alkoxide precursor solutions on Pt coated silicon substrates. In this work different carboxylates with different length of the alkyl chain i.e., acetates, propionates and 2-ethyl hexanoates with concentrations 0.3 to 0.1M were studied. Acetyl acetone was used as a stabilizer. In case of acetate based process for both $BaTiO_3$ and $SrTiO_3$ films the presence of an intermediate phase (stable in the temperature range between 550^{0}C and 650^{0}C) was observed [Fig.1.19]. The intermediate phase is attributed as an oxycarbonate phase. With decreasing sol concentration a columnar microstructure is developed with a decrease in porosity. Based on the above study a mechanism of crystallization process in BST films are proposed. According to them, the oxycarbonate

grains can act as nucleation seeds for the BST-perovskite grains, which results in a competition of heterogeneous nucleation events at the seed grains or at the substrate

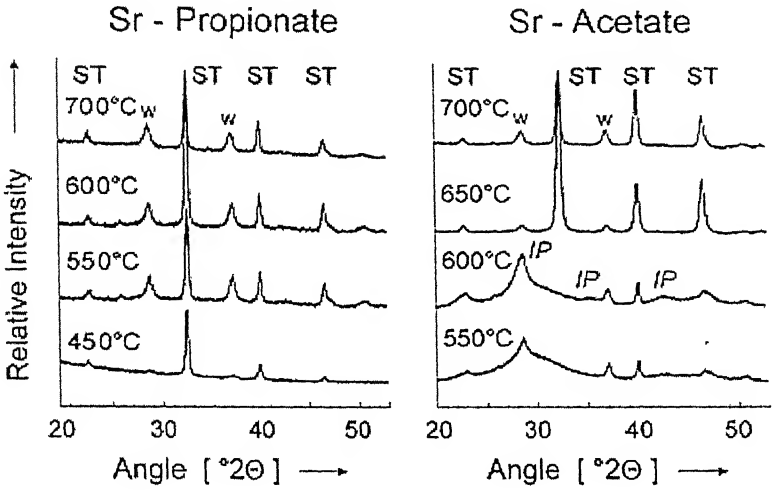

Fig. 1.19: XRD diagrams showing the phase evolution in $SrTiO_3$ thin films prepared from Sr-propionate and Sr-acetate based pre-cursor solutions. ST: $SrTiO_3$, IP: intermediate Sr-Ti-oxo-carbonate phase ($Sr_2Ti_2O_5CO_3$); w: substrate. [14]

interface. Thus, kinetic aspects that are based on the nucleation and growth rates of the two different event controls the film formation process in the BST system.

Tcheliebou et al[20] have found an intermediate Ba rich pyrochlore phase $(Ba,Sr)_2TiO_4$ for laser ablated $Ba_{0.5}Sr_{0.5}TiO_3$ films on(1 $\bar{1}$02)-oriented sapphire substrate[Fig. 1.20(i)]. In case of lead zirconate titanate (PZT) films this intermediate phase was reported. Yamamichi et al[21] studied $Ba_{0.5}Sr_{0.5}TiO_3$ films prepared by ion-beam sputtering. The film with a (Ba+Sr)/Ti ratio of 1.41 showed peaks near 28^0besides the perovskite peaks [Fig.1.20(ii)] This second phase is considered to be a $(Ba,Sr)_2TiO_4$

phase. Noh et al[22] have found a nanocrystalline intermediate phase by a real time synchrotron X-ray scattering study in BST films grown on MgO (001) crystals by rf sputtering. A broad hump appeared around 3.07Å^{-1} close to the substrate peak [Fig. 1.21] This metastable intermediate phase that was nucleated around 500-600^{0}C at the interface was believed to play a crucial role in the crystallization process. The nature of the intermediate phase is not fully understood.

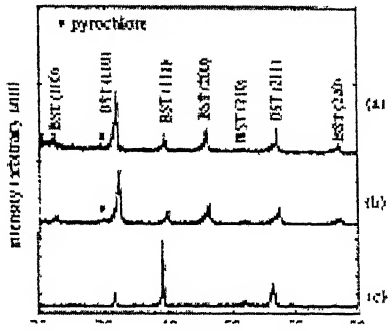

1.20 (i): XRD patterns of the BST films grown onto the 1 1¯ 02 oriented sapphire substrates using different laser wavelengths: (a) 532, (b) 355, and (c) 248 [20]

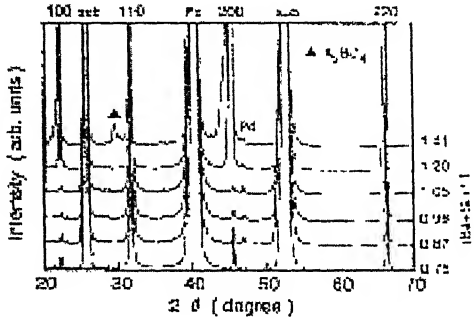

1.20(ii): XRD patterns of the films with (Ba+Sr)/Ti ratios of 0.75, 0.87, 0.99, 1.05, 1.20, and 1.41 [21]

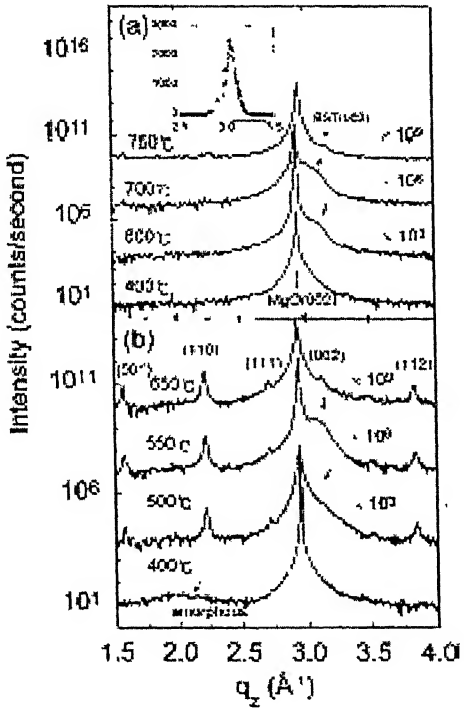

Fig. 1.21: The x-ray powder diffraction profiles of (a) 550 Å thick BST film and (b) a 5500 Å thick BST film measured during real time annealing .The inset of (a) represents the diffraction profile of the intermediate phase [22]

Cho et al[23] using x-ray photoelectron spectroscopy concluded that the intermediate phase forming in BST films is not a barium titanium oxycarbonate but hexagonal $BaTiO_3$ stabilizes with Ti^{3+} ions.

On the other hand Majumdar et al[4] in their study of sol-gel grain oriented thin films of BST on $LaAlO_3(100)$ substrate could not find any intermediate phases[Fig. 1.22] The thin film unlike the powdered sample crystallizes into the perovskite phase without the formation of any intermediate compounds.

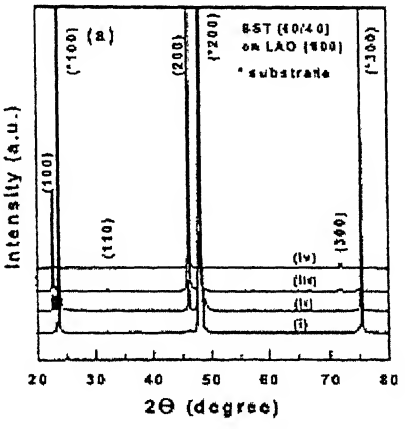

Fig. 1.22: X-ray diffractograms of BST (60/40) films annealed at (i) 600, (ii)900, (iii) 1000, and (iv) 1100 °C for 2 h in air. [4]

1.8.6 Dielectric properties of the films:

The study of BST as a dielectric is important from both fundamental and practical point of view. Due to its unique combination of high dielectric constant and low loss BST found use in some interesting device applications in the ULSI era. In this sub section different values of dielectric constant and loss reported in the journal articles and the factors affecting them are discussed.

Tahan et al[9] did a detailed study of sol-gel BST (0.8,0.2) thin film made with an optimum ratio of acetic acid and ethylene glycol as 3:1. They have studied the effect of Ba/Sr ratio, annealing temperature and annealing atmosphere on the dielectric constant and dielectric loss of the films. Dielectric constant and loss are measured for three different annealing temperatures 500, 600 and 700^{0}C at 1 kHz [Fig. 1.23]. It was seen that the dielectric constant increased significantly with annealing temperature while the dissipation factor increased only slightly from 0.025 to 0.04 over the temperature range. The grain size of the films ranged from 20-50 nm, depending on the annealing temperature. An oxygen-annealing atmosphere hindered the grain growth of the BST films, resulting in a decrease in the dielectric constant of the films when compared to those annealed in air. These results were explained by the increase in grain size with annealing temperature.

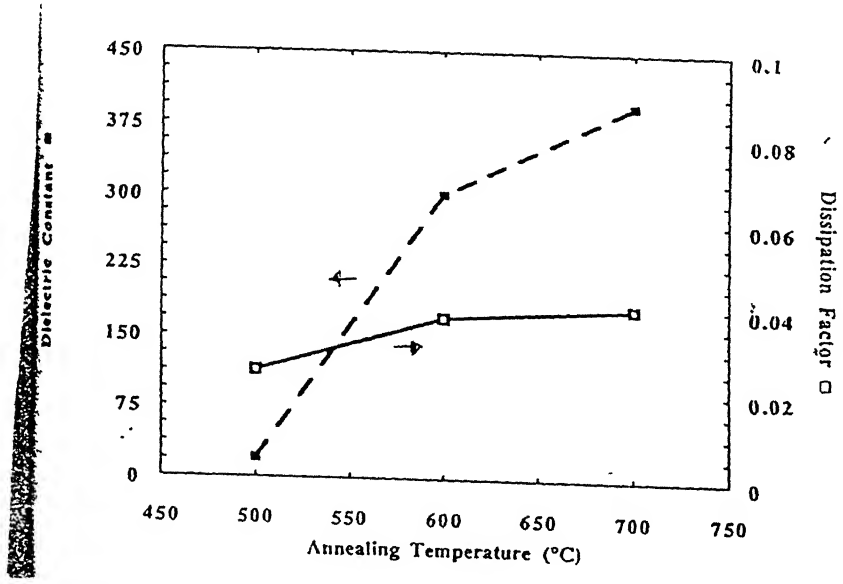

Fig. 1.23: Dielectric constant and dissipation factor versus annealing temperature

Dielectric constant has a strong dependence on the grain size in case of BST thin films. Horikawa et al [ ] studied the effect of grain size on the dielectric properties of $(Ba_{0.65}Sr_{0.35})TiO_3$ films grown by RF sputtering deposited at substrate temperatures of 500-700^{0}C. The correlation between the dielectric constant and broadness of XRD peak is investigated. According to their result, the polycrystalline film with grain size of 45nm had a dielectric constant smaller than 200, while the film with grain size of 220nm

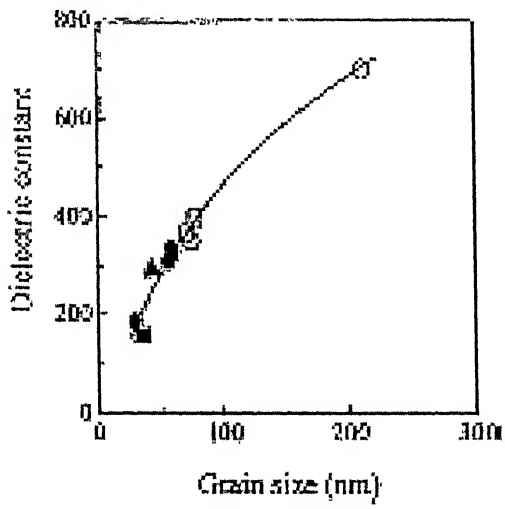

Fig. 1.24: The dependence of the dielectric constant on the grain size from XRD for the $Ba_{0.65}Sr_{0.35}TiO_3$ films deposited at the different substrate temperatures of 500–700 ^{0}C.

showed a dielectric constant larger than 700 [Fig.1.24].

The similar grain size effect on dielectric constant is seen in case of doped BST thin films[25].

Ichinose et al[26] studied the effect of rapid thermal annealing on the electrical properties of $(Ba_{0.5}Sr_{0.5})TiO_3$ thin films grown by rf magnetron sputtering. The dielctric constant was improved by RTA and a maximum value (~100) was obtained at 700^{0}C[Fig.

1.25]. The effective value of dielectric constant is estimated using a two-capacitor model made of the film and the interlayer between the BST film and Si substrate.

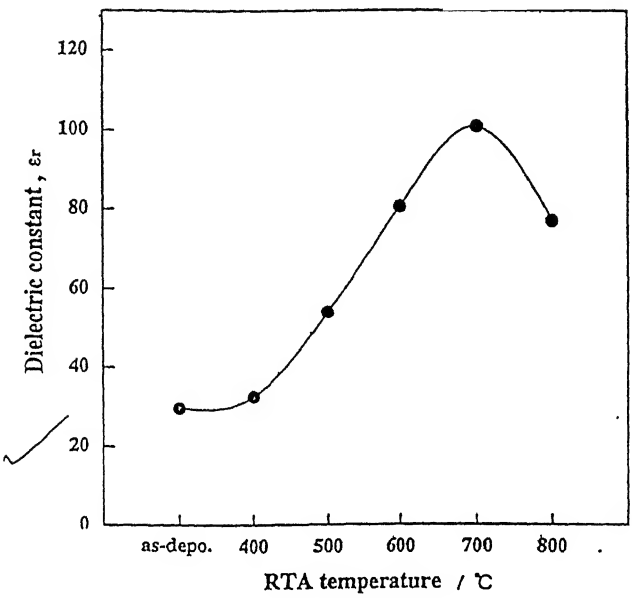

Fig. 1.25: RTA temperature dependence of dielectric constant

Jang et al[27] studied the electrical properties of a boron doped $(Ba_{0.5}Sr_{0.5})TiO_3$ thin films by a sol-gel method using an isopropoxide route. The variation of dielectric constant and dielectric loss with frequency and boron addition is shown in fig. . It is seen that the relative dielectric permittivity of the 250 nm thick BST film fired at 700^0C decreased with increasing boron content, from 420 for the undoped film to 190 for the 10 mol% boron-added film at 1 MHz [Fig. 1.26]. This observation was interpreted in terms

of a serial capacitance composed of the perovskite BST grain and the interfacial B_2O_3 glassy phase having a low dielectric permittivity.

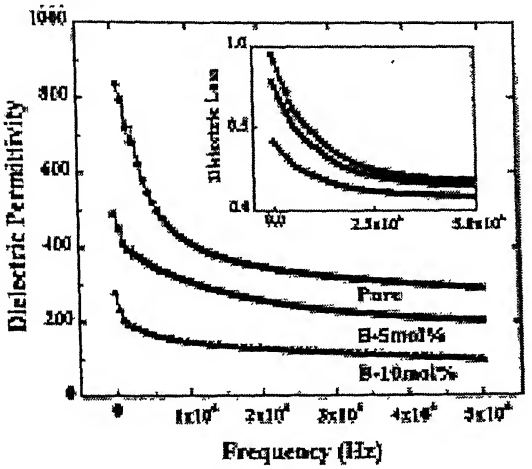

Fig. 1.26: Relative dielectric permittivity and the dielectric loss of BST thin films plotted as a function of the applied AC frequency. The thin films with a thickness of 250 nm were fired at 700^{0}C for 2 h.

1.9 Statement of the problem:

As discussed in the previous sections, thin films of BST are the potential candidates for device applications in the ULSI era. The quality of the films depend upon a series of interrelated factors like processing methods, film composition, crystalline structure, microstructure, surface morphology, film thickness, and electrode materials to name a few. In sol-gel processing, the chemistry of the precursor solutions plays an important role in determining the quality of the films. In the present work, the effect of different additives (acetyl acetone and DEA) on the evolution of phases especially in the formation of the intermediate phase(s) is proposed to be studied. The effect of additives on the microstructure and other dielectric and electrical properties are also to be investigated with a view to understand the underlying mechanisms.

Chapter 2

Experimental Procedure

In the present work thin films of barium strontium titanate (BST) of composition $Ba_{0.8}Sr_{0.2}TiO_3$ are prepared using a sol-gel method. First the details of the film preparation which includes preparation of the precursor sol, substrate preparation, film deposition, and heat treatment of the film are discussed. Then the characterization procedures used during the course of work including optical microscopy, scanning electron microscopy (SEM), thickness measurement, x-ray diffraction (XRD), and fourier transform infrared spectroscopy (FT-IR), thermogravimetric analysis (TGA) are described. Finally the dielectric measurements of the films using impedance spectroscopic techniques are described. For BST films various substrates are tried and the effects are reported in various papers and journal articles. They are noble metals (like Pt, Ir, and Ru), conducting oxides such as RuO_2, IrO_2, $BaRuO_3$, $YBa_2Cu_3O_7$, $SrRuO_3$ etc and silicon. Pt appears to be the material of choice for use as electrodes for BST capacitors due to its excellent electrical properties. In our laboratory we have used Si(100) n-type and p-type wafers, platinum, and glass substrates.

2.1 Sample Preparation:

Thin films and gel powders are made from BST sol of desired composition and concentration for different characterization studies. First the BST sol is prepared and used to coat different substrates. Si substrates were coated with Pt by sputtering prior to the film deposition. Pt coating on the substrate acts as the bottom electrode for the BST capacitor. After drying and gelling an amorphous film is formed. The film is then given

the proper heat treatment (annealing) in order to crystallize it. After that, the top electrodes of size 0.5 mm are deposited using a mask over this polycrystalline film. In this way a metal-insulator-metal (MIM) capacitor is made for the electrical characterization of the film. For the study of phase formation in BST, gel powders are made from the sol by keeping the sol in an oven at 120^0C for 12 hrs and then grinding it in an agate mortar. For the study crystallization by microwave, films were prepared on the glass substrate and films prepared on the uncoated Si (100) substrate was used for the studies on the crystallization of the film by hydrothermal method.

2.1.1 Sol Preparation:

2.1.1.1 Precursors: As mentioned earlier, a sol-gel method is used to prepare thin films of BST. The chemicals used for the preparation of BST sol is given in the Table 2.1.

Table 2.1: Chemicals used for the preparation of BST sol:

Serial number	Name of the compound	Molecular weight	Density (gm/cc)	Assay	Source
1.	Barium acetate	255.42	2.190	100%	Thomas Baker
2.	Strontium acetate	214.72	---	98.07%	Rolex Chem.
3.	Titanium butoxide	340.35	0.995	95.7%	Alfa Product
4.	Acetic acid (glacial)	60.04	1.049	99.8%	Thomas Baker
5.	2-Methoxyethanol	76.1	0.963	99.0%	S-d Fine Chem.
6.	Ethylene glycol	62.07	1.112	---	Nice Chem.
7.	Diethanolamine(DEA)	105.14	1.100	98%	S-d Fine Chem.
8.	Acetyl acetone	100.12	0.973	99.5%	S-d Fine Chem.

Six different sols of composition $Ba_{0.8}Sr_{0.2}TiO_3$ with and without different additives (acetyl acetone and DEA) and with the combination of different solvents (2-methoxyethanol and ethylene glycol) have been prepared. The concentration of the sol was kept around 0.20-0.25M.

2.1.1.2 Calculations:

To prepare a sol containing 0.01moles of $Ba_{0.8}Sr_{0.2}TiO_3$:

Ba-acetate required = 0.01×0.8×255.42 = 2.04336 gms/lit

Sr-acetate required = 0.01×0.2×214.72×100/98.07 = 0.43789 gms/lit

Ti-butoxide required = 0.01×1×340.35×100/95.7 = 3.55642 gms/lit

Density of Ti-butoxide = 0.995

Therefore, the volume of Ti-butoxide = 3.57429 ml/lit

Ratio of Ti-butoxide to additive is 1:2 (by mole)

$$\frac{\frac{Amount\_of\_additive}{Molecular\_weight\_of\_additive}}{\frac{Amount\_of\_butoxide}{Molecular\_weight\_of\_butoxide}} = \frac{2}{1}$$

We have used two different additives: acetyl acetone and DEA.

Amount of acetyl acetone = 2×3.55642×100.12/340.35 = 2.10 ml

Amount of DEA = 2×3.55642×105.14/340.35 = 2.20 ml

Total volume of the sol is made up either by the addition of acetic acid and 2- methoxy ethanol or by the addition of acetic acid and ethylene glycol in 3:1 ratio.

Concentration of the sol = 0.01×1000/Total volume of the sol (M)

Glassware used like pipettes, beakers, measuring cylinders, teflon coated magnetic beads are thoroughly cleaned with dilute nitric acid, then with a soap solution and finally with distilled water. For faster drying a quick rinsing of the glassware and bead with acetone is done before keeping in oven at 50°C for drying.

For the preparation of BST sol, Ba-acetate is taken as the Ba source, Sr-acetate as the Sr-source and Ti-butoxide as the Ti source. Acetyl acetone is used as the chelating agent. Acetic acid and 2-methoxyethanol are used as the solvent.

At first 2.0434 gms of Ba-acetate and 0.4379 gms of Sr-acetate are weighed and taken in a three necked flask containing a magnetic bead. Then 20 ml of acetic acid is added to it and the flask, fitted with one condenser system, is heated in an oil bath with constant stirring for 1 hr. The temperature of the oil bath is kept at 100^0C. After 1 hr of stirring 8 ml of 2-methoxyethanol is added and the solution is kept on stirring for another hr. Then 10 ml of acetic acid is again added to the solution and the temperature of the bath was lowered to 80^0C. Meanwhile in another 10 ml beaker inside the glove box (with the relative humidity level of 30%) 3.6 ml of Ti-butoxide is pipetted out from a measuring cylinder containing $\approx$ 4 ml of butoxide. The pipette is then washed with about 2 ml of 2-methoxyethanol and 2.10 ml of acetyl acetone is added to the beaker. The beaker is covered with an aluminum foil to avoid moisture absorption from the atmosphere. The mixture is then kept for stirring for 30 minutes inside the glove box. The butoxide solution is then taken out of the glove box, added to the Ba + Sr mixture and stirred for another 30 minutes at 80^0C in the oil bath. In this way a clear yellow in coloured BST sol is obtained. The sols where acetylacetone is not used are colourless.

Precautions to be taken in sol-preparation:

1. In order to obtain a sol with long shelf life, the glassware should be thoroughly cleaned and the Ba and Sr acetates should be completely dissolved in acetic acid before addition of Ti-butoxide in it. In order to dissolve acetates,

first the temperature of the oil-bath is increased to 110^0C. After dissolution of the salts the temperature of the bath was reduced to 100^0C.

2. Ti-butoxide is stirred inside the glove box at a relative humidity level ≤ 30%. This level is obtained by placing dried (at 120^0C for 10 hrs) silica gel inside the glove box for 3-4 hours. The low humidity level is needed as Ti-butoxide is highly hygroscopic and the sol gets gelled very soon when butoxide is kept outside for long.

2.1.2 Preparation of the substrates:

Substrates used in the present work are listed in the Table 2.2. Prior to film deposition the substrates are required to be optically or near optically flat. Substrates such as silicon(100) and (111) and quartz are already optically flat as received. However platinum required further polishing. The platinum substrates were first polished successively on 2/0, 3/0, and 4/0 emery papers to remove deep scratches. Finally they are mounted on a plastic stub and polished on a rotating velvet wheel with 0.05 μm alumina powder until mirror finish is obtained.

Table 2.2: Specifications of different substrates used for coating

Nature	Substrate
Single crystalline	Silicon(100)
Polycrystalline	Platinum
Amorphous	Sodalime glass slide

Before depositing the film, the substrates were cleaned thoroughly by the procedure described below.

1. Ultrasonicated in acetone for 5 minutes.
2. Ultrasonicated repeatedly in distilled water for 5 minutes.
3. Ultrasonicated in trichloroethylene for 5 minutes.
4. Dried in air and kept in sealed plastic containers.

2.1.3 Film Deposition:

The sol was coated on to the substrate by spin coating technique. Spin coating technique involves simple fluid flow and evaporation behaviours that generally give uniform coating. The films were deposited using a DUCOM (Bangalore) photoresist spinner. The substrate was fixed at the centre of the rotating vacuum chuck. This chuck has a small hole (~ 2 mm diameter) in its centre which is connected to a vacuum pump. When the LED glows, the required vacuum is created at the hole and the substrate is held firmly on the chuck. A dropper was used to drop ~0 05 ml sol onto the substrate during the initial few seconds of spinning. The sol immediately spreads on the substrate and a gel film is produced. The photoresist spinner was typically operated at 3000 rpm for 30 seconds duration. After each coating the film was dried in a quartz tube furnace at 200^0C for 2 minutes. Total number of coatings varied from 5 to 25 in order to obtain different thickness for different characterization study. Generally, 15 coatings of the sol on Pt substrate resulted in a film of 1.0 μm thickness. Initially Si-substrates coated with platinum by sputtering were used for film deposition. But XRD did not show any well developed BST peaks except for the Pt peak. After annealing to 650^0C films became conducting so they could not be used for electrical characterization. Use of Pt substrates are recommended for electrical characterization.

2.1.4 Heat treatment of the films:

The as deposited film contains large amounts of organics. Large shrinkage occurs during the heat treatment due to removal of the organics. Crystallization may start before the organics are completely removed, and sintering and crystallization process may also overlap. Thermal analysis such as differential thermal analysis (DTA), thermogravimetric analysis (TGA) and infrared spectroscopy (IR) are useful characterization tools to identify the physio-chemical changes that occur during the heat treatment of the films. Since the material content of the film is extremely small, the signal obtained is often beyond the detection limits of these techniques. To overcome this problem we have dried the coating sol at 120^0C overnight to prepare a gel powder of same composition. The gel-derived powder is ground in a mortar pestle to form fine powder. This powder is then used for further study. The heat treatment of the film and powder is performed in a quartz tube furnace equipped with a controller. A chromel-alumel thermocouple is kept close to the sample to monitor the process temperature. Typical heating rate used is 5^0C/min. Samples were also "rapid heated" by inserting the sample (kept on a quartz boat) directly in the furnace at a preset temperature. After holding in the furnace for required time, the sample is quenched to room temperature. Very high heating and cooling rates (~100^0C/min) can be achieved by this technique. It was observed that films were not able to sustain such treatments as this process of rapid heating generated cracks. Thus they cannot be used for characterization.

The process of film preparation is summarized in the flowchart in Fig. 2.1.

Fig. 2.1: Flowchart for preparation and characterization of BST film and gel powder

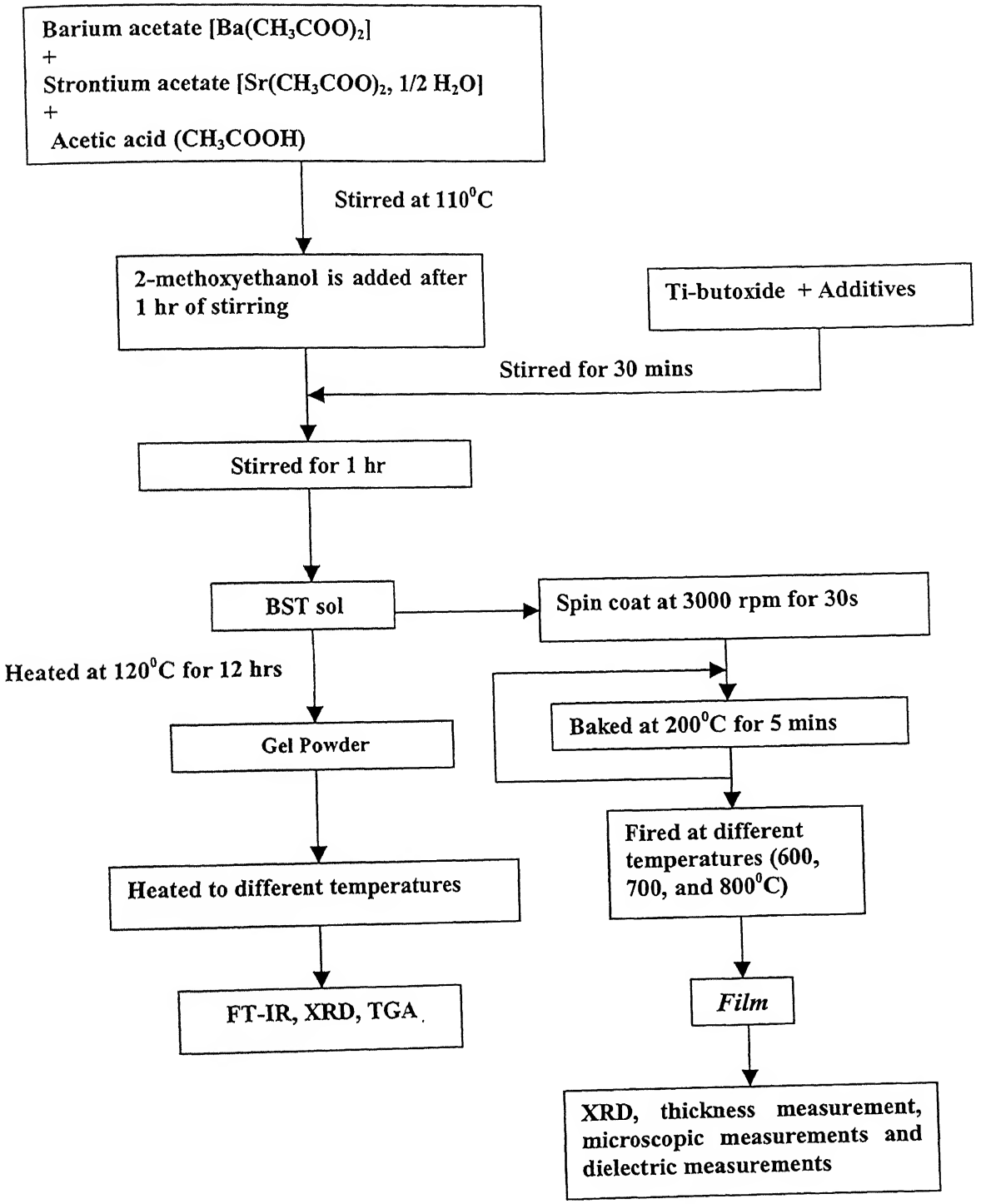

2.1.5 Sample preparation for microwave treatment of films:

For microwave treatment the films were prepared on a sodalime glass and Si substrates. The films were then put inside a glass petri-dish and kept inside an ordinary kitchen microwave oven (2450 MHZ, 1350W+/- 10%, BPL, India). Films were treated for different durations inside the microwave oven. A different configuration is used when the film is heated radiatively through graphite susceptors [Fig. 2.2]. Use of a thermocouple to measure the temperature was not successful due to generation of sparks for the thermocouple tip by the incident microwave radiation.

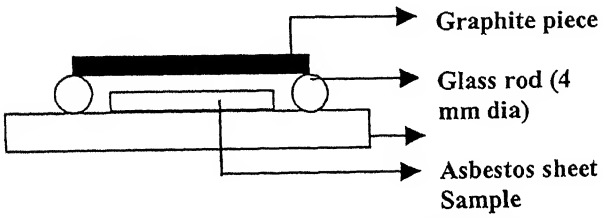

Fig. 2.2: Arrangement for heating the films radiatively using graphite susceptors

2.1.6 Hydrothermal crystallization:

Hydrothermal crystallization experiments were performed in sealed quartz tubes. The sample was prepared with 20 coatings of the sol on Si-substrates, each coating dried in the furnace at 200^0C for 1 hr. Some films were given an additional heat treatment at 350^0C for 1 hr in the furnace for better adherence with the substrate. A calculated amount of water (in some cases dilute NH_4OH with different concentration) were put into a quartz tube containing the sample. The tube was sealed and then put in a wrought iron tube. For experimental conditions involving temperature >150^0C, the wrought iron tube with the sealed quartz tube inside was placed at the centre of the furnace muffle. For

experiments involving temperature <150^{0}C, the sealed quartz tube was kept inside the preheated oven for required time. The different conditions used for hydrothermal treatment are tabulated below in Table 2.3.

Table 2.3: Details for hydrothermal experiment

Medium	Conditions (Temp/Press)	Time	Equipment used	Condition of water
Water	320^{0}C/2MPa	3 hrs	Furnace	Superheated steam
0 5 M NH_4OH	250^{0}C/2 MPa	3 hrs	Furnace	Superheated steam
1M NH_4OH	150^{0}C/not considered	6 hrs	Oven	Subcooled liquid
0.2M NH_4OH	150^{0}C/not considered	6 hrs	Oven	Subcooled liquid
0.2 M NH_4OH	150^{0}C/not considered	30 min	Oven	Subcooled liquid

Calculation of the amount of water/alkali:

The amount of water to be added is calculated using steam table software (Archon Engg., Demo version 5.0). Knowing the temperature and pressure, the specific volume i.e., the volume of the quartz tube after sealing is obtained (an allowance of 1 cm in the length of the tube is given for sealing). The different values used are tabulated below in Table 2.4.

Table 2.4: Calculation of the amount of water/alkali

Conditions Temp/Pressure	Available volume (cc)	Specific volume (cc/gm)	Mass (gms) Calculated	Mass (gms) Actual
320^{0}C / 2 MPa	33.08	130.8	0272	0.27
250^{0}C / 2 MPa	30.54	111.4	0.274	0.27
150^{0}C / not accounted	27.99	1.1	25.447*	12.7
150^{0}C / not accounted	38.17	1.1	34.70*	17.3

*In these cases the actual amounts taken are 12.7 and 17.3 gms respectively; the pressure is not calculated from the steam table.

2.2 Characterization of the films and gel powder:

2.2.1.Optical Microscopy:

After drying, the films are examined in an optical microscope (Carl Zeiss, Germany) under reflected light at ×100 and ×200 magnifications. Presence of any cracks after drying can be easily detected at these magnifications.

2.2.2 Scanning electron microscopy (SEM):

The presence of cracks, voids etc in the film as well as the grain size and other microstructural features of the films are studied by a scanning electron microscope (JSM 840A, JEOL, Japan). The insulating film cannot be directly observed under SEM due to electron charging effect. For this pupose the film surface is coated with a thin metal (Au-Pd) layer. The electroded film is fixed on the top of a 1cm cylindrical brass stub and observed under SEM. The typical operating conditions of the SEM are given in Table 2.5.

Table 2.5: Operating conditions for SEM

Acceleration Voltage	10-15 kV
Probe current	0.3 nA
Working distance	7-15 mm
Magnification	4000 - 20,000 ×

2.2.3 Thickness and surface roughness measurements:

The thickness and surface roughness of the film after the heat treatment are measured by a surface profilometer (Alpha step-100, Tencor Instruments, USA). This instrument requires a sharp step between the film and the substrate to measure film thickness. Since spin coating uniformly covers the substrate, a small part of the film is wiped off after deposition from the substrate by a mild etchant after each coating. A blade is kept vertically over the film each time at the same place (position is is kept fixed by observing under an optical microscope) and by brushing off the film with the etchant carefully so that no etchant seeps through the bottom edge of the blade.

Preparation of the etchant: The etchant solution is prepared by adding 2ml of HNO_3, 10ml of distilled water and 10 ml of ethyl alcohol together in a 25 ml beaker. The solution stored in a plastic container.

During thickness measurement the stylus of the surface profilometer first scans the bare substrate and then scans the film surface through the sharp edge. The difference in height between the two in the profilograph yields the film thickness. For a baseline correction, the step up (⇑) or step down (⇓) button is pressed a number of times as needed. A chart recorder produces the output of the measurement. To measure the surface roughness of the film the stylus is scanned on top of the film surface and the roughness is read from the profilograph output.

2.2.4. X-ray diffraction (XRD) study:

The X-ray diffraction technique has been used to analyze the phases and to determine the crystal structure, lattice parameter and the crystallite size of the phases present in the film.

2.2.4.1 Phase analysis:

Phase analysis is carried out for the thin films derived from different sols and gel derived crushed powder of the same composition of the sol. X-ray diffraction patterns are recorded by a fully computerized X-ray diffractometer (Rich Seifert Iso-Debyeflex-2002, Germany). CuK_α radiation (λ = 1.5405 Å) is used with a Ni monochromator for probe. The following operating conditions have been used.

Table 2.6: Operating parameters for X-ray diffractometer

Accelerating voltage and current	30kV, 20mA.
Scanning speed (SS)	3^0/minute
Counts per minute(CPM)	5k
Time constant	10 seconds

The substrate coated with the film is held in a Perspex holder with small amount of plasticine. The sample is made horizontal by pressing it down lightly with a glass slide. The powder samples are spread evenly on the surface of a glass slide with the addition of a few drops of acetone so that the powder sticks to the glass slide.

The X-ray diffraction plots (intensity vs 2θ) of the samples are recorded in the 2θ range from 20^0 to 60^0 with the step size of 0.05^0. The 2θ values and the corresponding relative intensities are compared with the standard data for determination of phase or phases present.

BST crystallizes in perovskite form. The interplaner spacing 'd' is noted from the data of the diffractogram. For BST composition $Ba_{0.8}Sr_{0.2}TiO_3$ the structure is tetragonal. The standard data was not available for this composition. So the data from the diffractogram given in Ref. 30 is read using Tracer 1.5 software. The data in reference

shows splitting of (001) and (200) lines, which is a sign of obvious teragonality. Our system was not precise enough to detect the splitting clearly. A slow scanning (0.3^0/min) was tried but the noise level was so high that the peaks could not be distinguished. The data was not accurate enough to calculate the lattice parameter and crystallite size.

2.2.5 Fourier Transform Infrared spectroscopy (FT-IR):

The broadband spectra like Raman and IR are presently becoming more popular as the useful tools to study the structural aspects of the material under study, which are sensitive to compositional variations. Infrared spectroscopy, in particular involves the absorption of electromagnetic radiations by matter, the existence of which is known since a long time with the discovery of Sir William Herschel in 1800[28]. Today Infrared spectroscopy ranges approximately from *0.78 μm* ($1/\lambda = 12500cm^{-1}$) to *1000 μm* ($1/\lambda = 10cm^{-1}$). However the most useful range is from *2 μm* to *16 μm*. The absorption bands, which occur in this region, are due to the fundamental molecular vibrations. IR technique is used for the identification of specific functional groups especially in organic molecules or covalently bonded groups such as hydroxyl, carbonate, trapped water etc in inorganic solids.

It is well-accepted fact that the matter absorbs infrared radiation selectively with respect to the wavelength. The two necessary conditions, which must be met before the absorption of infrared radiation by the molecule can occur, are

1) There must be a change in dipole moment of a molecule, and this will occur only when the electrical charges on the atoms are unequally distributed. Under these conditions, a stationary alternating electric field is produced whose magnitude

changes with the frequency; and it is this electric field which interacts with the field of electromagnetic radiation.

2) The molecular vibration frequency must be identical to that of incident electromagnetic radiation, failing which the radiations transmit through the molecule without any loss of energy.

As a result, when infrared radiations of successive frequencies are passed through the molecule and the fraction of transmitted energy is plotted against the frequency or wavelength, the result is a series of minima and maxima, which is referred to as an infrared absorption spectrum. The absorption or transmission of this electromagnetic energy is dependent on the number of atoms, their mass, their way of stacking in the material and the force constant of interatomic bonds. The vibrations between various atoms within the molecule could be described as stretching vibrations, bending vibrations, involving groups of atoms within the molecule and the vibrations of the molecule as a whole. These vibrations can occur at various frequencies and are characteristics of groups of atoms within the molecule. Thus, absorption peaks at various wavelengths are correlated with the molecule, using which, the structural studies can be carried out. The depth of the absorption bands is directly related to the number of molecules in the beam of radiation, and this feature is often used for qualitative measurements.

The Fourier Transform Infrared Spectroscopy (FT-IR) studies were carried out with a spectrophotometer model Vector-22 (Bruker) in the range *400-4000cm*$^{-1}$. BST gel powder is mixed thoroughly with KBr powder and pressed in a 0.5 mm thick pellet of 1

cm diameter. The pellet is inserted into the sample holder and IR absorption is recorded. A pure KBr pellet of same size and thickness is used as reference.

2.3.6 Thermogravimetric analysis (TGA):

In the present work TGA has been carried out in order to identify the thermal decomposition, solid-state reactions and phase transition of BST gel powder during heating. In TGA % weight of the sample is recorded as a function of heating temperature. Gel powders made from the sols are used as samples for TGA. A small amount of powder (W_1) is taken in a platinum crucible, which is hung from an electronic balance (ER-100A, Afcoset, India), into an electrically heated vertical furnace. The sample is heated at a constant rate of 5^0C/min. The weight of the sample (W_2) is recorded as a function of temperature from room temperature to 900^0C. The weight percent of the sample, $\frac{W_1 - W_2}{W_2} \times 100$ Vs temperature (T) yields the TGA plot.

2.2.7 Electrical measurements:

2.2.7.1 Sample configuration:

For all the electrical measurements films are deposited on polished platinum plates. After annealing, 0.5 mm diameter dot electrodes are deposited through a mask. The electrodes are of gold-palladium (Au-Pd) deposited by d.c. sputtering. The thickness of the electrodes is estimated to be 1000Å. The sample configuration is shown in Fig. 2.1. After top electrode deposition the films are heated to 300^0C for 10 minutes to impart better adhesion between the electrode and the film surface.

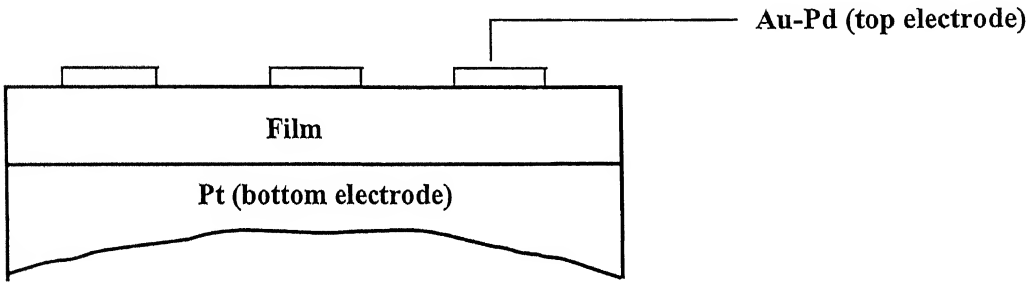

Fig. 2.3 Sample configuration for electrical measurement

2.2.7.2 Top electrode deposition:

Hummer (VI-A) sputtering unit (Anatech Limited) with Au-Pd target in a shape of circular disc is used to deposit top electrode of Au-Pd on ceramic thin films. A mask with several circular holes (~ 0.5 mm diameter) is kept on the films. So only the spare small circular areas is deposited with Au-Pd thin films. The steel substrate is conducting and acts as bottom electrode.

For sputtering, following conditions are used:

Vacuum in sputtering chamber = 80 mT (milliTorr),

Plasma discharge current = 10 mA (milliAmpere),

Voltage control setting = 3.5 to 4.5,

Total time for sputtering = 15 to 20 minutes.

2.2.7.3 Sample holder:

Fig 2.3 shows the schematic diagram of the sample holder used for electrical measurements. A mica-sheet is wound with a heating coil and positioned between two stainless steel plates, insulated from the coil. The top stainless steel plate is partly covered with a silver foil of about 0.2 mm thick. Two adjustable silver probes, insulated from each other are fixed on the top plate. A chromel-alumel thermocouple is also kept in the close proximity of the probe to monitor the sample temperature during high temperature measurements. In the present work only room temperature measurements were carried out.

2.2.7.4 Impedance analyzer:

An impedance analyzer (Model HP 4292A LF) with a HP 1607A test fixture is used for electrical measurements. The impedance Z, phase angle θ, dielectric loss (D) and capacitance (C) of the films are measured as a function of frequency between 100 Hz to 13 MHz. The built in frequency synthesizer is used to generate frequency in the range of 5 Hz to 13 MHz with 1 mHz resolution. The a.c. voltage peak amplitude and the frequency range over which measurements are desired are set while calibrating the instrument. There are two display modes 'A' and 'B', which can be selected to measure the desired quantities.

Table 2.7: The displays 'A' and 'B' of impedance analyzer

Display 'A' Function	Display 'B' Function
|z| : Absolute value of Impedance |Y| : Absolute value of Admittance	θ (deg/rad) : Phase Angle
R : Resistance	X : Reactance
G : Conductance	B : Susceptance
L : Inductance C : Capacitance	Q : Quality factor D : Dissipation factor R : Resistance G : Conductance

The equivalent modes are auto, 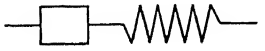 (series) and

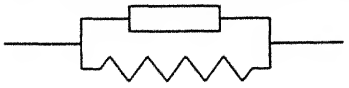 (parallel).

For dielectric measurements, the display can be set to 'C' and 'D' to calculate dielectric constant (k). These measurements are done as a function of frequency.

2.2.7.5 Dielectric constant and dielectric loss measurements:

The dielectric properties such as dielectric constant, dielectric loss factor, dielectric resistivity, dielectric strength and magnetic permeability are very useful for ceramic applications. The capacitance (C) and dielectric loss factor (D) are measured directly by impedance analyzer for all the samples. The thin film sandwiched between the top and bottom electrodes acts as a parallel plate capacitor.

The capacitance of the dielectric/ceramic materials is given by

$$C = \varepsilon_o \varepsilon_r \frac{A}{d} \qquad \text{---------- (5)}$$

where, ε_o = permittivity (dielectric constant) of free space (vacuum),

ε_r = dielectric constant of the film,

A = area of the top electrode,

and, d = thickness of the thin film.

From equation (5),

$$\varepsilon_r = \frac{1}{\varepsilon_o}\left(\frac{C \times d}{A}\right) \qquad \text{---------- (6)}$$

Hence, ε_r is calculated in the frequency range of 10 kHz to 13 MHz for all the samples at room temperature. The dielectric loss is directly read from the impedance analyzer.

भारतीय ... 143521

Results and Discussions

This chapter deals with the experimental results on the structural and electrical properties of the BST thin films made by sol-gel route. The BST films are made with different additives and solvents and characterized with respect to their phases, microstructure, and electrical and dielectric properties. Thermogravimetric analysis (TGA), X-ray diffraction (XRD), and fourier transform infrared spectroscopy (FT-IR) are used to obtain the structural information on BST films and gel powders. The dielectric properties of the film are studied through complex impedance analysis (CIA). Results are presented in three sections.

1. Studies on intermediate phase
2. Studies on the crystallization by unconventional method (microwave and hydrothermal)
3. Structural and electrical properties of thin film samples.

TGA results are presented first, followed FT-IR and XRD results. Then the results of the studies on the crystallization by microwave and hydrothermal method are discussed. Data on the microstructure and physical properties of the film are presented next. The dielectric and electrical properties of the film obtained from the complex impedance analysis are discussed thereafter. The results have been discussed and compared in light of the existing data given in the recent literature.

3.1 Studies on the intermediate phase of BST:

In the sol-gel processing of BST films precursors are Ba - acetate and Sr - acetate dissolved in heated acetic acid and Ti - butoxide. The precursors react to form a sol of barium strontium titanate (BST). The sol is used to coat the substrates. The as - deposited films are amorphous and need to be annealed at 600^0 - 700^0 C to form the crystalline perovskite phase. It is believed that the crystallization to the final perovskite phase proceeds via the formation of one or several intermediate phase(s). The crystallization behavior, phase formation and microstructure evolution in BST films depends upon a series of interrelated factors like sol concentration, thickness of the films, nature of substrates, effect of annealing temperature, annealing atmosphere, post - annealing treatment and use of different additives. The aim of the present study is to investigate the effect of different additives like acetylacetone, DEA and ethylene glycol on the structural and electrical properties of BST thin films and evolution of intermediate phase(s). Efforts are made to find out the structural information by a systematic study carried out for thin films and gel powders prepared from sols with different additives as tabulated in Table3.1.

Table 3.1: Specification of the gel powders made from sols of different additive

Sample name	Additive used	Solvent used
SWA	None	Methoxyethanol/acetic acid
FS	Acetylacetone	Methoxyethanol/acetic acid
SDM	DEA	Methoxyethanol/acetic acid
SWG	none	Glycol/acetic acid
SEG	Acetylacetone	Glycol/acetic acid
SDM	DEA	Glycol/acetic acid
OS	Acetylacetone	Glycol/acetic acid

All the sols are of composition $Ba_{0.8}Sr_{0.2}TiO_3$. The gel powders made from the sol are heated to different temperatures from 200^{0}C to 800^{0}C. The results are summarized below.

3.1.1 Thermogravimetric Analysis (TGA):

Figure 3.1 show the TGA plots for three different samples with acetylacetone, without additive and with DEA respectively. In all the samples weight loss occurs in three distinct steps. First one occurs between 50 - 150^{0}C, second one between 225-400^{0}C and the last one occurs between 600 to 700^{0}C. The TGA curves show a small weight loss of about ~10% between 50 and 200^{0}C which corresponds of absorbed water, a major weight loss (~25%) between 300^{0}C and 400^{0}C, which is probably due to drastic removal of carboxylic groups and their combustion [29] and a weight loss (~13%) in the range of 600 - 690^{0}C. In case of sample with acetylacetone the weight loss between 300^{0}C - 400^{0}C is more gradual compared to the other two. So it can be said that the addition of acetylacetone slows down the weight loss due to organic burn out and it is expected in case of BST film it will minimize cracking. It appears that the removal of organics is more difficult when an additive is used and the organics may not be getting removed completely even upto 900^{0}C.

3.1.2 FT-IR analysis:

The FT-IR absorption spectra from gel powders made from the sols of different compositions were obtained. The powder is made by keeping the sol at 120^{0}C in an oven for 12 hrs. The resulting gel powder is ground in an agate mortar. Pellets of the powder were made in KBr in the ratio of 1:30 and the FT-IR spectra were obtained using a spectrometer model vector-22 (Bruker) in the range 400 - 4000 cm $^{-1}$.

The absorption spectra of gel powder made from the sol with 2-methoxyethanol and without any additive and heated to 400^0C, 500^0C, 650^0C and 800^0C each for 1 hr are shown in figure 3.2. A broad peak ranging from 1700 - 950 cm^{-1} appeared with maximum at 1430 cm^{-1} for the sample heated at 400^0C for 1 hr. On heating to 500^0C the peak shifts to 1440 cm^{-1} indicating the formation of carbonates [17]. On further heating to 650^0C this peak shifts to 1441.31 and some strong peaks appear between 650 - 430 cm^{-1} indicating the onset crystallization. On further heating to 800^0C the CO_3^{2-} peak shifts 1444.38 cm^{-1} and becomes much weak in intensity.

A prominent hump at 3446.09 cm^{-1} due to hydroxyl (-OH stretch) is observed for the sample heated at 400^0C. This peak decreases in intensity with increase in treatment temperature.

In figure 3.3 spectra for the gel powder made from sol with 2-methoxyethanol and acetylacetone as additives are shown for three different temperatures 400^0C, 500^0C and 650^0C. A peak corresponding to carbon - oxygen stretch in organic acids (C-OH) appeared at 1432 cm^{-1} for sample heated at 400^0C. On heating to 500^0C the peak shifts towards lower wave number i.e., 1429 cm^{-1}. This peak is broader but much less intense. On further heating to 650^0C this peak shifts towards even lower wavenumber (1425cm^{-1}). No characteristic peak for carbonates (1440-1450 cm^{-1}) was observed for these samples.

In figure 3.4 the spectra for gel powder made from sol with 2-methoxyethanol and DEA as additive are shown for three different temperatures 400, 500 and 600^0C. All of them showed the presence of CO_3^{2-} peak around 1441 cm^{-1} and a broad hump for hydroxyl (-OH) stretch.

Figure 3.5 presents the spectra of gel powder of sol made with ethylene glycol and without any additive at 400^0C, 500^0C and 650^0C. A sharp peak at 1437 cm^{-1} is obtained which shifts to 1438 cm^{-1} and 1434 cm^{-1} with heating to higher temperature.

In figure 3.6 the spectra for gel powder of sol with ethylene glycol and acetylacetone as additive are shown. At 400^0C a peak corresponding to 1436 cm^{-1} appeared which shifted towards lower wave-numbers i.e. 1435 cm^{-1} (at 500^0C) and 1431 cm^{-1} (at 650^0C) indicating C-OH stretch of organic acids[30]. At 800^0C no peaks in the concerned region (1400 - 1700 cm^{-1}) are observed.

Figure 3.7 represents the spectra of gel powder made from sol with ethylene glycol and DEA. For 400^0C a sharp peak corresponding to wavenumber 1438 cm^{-1} appeared. On heating further to temperatures 500^0C and 600^0C the peak position did not change much (1437.37cm^{-1} for 500^0C and 1438.68cm^{-1} for 600^0C). For all these samples an hump corresponding to hydroxyl (-OH) stretch is also observed.

Figure 3.8 represents the spectra for the gel powders of an aged sol containing methoxyethanol and acetylacetone. The sol was aged for 30 days at room temperature and then gelled into powder as before. In these powders, a broad absorption peak due to hydroxyl (-OH stretch) is observed at wave number 3356 cm^{-1}. This peak decreases in intensity with increase in treatment temperature but may still be very weakly present after treatment at 650^0C. A distinct peak at 1442 cm^{-1} remains after the heat treatment at 650^0C in addition to several strong peaks below 670cm^{-1}. The position of the peak shifts towards the lower wave numbers as the treatment temperature is lowered. At 200^0C there is a broad peak between 1800-1500cm^{-1}. It appears that the peaks are due to the asymmetric carboxylate stretch of CO_2^- [30] and also due to C-OH stretch from the acetic acid. As the temperature is increased, the antisymmetric CO_2^- stretch disappears and finally at 500^0C

the peaks due to acid totally disappear and carbonate (CO_3^{2-}) peak appears. On heating to 800^{0}C the peak corresponding to carbonate disappears.

From the above results, it is seen that in some cases a peak at ~1440 cm^{-1} corresponding to CO_3^{2-} is present. On heating, this peak either remains unchanged or shifts to slightly higher wave numbers. This agrees with the position of the peak in the range 1440-1450 cm^{-1} reported for carbonate group [16]. In the other sample a peak is present at ~1435 cm^{-1} and its position shifts to the lower position. This corresponds to C-OH stretch.

As the peaks observed are somewhat broad and the position of the two sets of peaks are close to further clarify the matter, the peaks for samples treated at 500^{0}C were resolved into individual peaks by peak fitting (Peakfit 4.0). The results are shown in Fig. 3.9 and tabulated in Table 3.2.

Table 3.2: Consolidated data of the peak-fitting results

Additives to the sol/Temperature	Peak positions	Peak Intensity	Identification
None/500^{0}C	1442.7 1335.3	100% 26.77%	$-CO_3^{2-}$ $-CH_2-$
Acetylacetone/500^{0}C	1468.75 1426.56 1350.00	12.7% 100% 21%	$-CH_3$ -C-OH $-CH_2-$
DEA/500^{0}C	1561.65 1443.41 1339.45	1.98% 100% 14.05%	$-CO_2^-$ $-CO_3^{2-}$ -CH
Ethylene glycol/500^{0}C	1442.1	100%	$-CO_3^{2-}$
Ethylene glycol, acetyl acetone /500^{0}C	1466.42 1432.38 1383.83	45.54% 100% 9.5%	$-CH_3$ -C-OH $-CO_2^-$
Ethylene glycol, DEA/500^{0}C	1501.01 1437.01 1348.07	13.2% 100% 9.29%	- $-CO_3^{2-}$ -CH
Acetylacetone(aged sol)/500^{0}C	1442.7 1355.3	100% 26.77%	$-CO_3^{2-}$ $-CH_2-$

an additive to the sol, the hydrolysis and condensation reactions are slowed down and no segregation of different ions occurs. This avoids the formation of the intermediate carbonate phase.

3.1.3 X-ray diffraction analysis:

X-ray diffraction is carried out on the gel-powder samples made from sols containing different amounts of additives and solvents and heated to different temperatures in order to get information about the phases present and formed during the course of heating to higher temperatures for crystallization. Figure 3.10 shows the XRD patterns of the gel powder made from a sol containing methoxyethanol but without any additive. The x-ray peak for $BaCO_3$ is expected at $2\theta = 24.68$ and for oxycarbonate is at 27.0^0 [1]. The high intensity broad hump at $\theta = 20^0 - 30^0$ after 400^0C treatment [Fig. 3.9 (a)] is indicates the presence of a carbonate/oxycarbonate phase. A broad peak at 24.5^0 superimposed on this hump appears at 450^0C. At 500^0C the hump height decreases, the carbonate peak disappears and many peaks correspond to BST appear. At 600^0C the hump is almost gone and 5 distinct BST peaks are present. After the 650^0C treatment, the peaks become sharper. The XRD patterns are shown for the samples made from sol with acetylacetone and methoxyethanol in Fig. 3.11. It is observed that at 400^0C BST the peaks start appearing alongwith a broad hump in the range $20 - 30^0$. It seems that there is a peak superimposed on that hump at 24.2^0 value of 2θ. On heating to 500^0C the BST peaks get sharpened but a peak at 23.98^0 remained which does not match with either $BaCO_3$ or oxycarbonate peak. Such a peak has also been reported by Ding et al[10]. They attributed it to an unidentified intermediate phase, possibly $(Ba_2Sr)TiO_2CO_3$. Further heating to 600,650, 750^0C reduce the intensity of this peak (around 24^0) and BST peaks get stronger. After heating to 750^0C only the peaks corresponding to the perovskite phase

of BST are present. The composition corresponding to $Ba_{0.8}Sr_{0.2}TiO_3$ is expected to crystallize to a tetragonal phase. The XRD pattern of a tetragonal phase as characterized by the splitting of the (100) and (200) peaks. It can be seen that the (200) peak is asymmetric. Fig.3.12 shows a slow scan plot of the peak. The composite peak can be resolved into in to two peaks in peak fitting. In this case, the noise level was so high that the peak fitting gave many peaks rather than two distinct peaks. The XRD patterns for the sample with and without acetylacetone and with glycol are shown in figures 3.13 and 3.14 respectively. It can be concluded from these graphs that the samples made with acetylacetone crystallize at comparatively lower temperature than that made without acetylacetone. The sample made without acetylacetone shows the presence of additional peaks even at the temperatures of 650^0C. In case of samples made from aged sol with acetylacetone (fig. 3.15) showed well-crystallized BST phase from 500^0C onwards.

In figures 3.16 and 3.17 the results of XRD are shown for the samples made using DEA and methoxyethanol and DEA and glycol. The samples with methoxyethanol started crystallizing from 500^0C. At 400^0C some peaks corresponding to $BaCO_3$ and $SrCO_3$ were observed. Heating to 500^0C replaced those peaks by BST peaks. On further heating to 600^0C intensified the BST peaks. But for the samples with DEA and glycol till 600^0C some additional peaks were observed. The overall pattern is altogether different from the conventional BST peaks specially around $2\theta = 42 - 48^0$. The additional peaks can be identified as $BaCO_3$ and $SrCO_3$ peaks.

Discussions:

As seen in the FTIR data that CO_3^{2-} peak starts appearing in samples heated to 500^0C/hr when no acetylacetone is used. On the other hand, the XRD plots show that there exist some broad peaks in the region $\theta = 20^0 - 30^0$. When heating to higher temperature some

distinct peaks superimposed on this broad hump start appearing. These peaks neither correspond to $BaCO_3$ (24.68^0) nor oxycarbonate (27^0) peaks. So it is difficult to draw any conclusion from the XRD data about the intermediate phases. But in case of the samples with DEA the $BaCO_3$ and $SrCO_3$ peaks appeared which corresponds well with the FT-IR data. So it can be concluded that XRD was not sensitive enough to detect that the carbonate phases present in the BST, which was detected by FT-IR. Although there is no clear - cut indication about the presence or absence of carbonate phases from XRD, it is evident that in case of the sample with acetylacetone BST peaks starts appearing from 400^0C itself, which is unique and not seen in any other samples. Use of ethylene glycol in the sol improves the situation further, as when glycol is used peaks of BST become even stronger. Thus use of acetylacetone and glycol in the sol reduces the crystallization temperature of BST in its perovskite phase.

3.2 Studies on the crystallization of BST thin films by microwave radiation and by hydrothermal treatment:

Conventionally, the as deposited amorphous films are crystallized by means of IR i.e., by heating inside a conventional furnace to high temperature (650^0C). In this work two unconventional methods for crystallizing BST were also tried

i) Crystallization using microwave energy and

ii) Crystallization by hydrothermal method.

These are discussed below.

3.2.2 Crystallization using microwave energy:

The use of microwave energy for material synthesis and processing is a rapidly expanding field. Rapid sintering of ceramics using microwave energy offers many advantages over the conventional heating techniques. Fine grain size, high toughness and substantial energy saving have been achieved by microwave sintering[31]. So far, there is no report on the crystallization of thin films by microwave energy. In our lab using an ordinary kitchen microwave (2450 MHz, 1350W ± 10%, BPL, India) experiments were performed on crystallization of the BST film. Films on glass and silicon substrates are used for this study. Use of microwave in full power for 15 minutes also did not result in crystallization. Use of graphite susceptors for both the substrates did not result in crystallization [Fig. 3.18 (a) and (b)]. Thus the film is not getting heated to high enough temperature by the microwaves required for crystallization. Fig. 3.19(a) shows the FT-IR spectra of a gel powder subjected to same microwave treatment as the film.Fig 3.19(b) shows the FT-IR spectra of the same gel powder heated to 200^0C in the conventional manner. The spectra for the samples heated at 200^0C/ 1hr and treated in microwave for 15 minutes yield very similar graphs. Thus it can be concluded, with the existing set-up in the lab is not possible to crystallize the film. Either the microwave should be guided or a suitable susceptor should be used to heat the film rapidly. Moreover the auto cut-off circuit inside the microwave oven should be removed in order to get radiation continuously for a longer duration.

3.2.2 Crystallization using hydrothermal method:

Hydrothermal processing is a technique where high temperature and high pressure aqueous solutions, vapours and or fluids react with solid materials in order to yield new

or modified products[32]. But the temperature used in the hydrothermal technique is much lower compared to that used in the conventional sintering or calcination processes. Efforts were made to crystallize BST films on silicon by hydrothermal technique in the laboratory. Different temperature, pressure and medium for hydrothermal technique were used for different duration ant the results are tabulated below. The experiments regarding crystallization by hydrothermal technique was a failure, as the films did not crystallize by the conditions used in the present work. The gist of hydrothermal experiments and results are given in Table 3.3.

Table 3.3: Excerpts of the experiments on hydrothermal crystallization

Expt No.	Sample specification	Medium of hydrothermal treatment	Conditions for hydrothermal treatment	Film morphology	Remarks
1	20 coats of BST on Si, each coating dried at 200^{0}C for min in furnace	Water (0.27 ml)	320^{0}C, 2MPa, 3 hrs.	No apparent change in film morphology	Alkaline medium instead of pure water and a lower temperature (250^{0}C) is to be tried.
2	Same as the above	0.5M NH_4OH (0.3 ml)	250^{0}C, 2MPa, 3 hrs.	Film became white in colour cracks are developed.	Film did not crystallize. Only a Si peak at 28.45 is observed.
3	A sample treated by expt. 1 annealed in furnace at 650^{0}C for 1 hr.				The film did not crystallize. Perhaps the film gets removed/dissolved during the hydrothermal treatment.To avoid removal of film during hydrothermal treatment, the film is to be heated to an intermediate temp. of 350^{0}C for 1 hr.

Expt No.	Sample specification	Medium of hydrothermal treatment	Conditions for hydrothermal treatment	Film morphology	Remarks
4	Si coated with BST sol (25 times). Each coat dried at 200 ^{0} C for 2 min then treated at 350^{0}C/hr	NH_4OH (1M) (12 ml)	150^{0}C, 6 hrs ~1 MPa (not considered)	The Si wafer surface became very rough. Seemed that the solution reacted with Si. No film were identified.	Concentration of the alkali should be reduced
5	Same as the above	NH_4OH (0.2 M)	150^{0}C, 6 hrs.	Again Si surfaces are getting chipped off and no film was observed.	The time of treatment should be reduced.
6	Same as the above	NH_4OH (0.2 M)	150^{0}C, 30 min	The sample changes colour (yellow). The film is seen under the microscope and certain grain like structures are observed. FT-IR was very different in nature as observed before the treatment.	The film did not crystallize. Hydrothermal treatment for another 30 min also did not help in crystallizing the sample.

As discussed in the earlier table the films did not crystallize as shown by XRD pattern in Fig. 3.20 by the conditions used in the hydrothermal technique. The FT-IR spectra of as deposited, after 30 min and after 1 hr treatment are shown in Fig. 3.21. It is not possible

to conclude anything from those spectra. A detailed and systematic study is needed with different concentration of the alkali and time of the treatment to optimize the conditions to be used for hydrothermal treatment.

3.3 Results on the thin film samples:

3.3.1 Thickness and roughness measurements:

The thickness and roughness measurement is carried out using surface profilometer. Some examples of the profilometer plots are shown in Fig 3.22 (a)- (c). The thicknesses of the films are in the range of 0.8 μm to 2.0 μm. The measurements were done at 2-4 spots to determine the uniformity of thickness of the film. Fig 3.22(a) shows the profilograph of a film made by 15 coatings of sol on Pt and annealed at 650^0C for 1 hr in furnace. The film is uniform and almost smooth except for some unevenness at the step.Thickness of the film is around 1 μm. This is a typical sample used for electrical characterization. Samples with DEA as additive showed a rougher film with a slightly high value of thickness Fig. 3.22(b). 20 coatings of the sol resulted in a much thicker film.

3.3.2 Optical microscopy:

Figure 3.23 shows the optical micrograph of the film annealed at 650^0C/1hr. Films annealed to 800^0C /2 hrs had a similar structure. The film features are the scratches on the substrate formed during polishing. The films are crack-free under the optical microscope.

3.3.3 Scanning Electron Microscopy:

Fig. 3.24 (a)-(b) and Fig. 3.25 (a)-(b) show the SEM pictures of the films made with different additives and taken at different magnifications. Fig. 3.24 (a) shows the sample made without any additive, annealed at two different temperatures 600 and 800^0C. Fig.

3.24 (b) shows pictures of the samples made with acetyl acetone annealed at 600 and 800^0C. All these photographs are taken at ×5000 magnification. Figures 3.25 (a) and (b) depict the SEM pictures of the film with DEA taken at two different temperatures and two different magnifications (×5000 and ×15000). All the SEM pictures are very different from the published data in the journals. No grainy microstructure is seen in those films. In case of the film made with acetyl acetone and annealed at 800^0C, an altogether different microstructure from the rest is observed.

3.3.4 XRD results:

The XRD patterns for the thin film samples (~ 1 μm) containing no additive, acetylacetone and DEA and annealed at 600^0C for 1 hr are shown in Fig.3.26 (a), (b) and (c) respectively. In Fig. 3.27 plots of these three samples annealed at 800^0C for 1hr are shown. All the data are tabulated in Table 3.4.

Table 3.4: Comparison of the data obtained in different films with published data

Serial no.	From reference 29			Experimental Data											
	hkl	2θ	I/I_0	No Additive				With Acetylacetone				With DEA			
				600^0C/1 hr		800^0C/1 hr		600^0C/1 hr		800^0C/1 hr		600^0C/1 hr		800^0C/1 hr	
				2θ	I/I_0	2θ	I/I_0	2θ	I/I_0	2θ	I/I_0	2θ	I/I_0	2θ	I/I_0
1	001	21.827	63.2	-	-	-	-	-	-	-	-	-	-	-	-
2	100	22.404	40.8	22.36	54.15	22.21	18.80	22.47	56.5	22.34	45.58	22 32	47.89	22.26	45.62
3	101	31.73	100	31.78	100	31.73	47.5	31.79	94.47	31.89	100	31.87	99.53	31.66	100
4	110	32.02	71.2	-	-	-	-	-	-	-	-	-	-	-	-
5	111	39.038	50.4	39.15	30.82	39.14	15.65	-	-	39.25	30.21	39.23	31.09	39.04	26.39
6	002,200	45.48	61 6	45.56	38.31	45.67	19.06	45.60	34.58	45.72	38.25	45 81	32 01	45 58	26.90
7	102,210	50.865	44.8	51.22	14.27	-	-	51.22	16.35	51.39	16.11	51 55	12 84	51.14	10.54
8	112,211	56.36	61.6	56.59	37 44	56 61	14.49	56.65	31.44	56.62	30.67	56.64	33.50	56.61	38.46

3.3.5 Dielectric Measurements:

3.3.5.1 Dielectric constant:

The dielectric constant is calculated using the following relationship:

Capacitance of the film is given by

$$C = \varepsilon_0 \varepsilon_r \frac{A}{d} \qquad \text{---------- (1)}$$

where, ε_0 = permittivity (dielectric constant) of a vaccum,

ε_r = relative dielectric constant,

d = thickness of the film,

and A = area of the electrode.

From equation (1),

$$\varepsilon_r = C \times d / \varepsilon_0 A \qquad \text{---------- (2)}$$

The capacitance and dielectric loss of the film are measured directly from the impedance analyzer at various frequencies at room temperature. The films were about 1 μm thick and the top electrode diameter was 0.5 mm. The oscillator level was 50 mV and the measurements were carried out in the frequency range 1 kHz to 11 MHz. Measurements were carried out on three devices in each sample and the average of the three measurements for each sample is presented. Six different samples were made with three different sol (i) without any additive, (ii) with acetyl acetone, and (iii) with DEA and annealed at two different temperatures 600^0C and 800^0C for 1 hr each. The variations of the dielectric constant with frequency for the samples are shown in Fig. 3.28 and 3.29 as a function of annealing temperature and additive in the sol respectively. As seen from these curves, the dielectric constant increases with increase in annealing temperature in

all the three samples. The dielectric constant is high at low frequencies and decreases as the frequency increases first rapidly till 10 kHz and then slowly. In case of sample with DEA, annealing at 800^0C increased the dielectric constant significantly compared to the other two samples (with acetyl acetone and without additive). The values of dielectric constant is very low (maximum value ~ 42) compared to the available data in the literature (~ 300). These discrepancies may arise when

1. A layer exists at the grain boundaries having a very low value of dielectric constant
2. There is formation of interfacial layers with low dielectric constant between the substrate and the film.
3. Grain size is very small
4. Porosity in the film

A model of capacitance in series can realize the effects of 1 and 2[26]. The local field caused by the space charge layers at the grain boundaries can be expected to work as parasitic capacitors having a small capacitance[33]. In other way, this may be explained by a dielectric system represented by two extreme connectivity structure, with an effective dielctric permittivity given by [34]

$$\varepsilon_m^n = (1-V_f)\varepsilon_{low}^n + V_f\varepsilon_{high}^n \quad \text{----------(3)}$$

where n = ±1, V_f = partial volume, ε_{high} refers to the intrinsic dielectric permittivity of BST grain and ε_{low} is that of a second phase having a low dielectric permittivity. The exponent n is +1 for parallel and -1 for series combination. However, a lowering of the dielectric constant from an expected value of 300 to the measured value of ~ 20 can not be explained by such an argument. The grain size of the film, as observed the SEM is

also sufficiently large. It appears that the films have extensive microporosity as discussed in section ---- which may be responsible for the low dielectric constant.

3.3.5.2 Dielectric loss:

The frequency variation of average dielectric loss as a function of temperature and additives are plotted in Fig. 3.30 (a)-(c) and 3.31 (a)-(b) respectively. It is seen in all the cases that at low frequencies the dielectric loss is very high and decreases very rapidly below 100 kHz. For samples annealed at 800^0C it is seen that the value of dielectric loss is much less in case of the sample prepared with acetyl acetone. There is not much change in the dielectric loss values with annealing temperature in case of samples prepared with acetyl acetone and DEA. But in case of sample without additive dielectric loss differs in large amount at low frequencies for annealing temperatures 600^0C and 800^0C. The value of high dielctric constant and high dielectric loss at lower frequency can be attributed to the contribution of grain boundary and electrode[33]. The high value of the dielectric loss at low frequencies again appears to be related to the microporosity of the film. It could also be due to some organic residue remaining in the film.The significant differences in the dielectric loss in the samples with different additives [Fig. 3.43(b)] may be due to this reason.

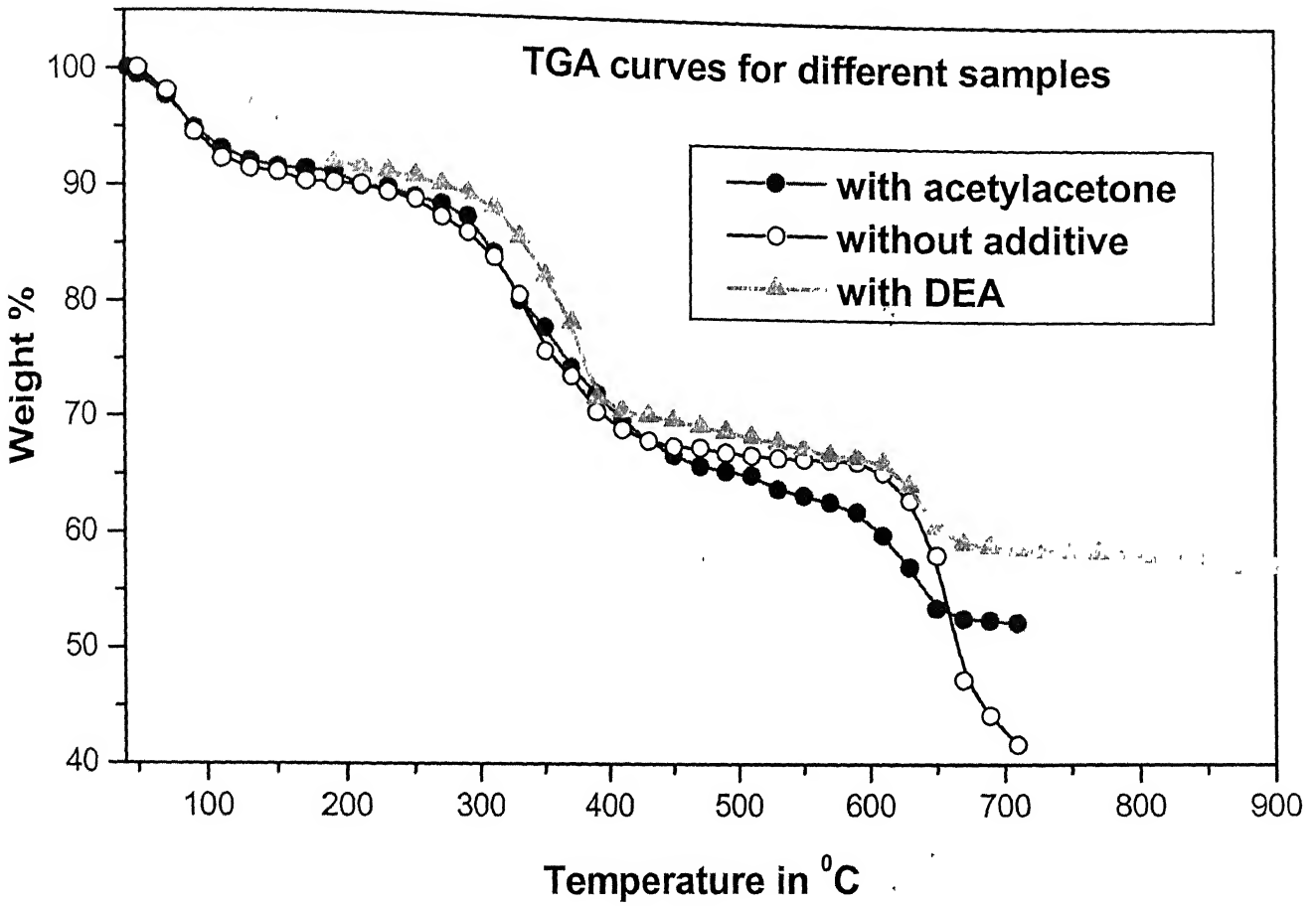

Fig. 3.1: TGA curves of the gel powder made from sols (without additive, with acetylacetone and with DEA)

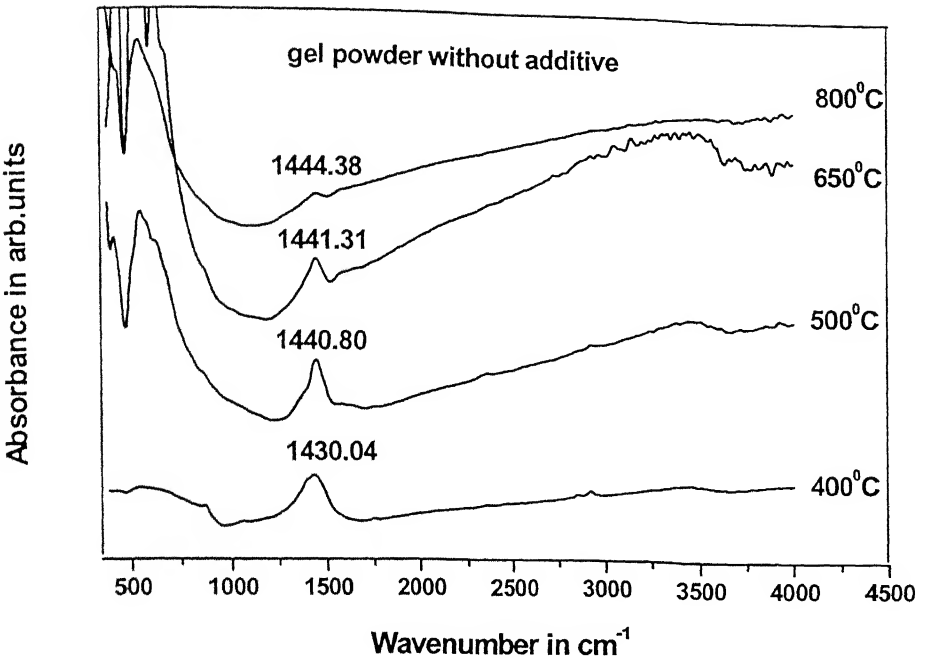

Fig. 3.2: FT-IR spectra of gel powders without additive at different temperatures

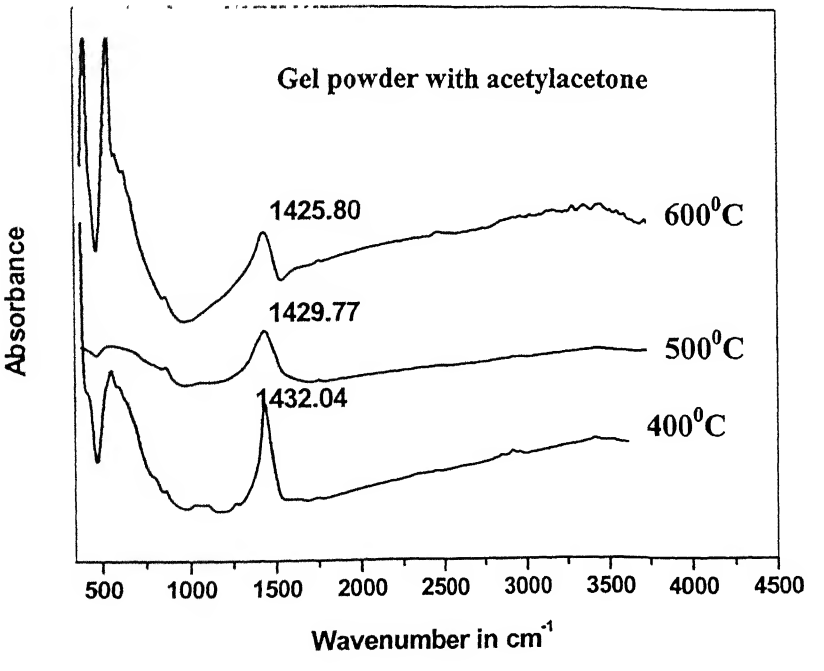

Fig. 3.3: FT-IR spectra of gel powders with acetylacetone at different temperatures

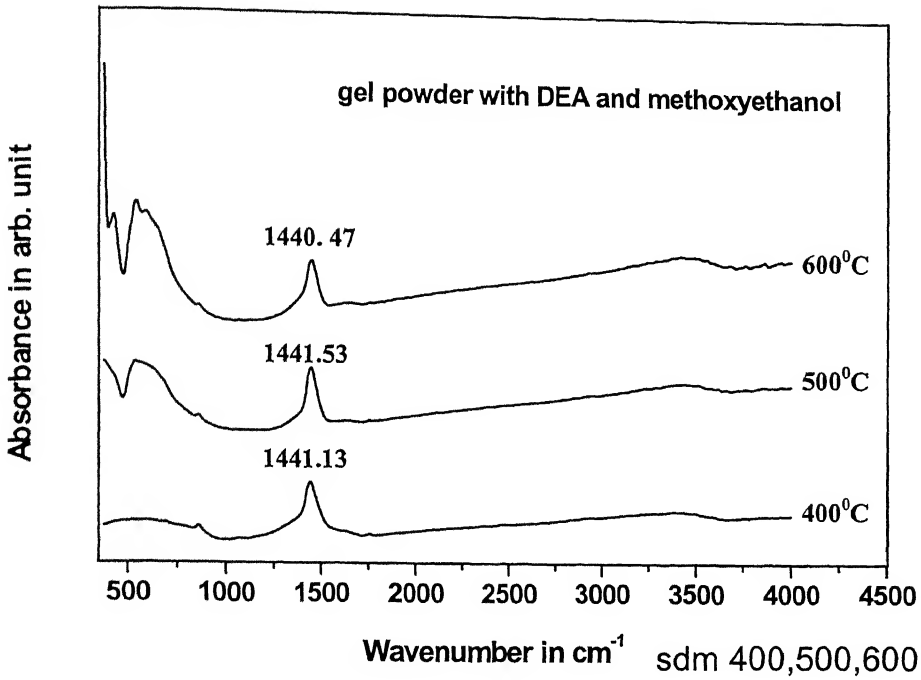

Fig. 3.4: FT-IR spectra of gel powder with DEA and methoxyethanol

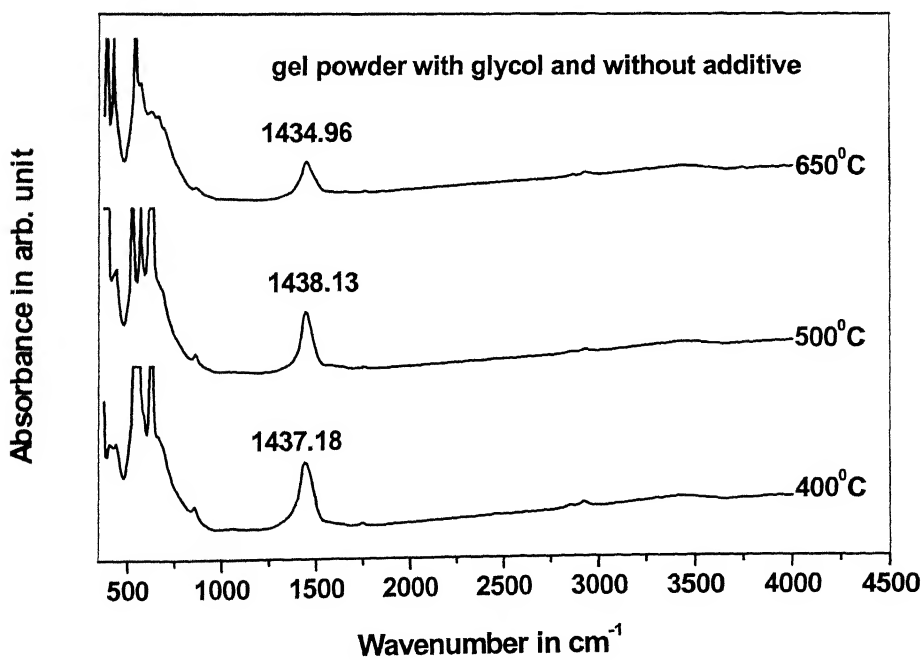

Fig. 3.5: FT-IR spectra of gel powder with glycol and without additive

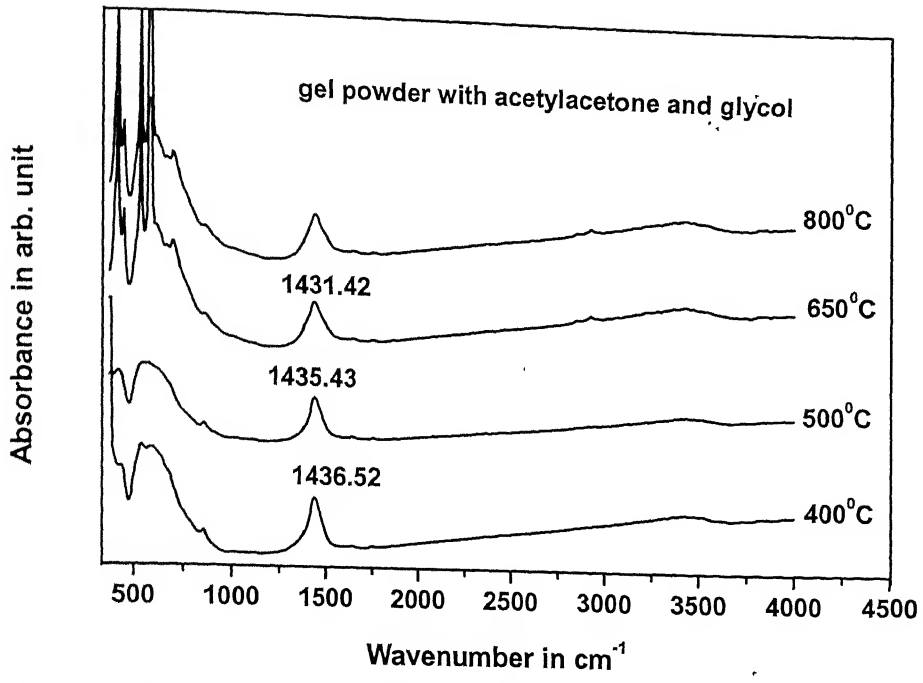

Fig. 3.6: FT-IR spectra of gel powder made with acetylacetone and glycol

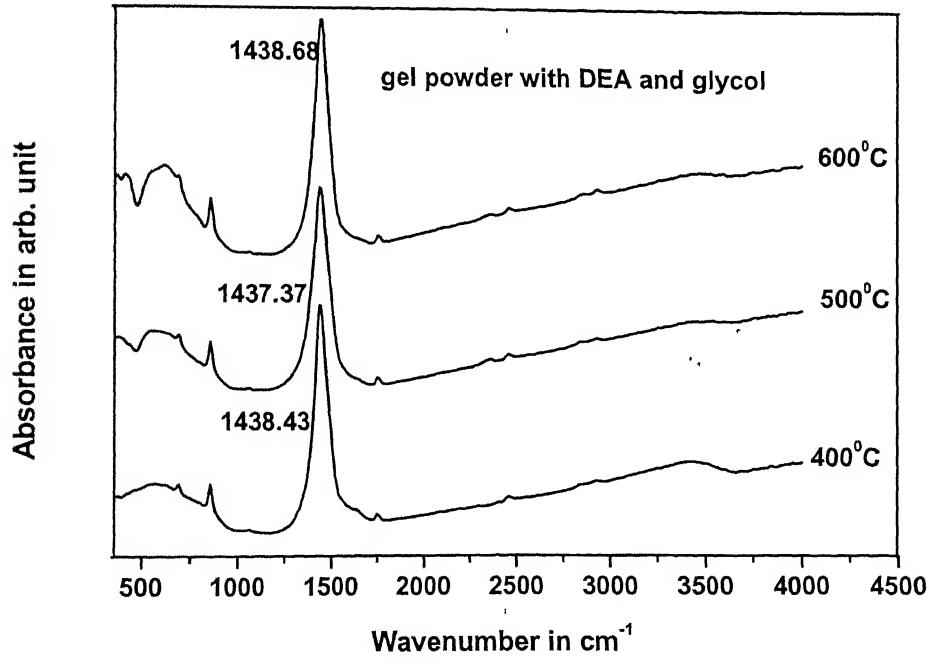

Fig. 3.7: FT-IR spectra of gel powder made with DEA and glycol

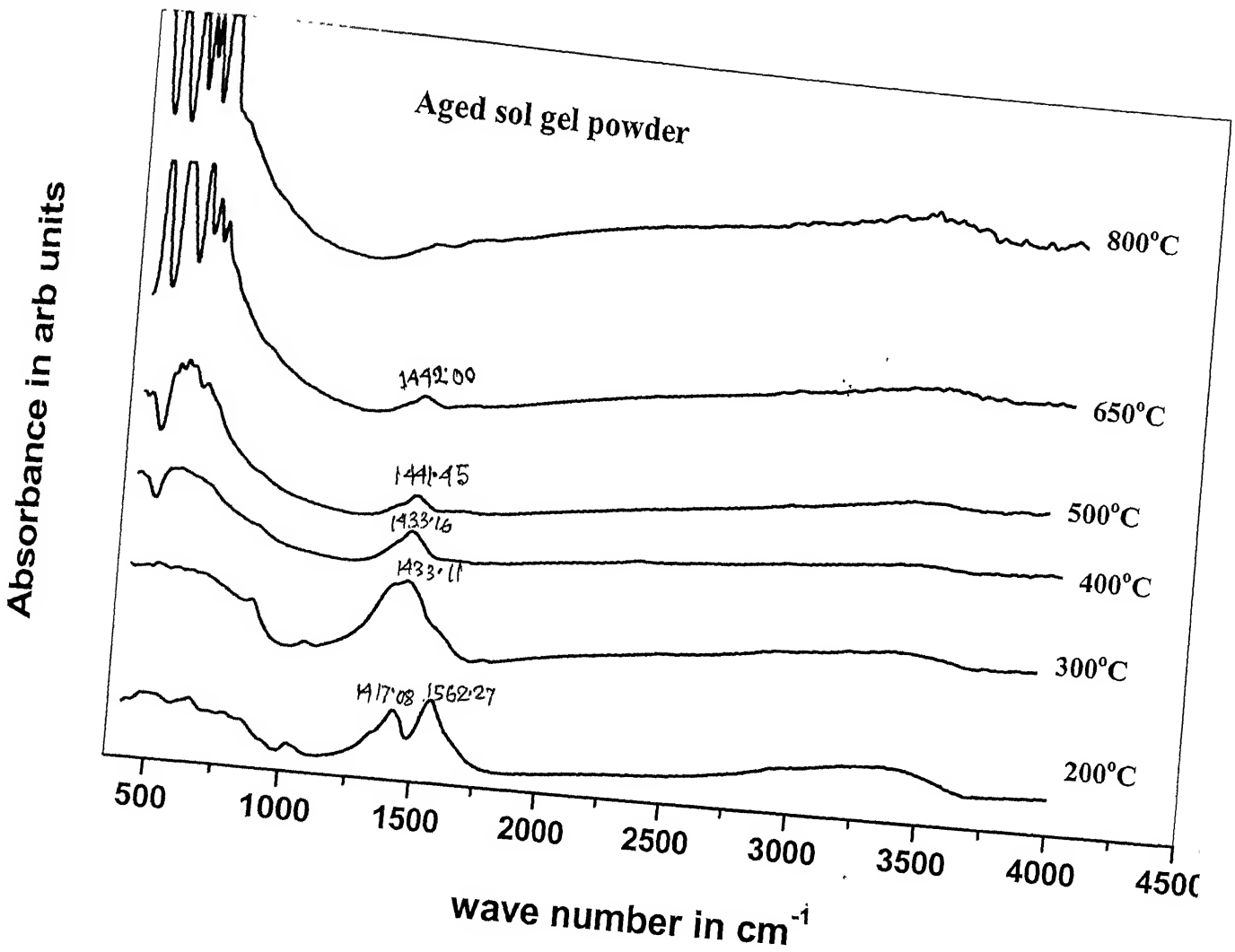

Fig. 3.8: FT-IR spectra of gel powder made from aged sol with acetylacetone

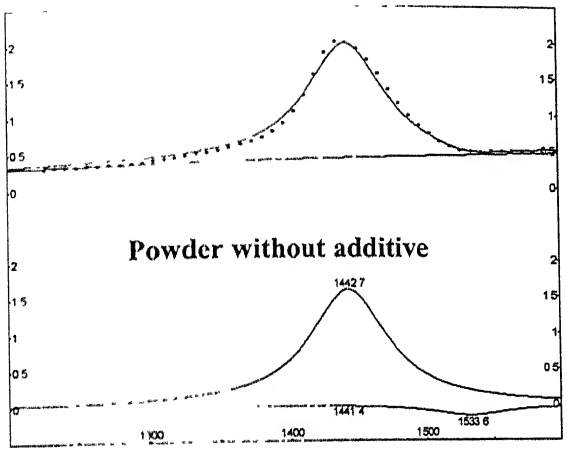

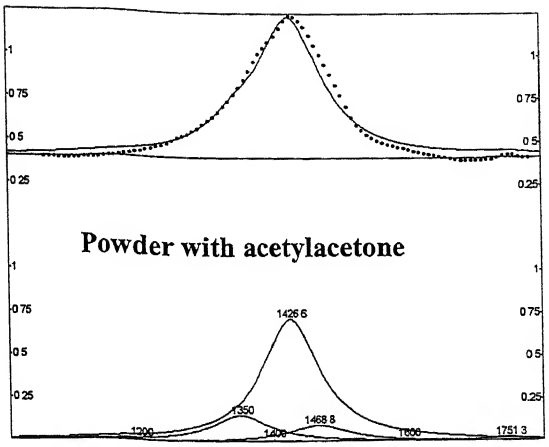

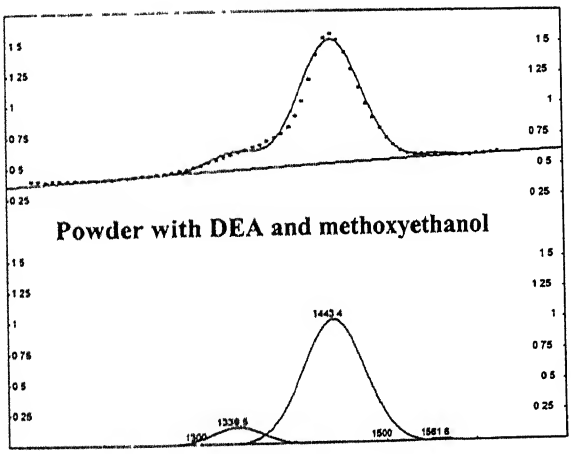

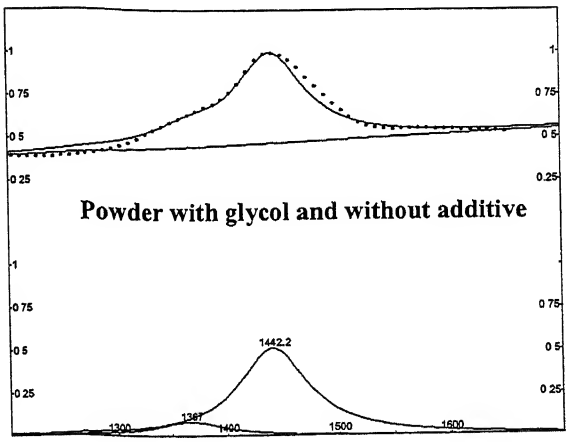

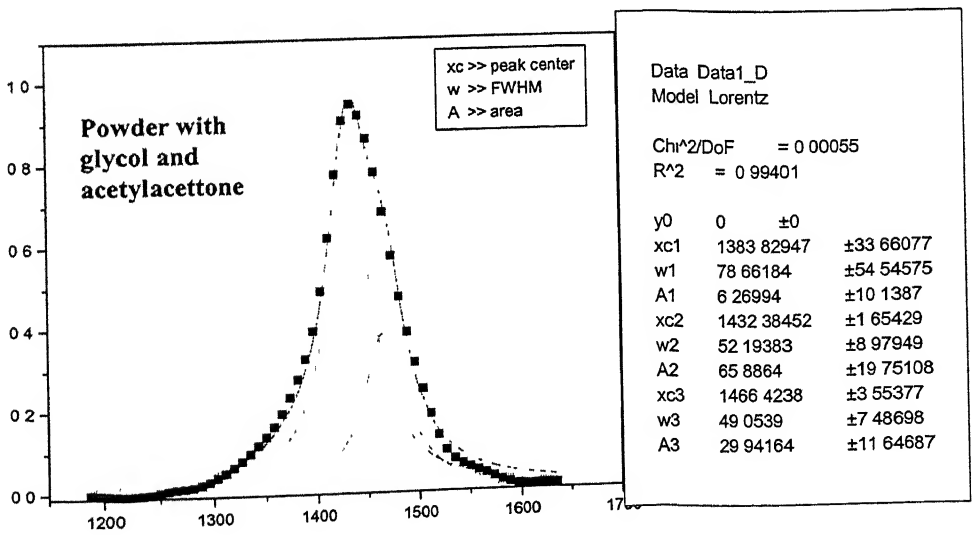

Fig. 3.9: FT-IR peak fitting results for different samples heated to 500^{0}C

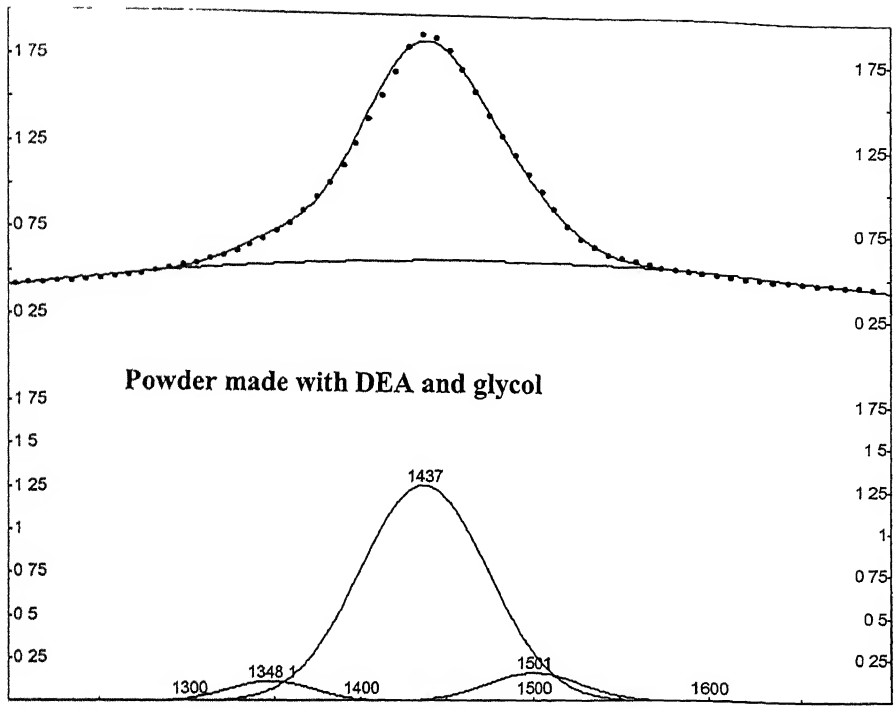

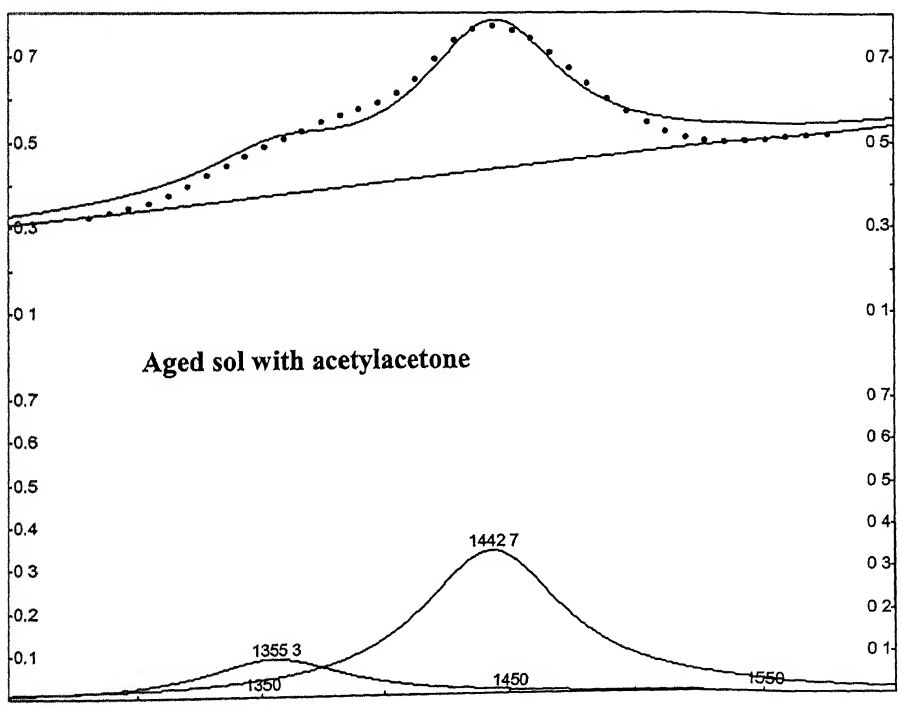

Fig 3.9: FT-IR peak fitting results for different samples heated to 500^{0}C

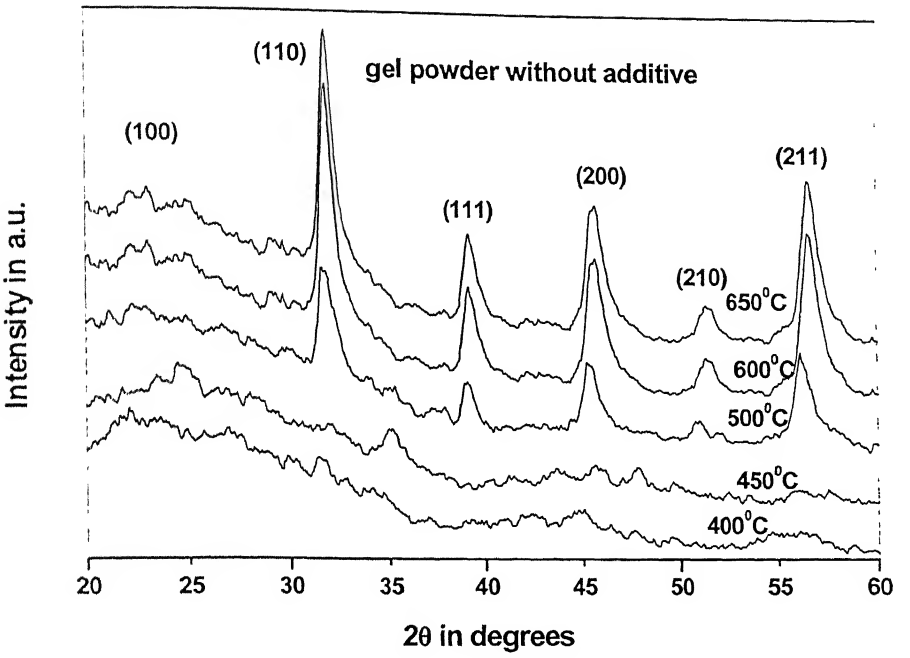

Fig 3.10: XRD plots of gel powder without additive and with methoxyethanol at different temperatures

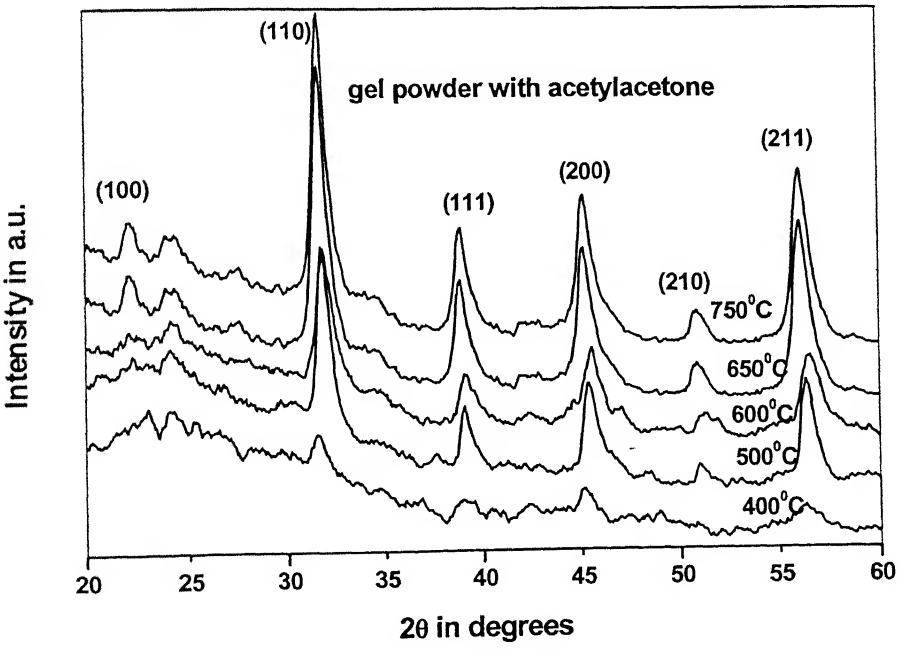

Fig 3.11: XRD plots of gel powder with acetylacetone and methoxyethanol at different temperatures

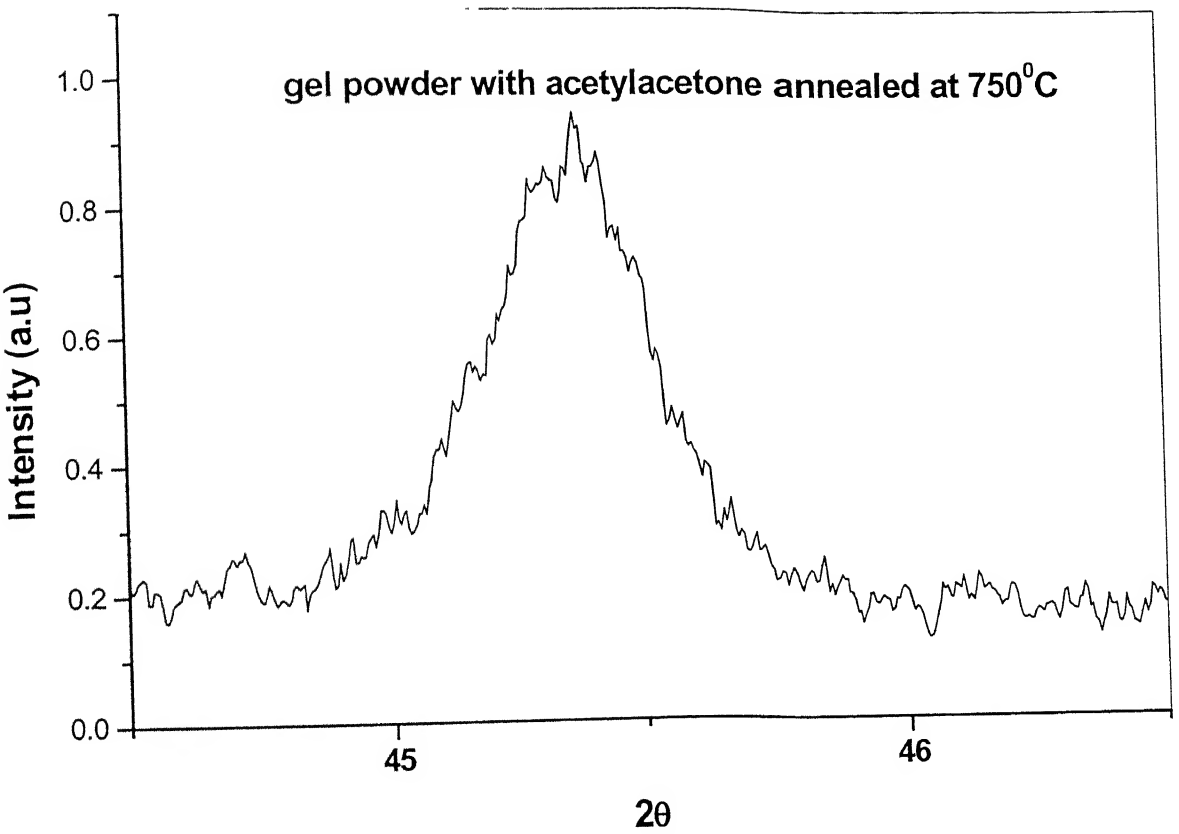

Fig. 3.12: Slow (0.3^0/min) scan of the (200) peak of gel powder sample made with acetylacetone and heated to 750^0C/1hr.

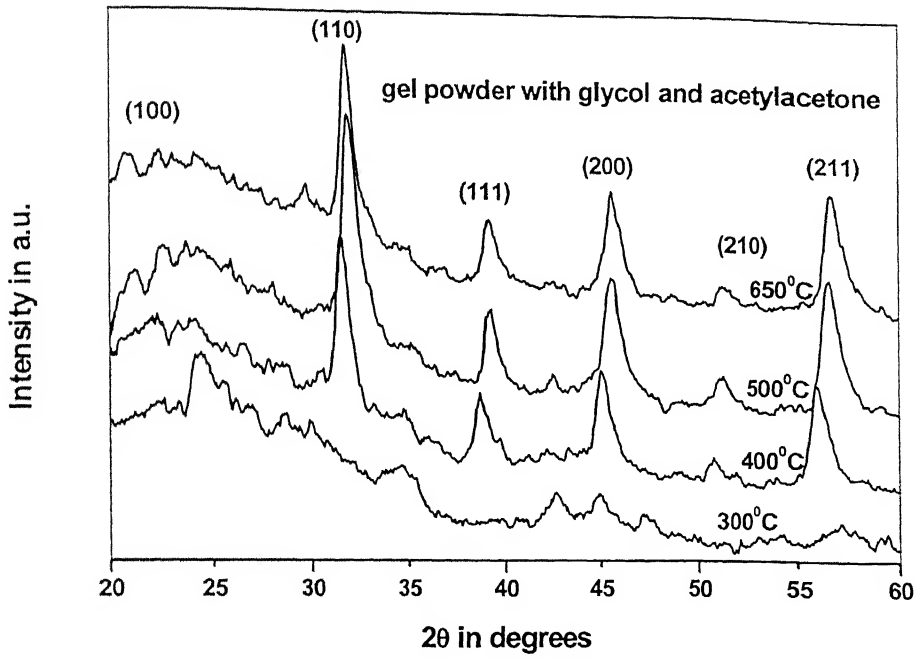

Fig 3.13: XRD plots of gel powder with acetylacetone and glycol at different temperatures

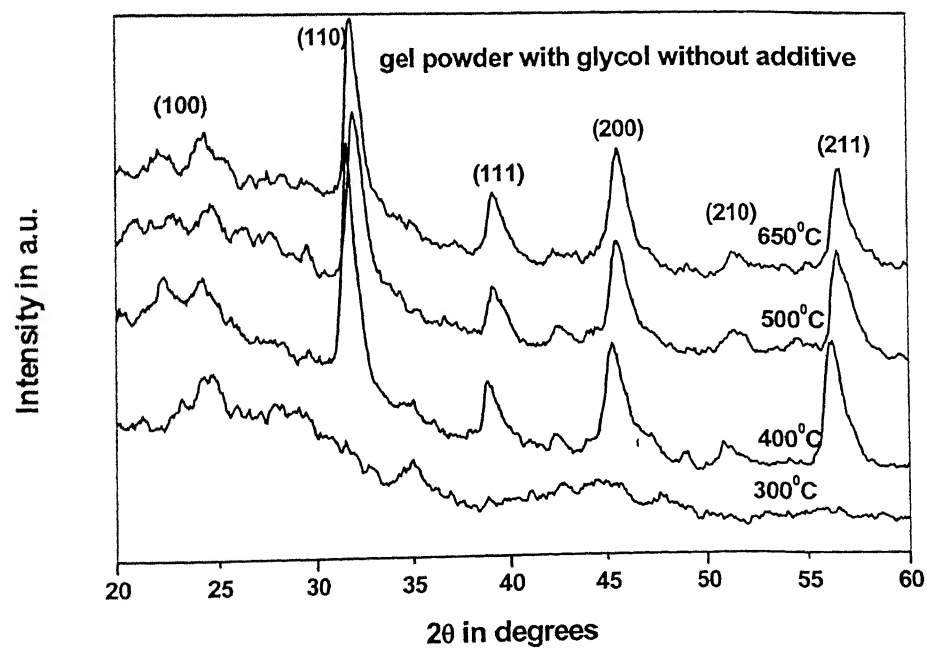

Fig 3.14: XRD plots of gel powder without additive and with glycol at different temperatures

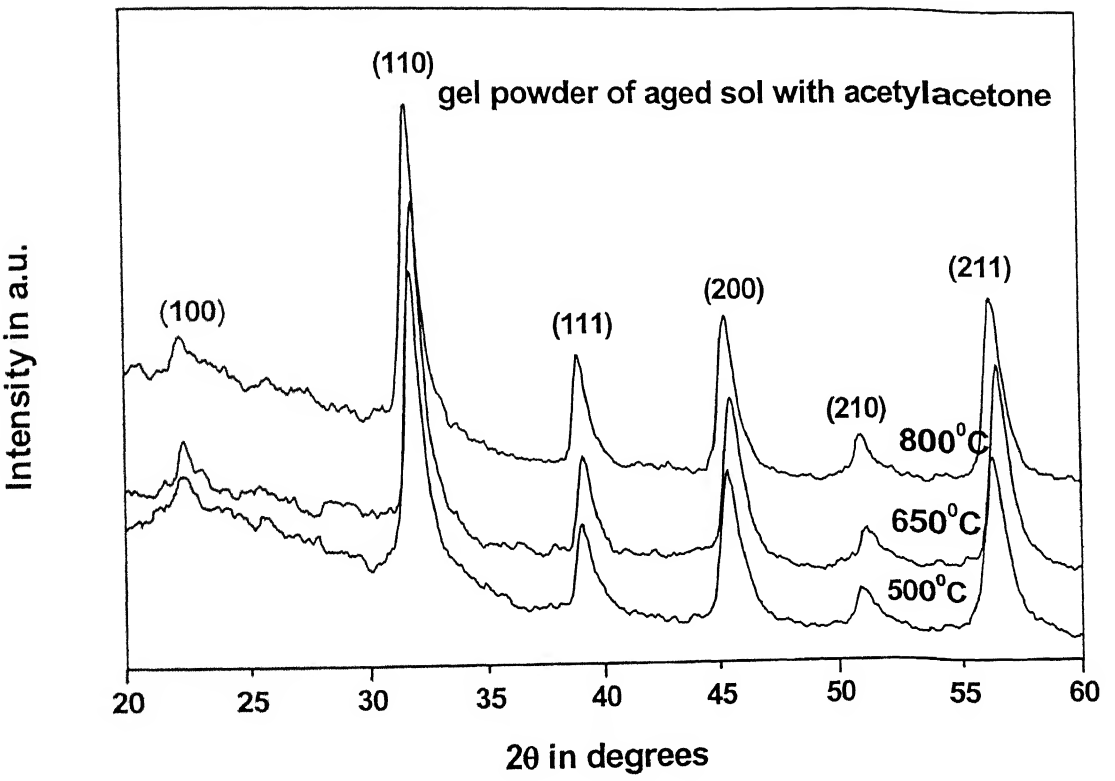

Fig. 3.15: XRD plots for the gel powder of aged sol at different temperatures

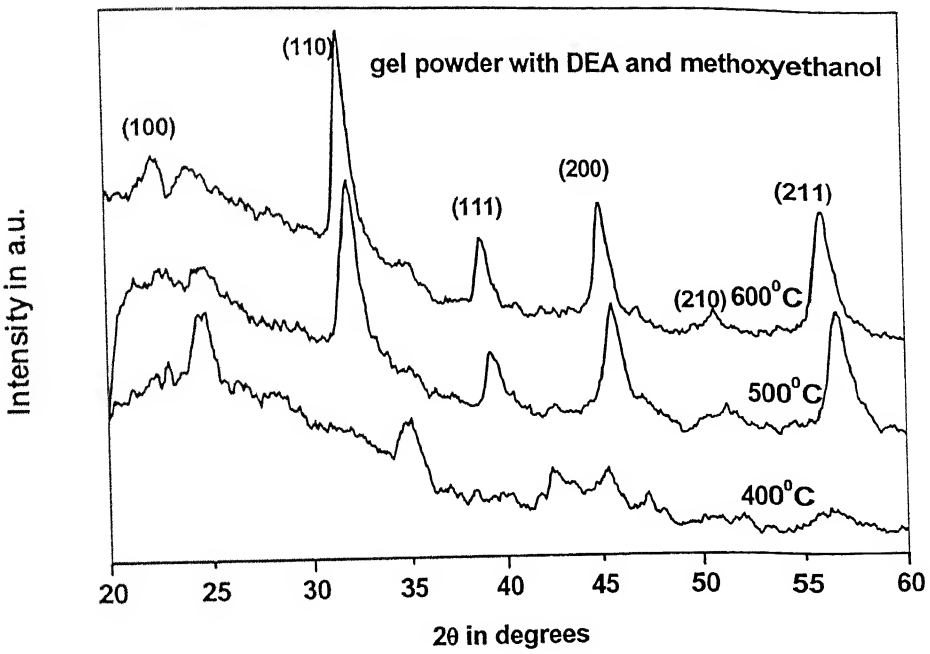

Fig 3.16: XRD plots of gel powder with DEA and methoxyethanol at different temperatures

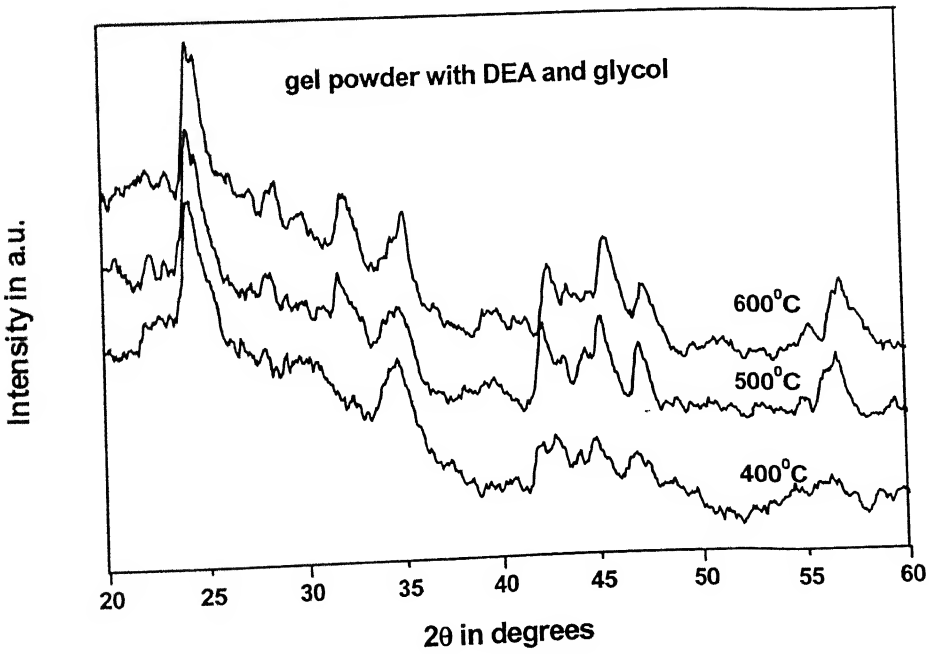

Fig 3.17: XRD plots of gel powder with DEA and glycol at different temperatures

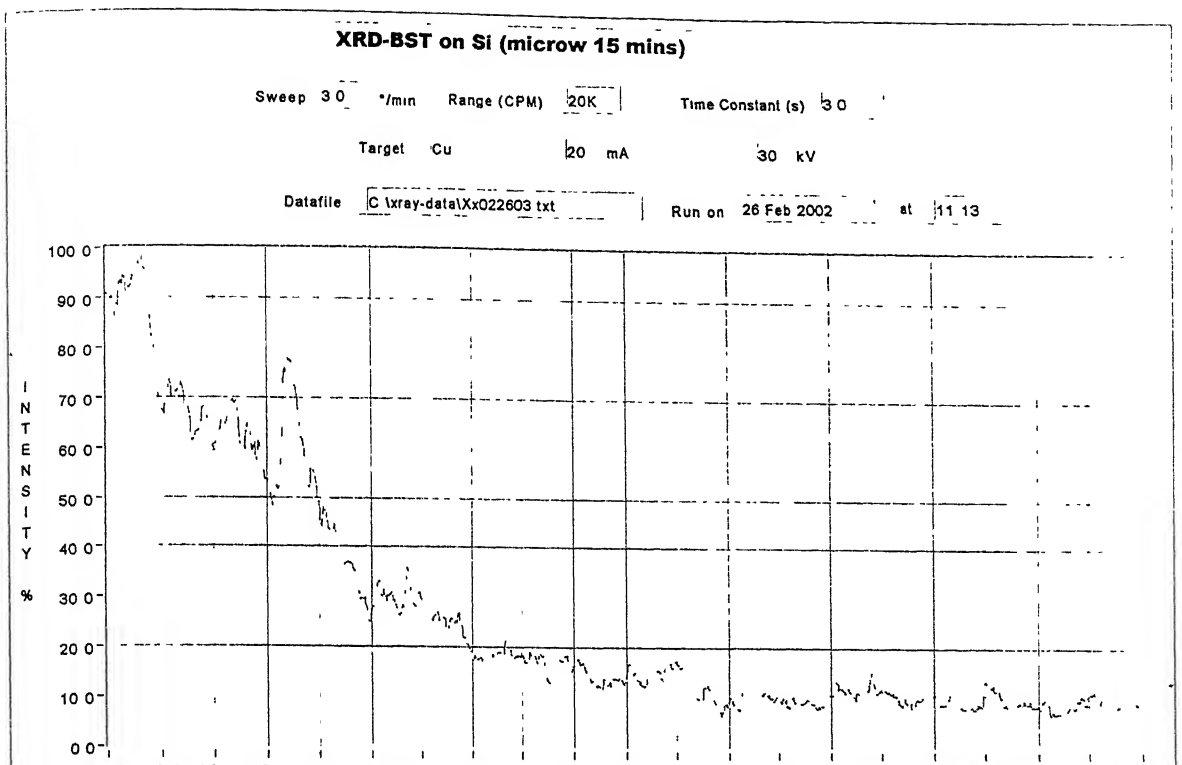

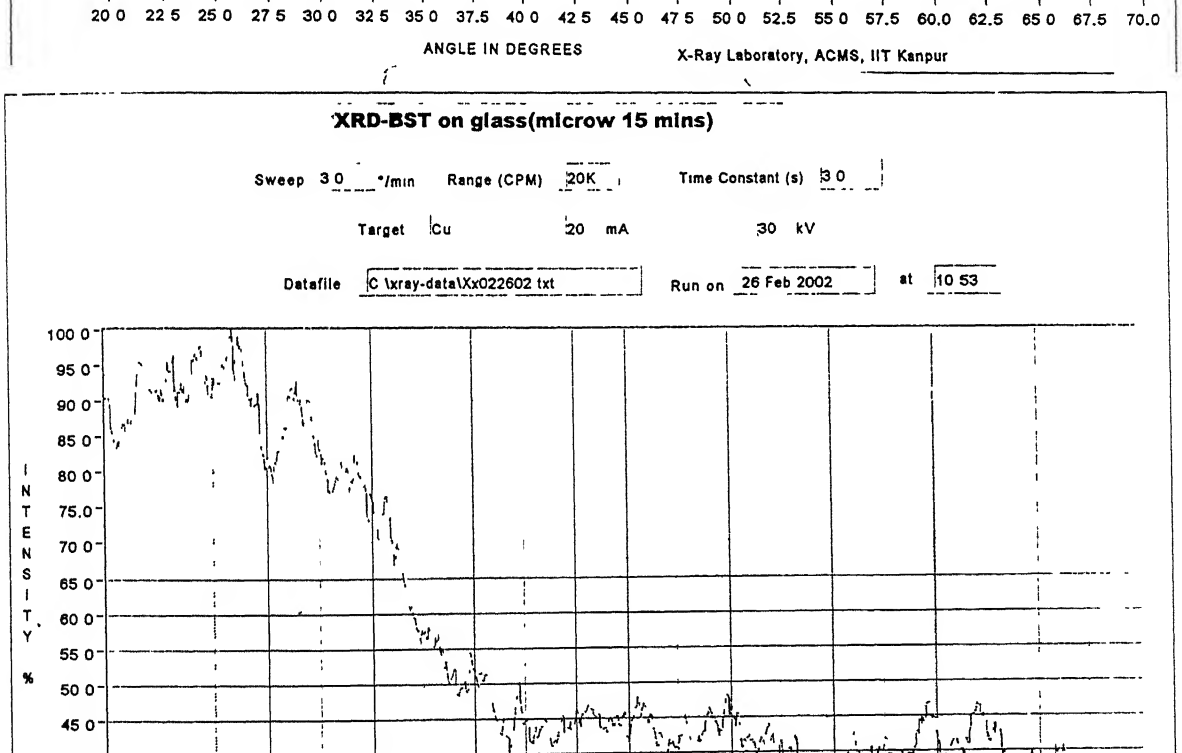

Fig. 3.18: XRD plots of the thin film sample after microwave treatment (a) on glass substrate (b) on silicon substrate

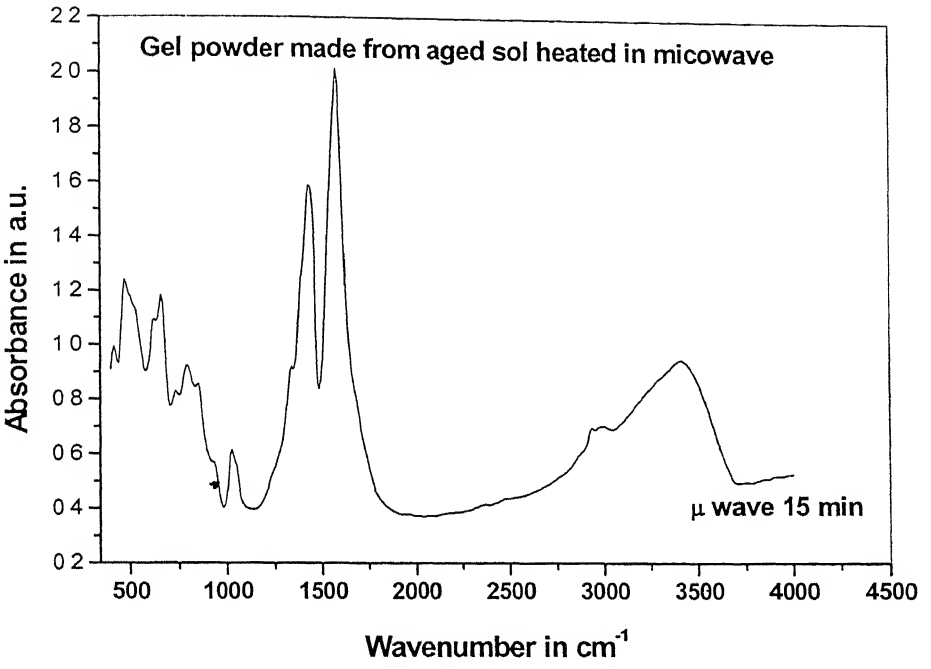

(a)

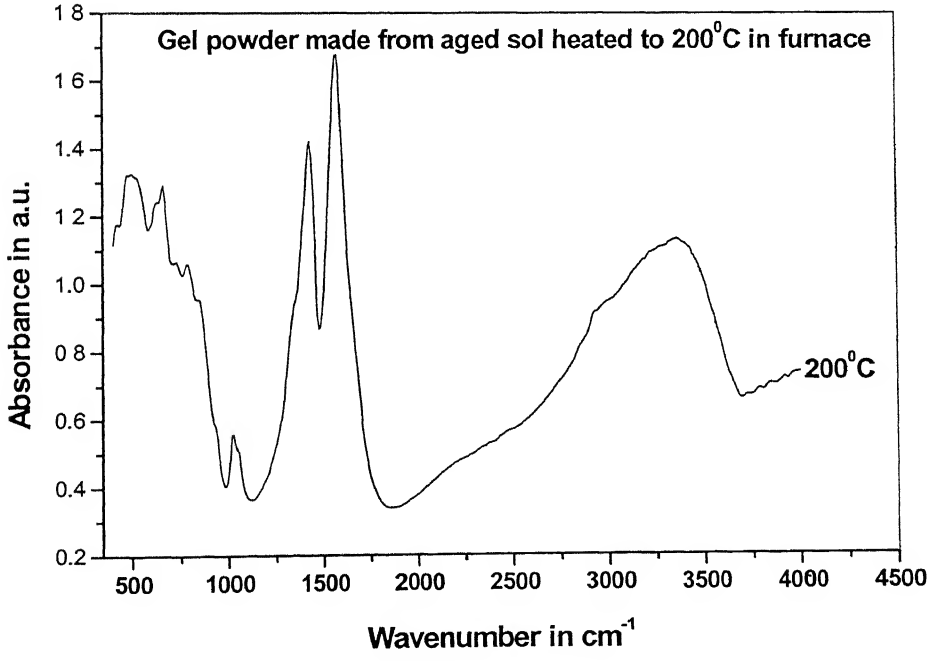

(b)

Fig. 3.19: FT-IR spectra of gel powders made from aged sol (a) in microwave (b) in furnace at 200°C

Fig. 3.20: XRD plot of thin film sample after hydrothermal treatment

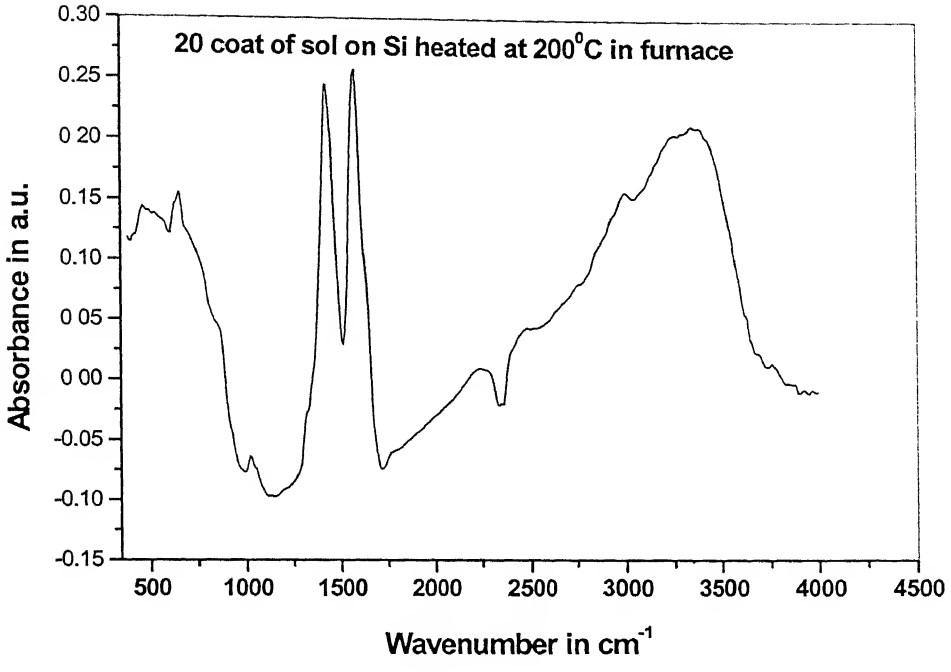

(a)

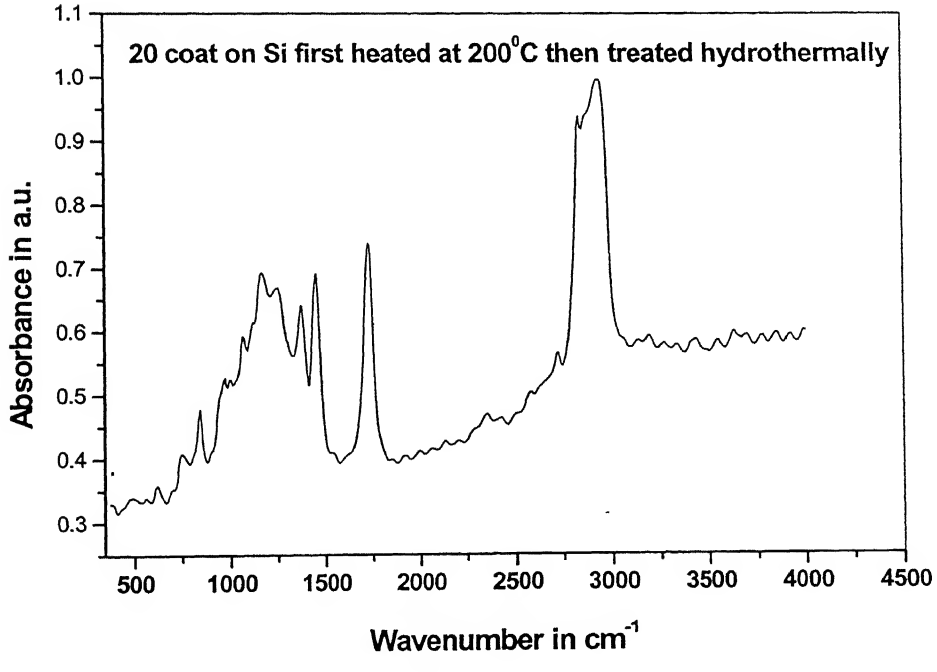

(b)

Fig. 3.21: FT-IR spectra of (a) before and (b) after hydrothermal treatment for 30 mins.

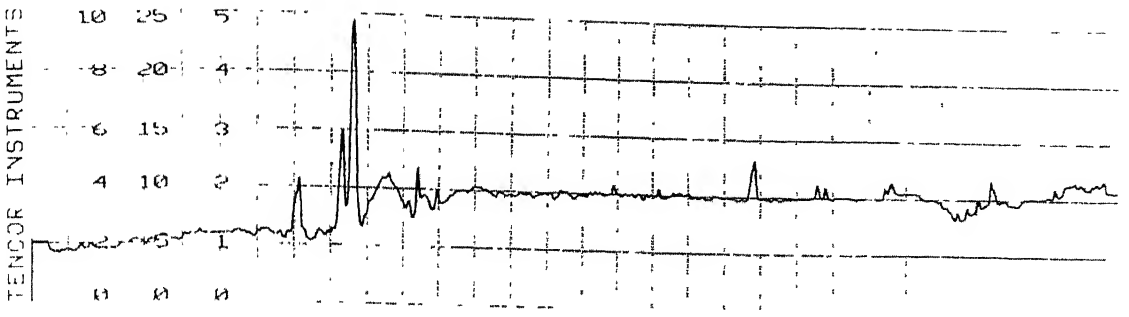

(a)

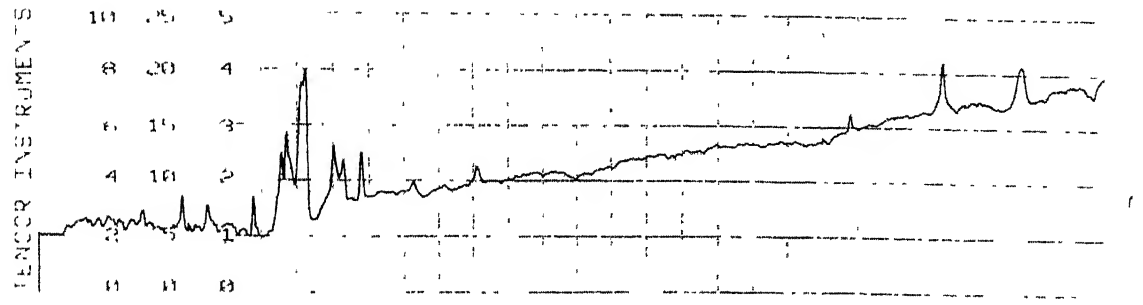

(b)

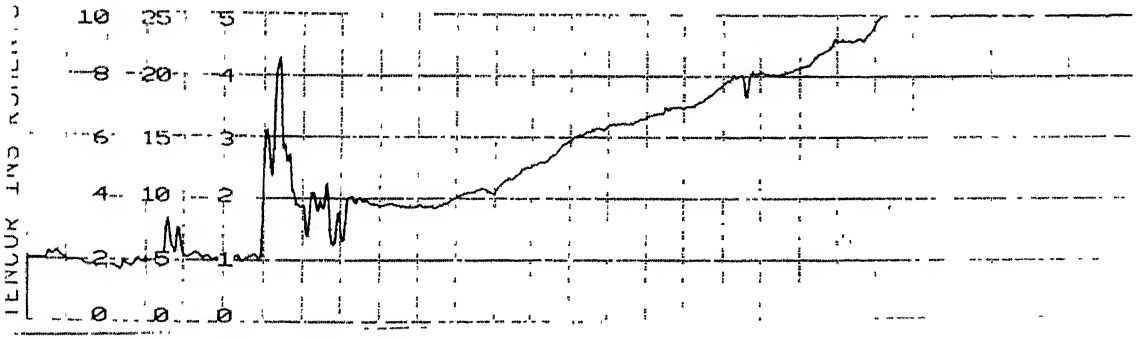

(c)

Fig. 3.22: Profilograph of some of the films (a) 15 coatings of sol with acetylacetone on Pt, (b) 15 coatings of the sol with DEA on Pt, and (c) 20 catings of the sol on Pt

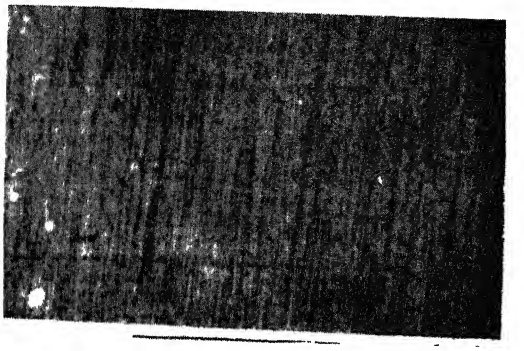

Fig. 3.23: Optical microscopic photograph of the film

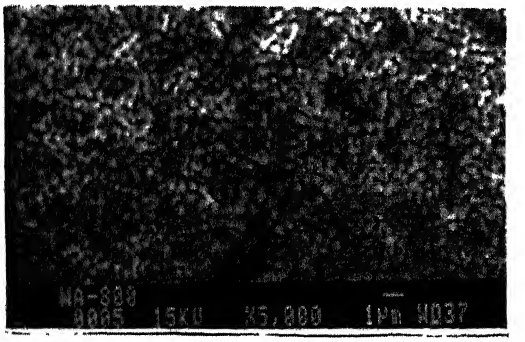

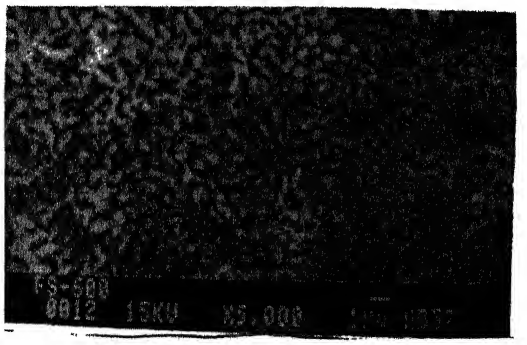

Fig.3.24: SEM pictures of the films (a) without additive (b) with acetylacetone

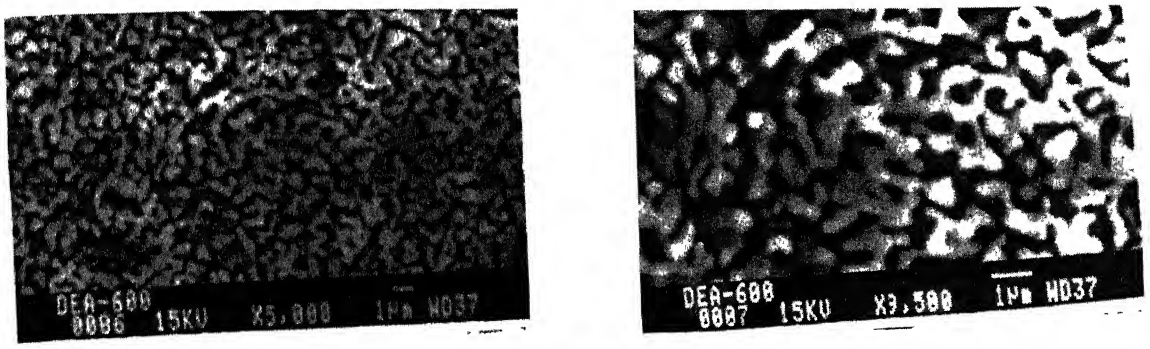

(a)

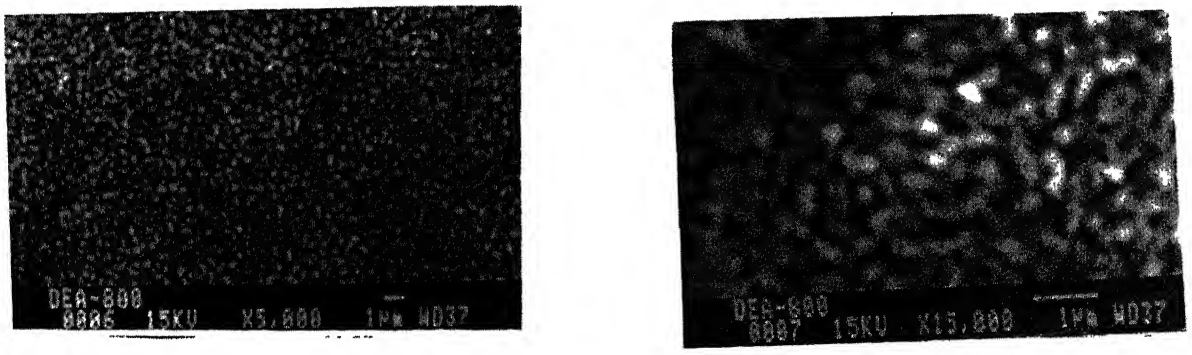

(b)

Fig. 3.25: SEM pictures of the films treated DEA and annealed at two different temperatures (a) 600^0C (b) 800^0C

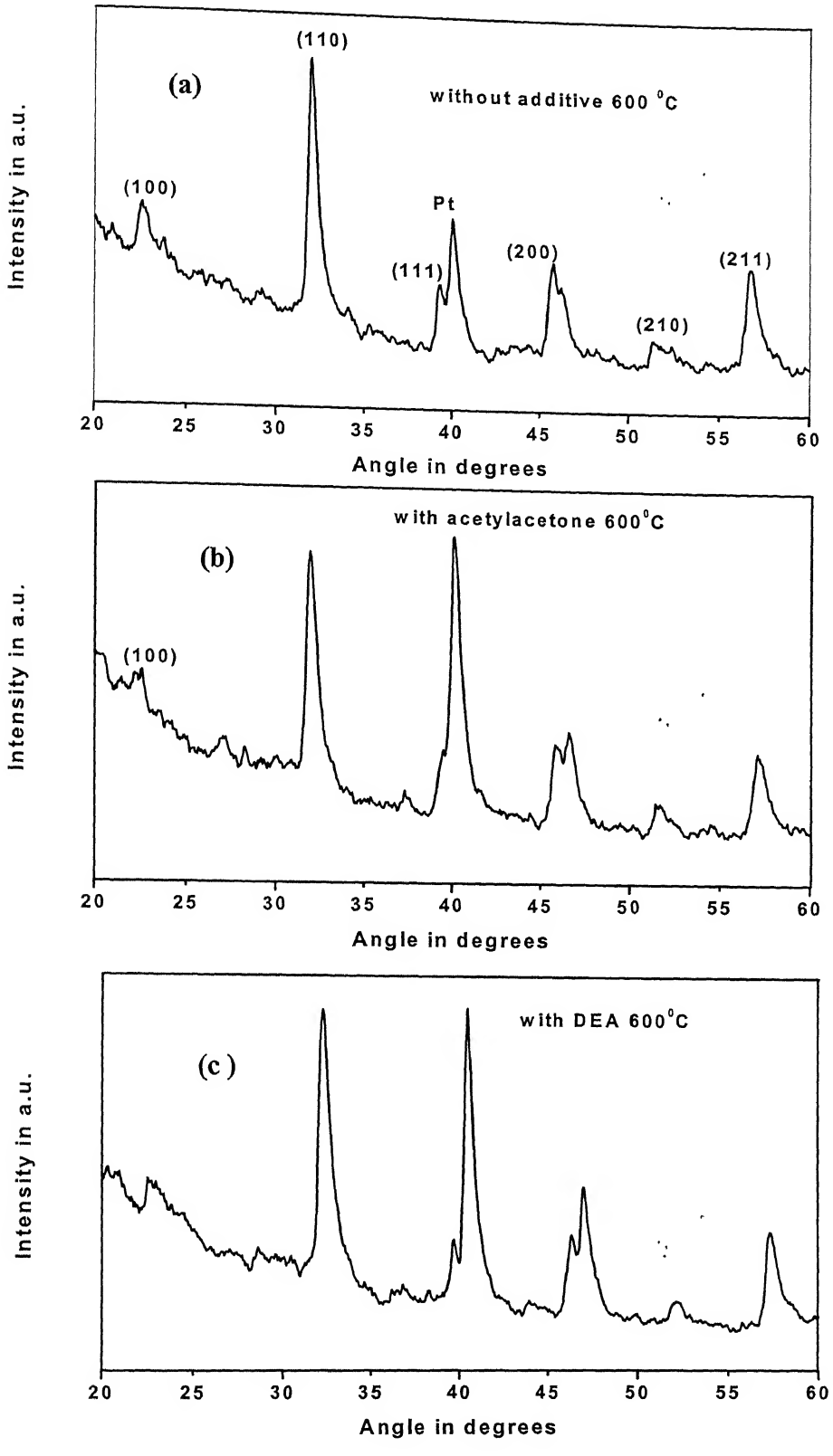

Fig. 3.26: XRD patterns of thin film samples annealed at 600^{0}C (a) without additive, (b) with acetylecetone, and (c) with DEA

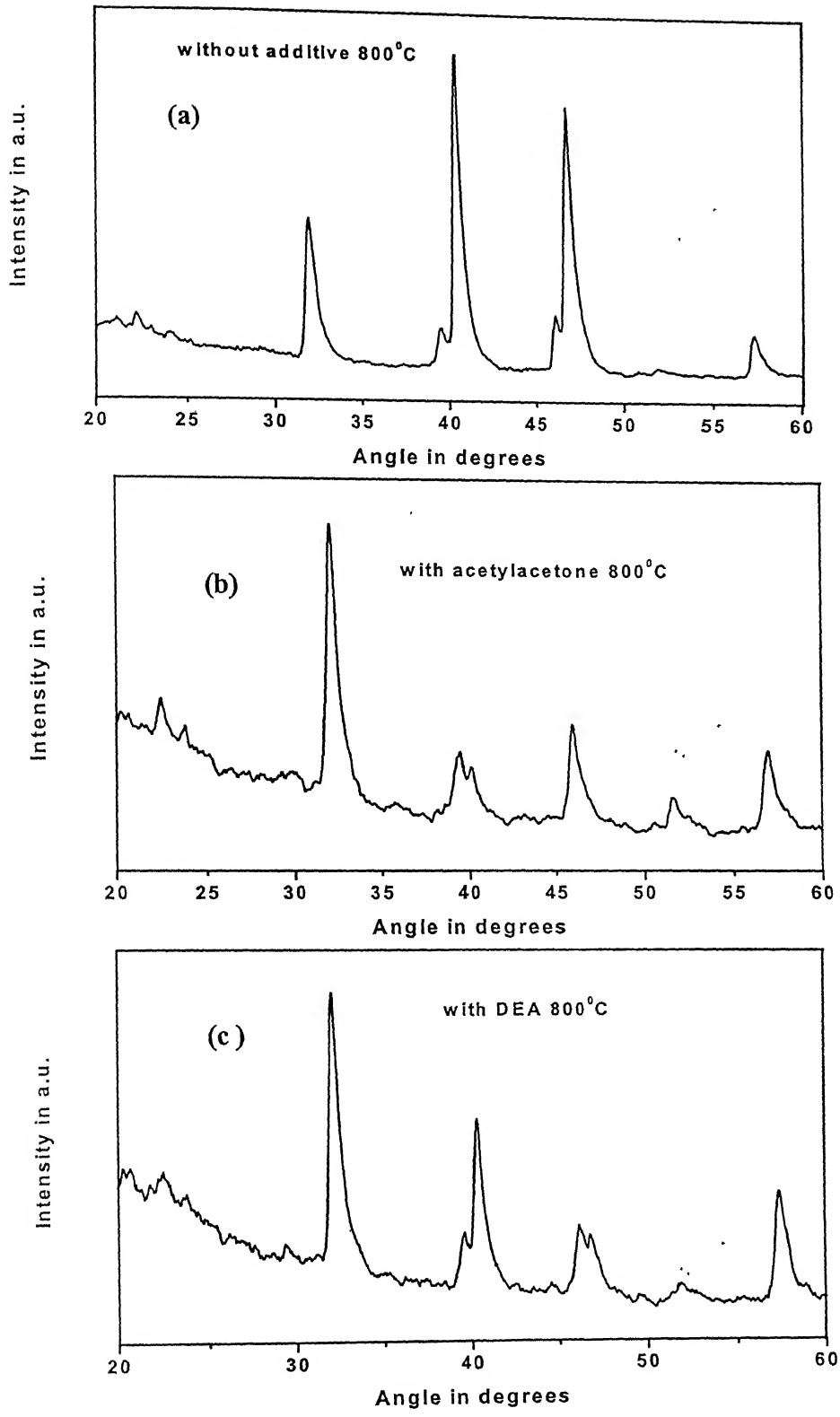

Fig. 3.27: XRD patterns of thin film samples annealed at 800^0C (a) without additive, (b) with acetylecetone, and (c) with DEA

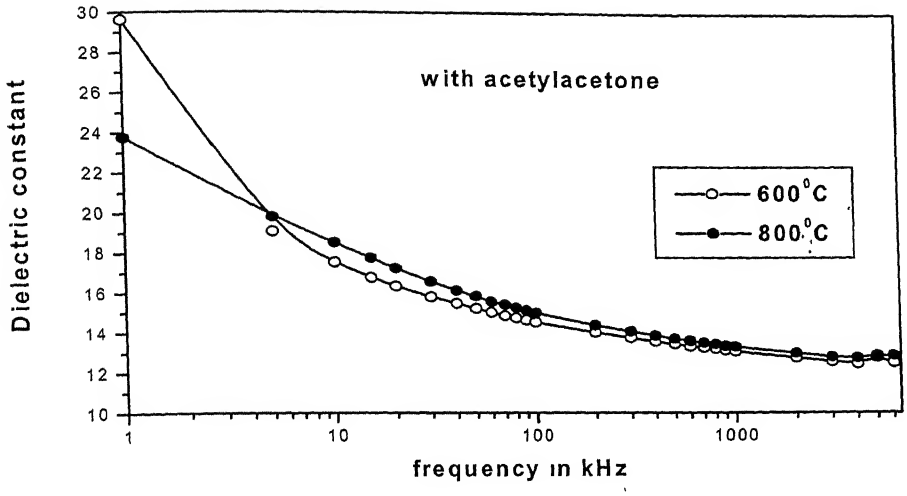

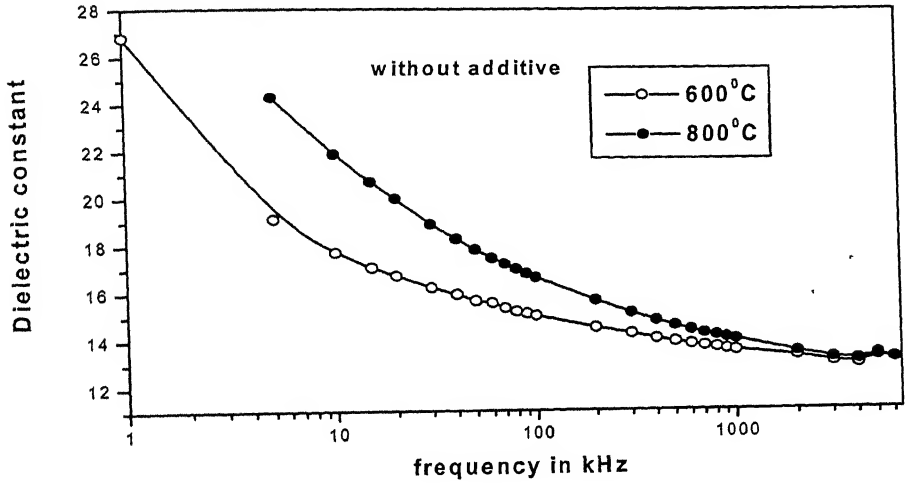

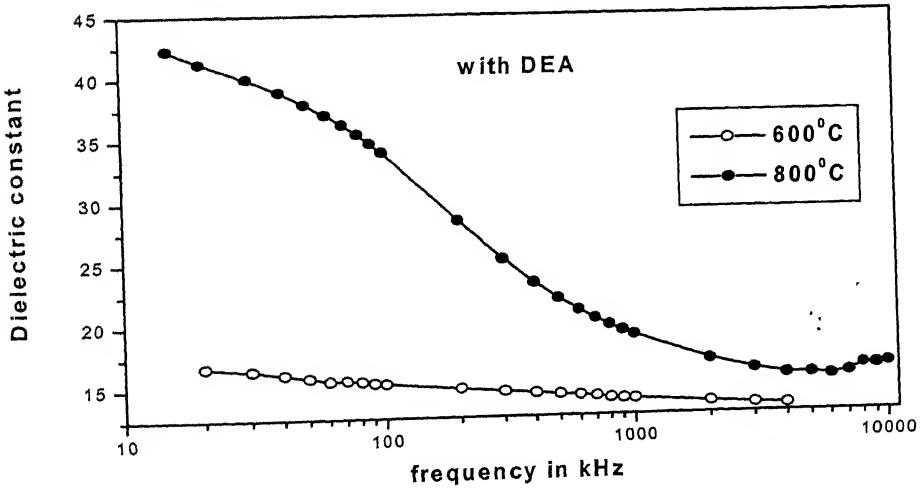

Fig. 3.28: Dielectric constant Vs frequency plot at two different temperatures (600^{0}C and 800^{0}C) for (a) with acetylacetone (b) without additive and (c) with DEA

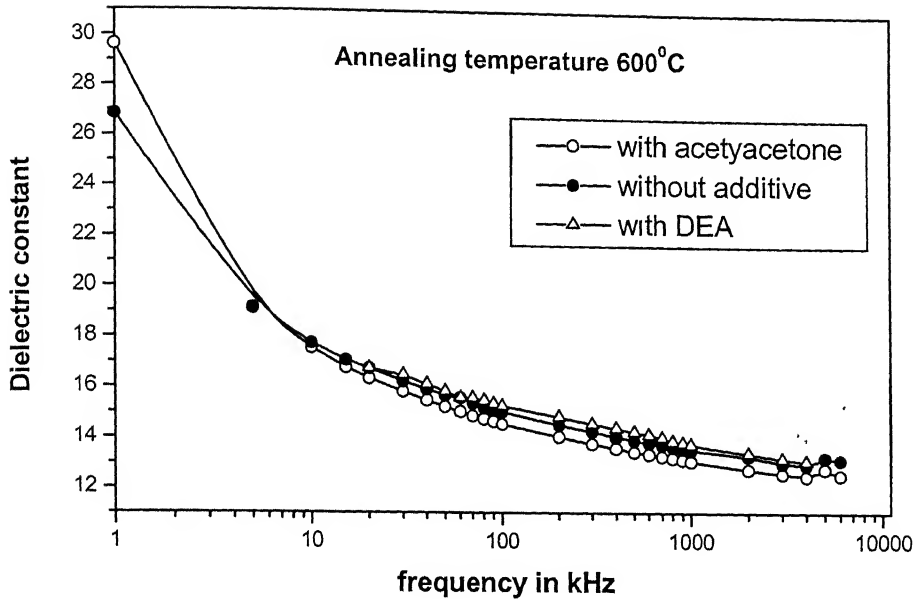

(a)

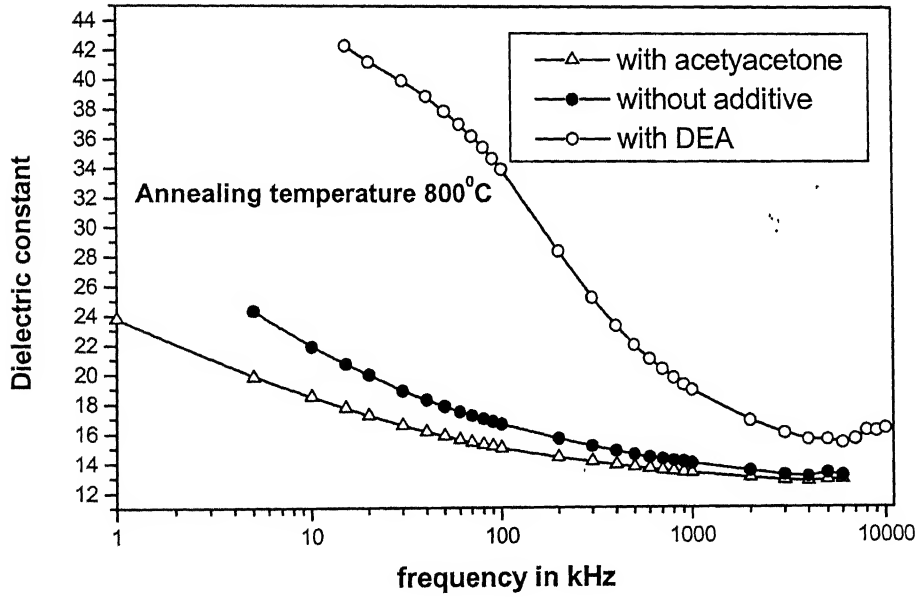

(b)

Fig. 3.29: Plot of average dielectric constant Vs frequency for three different sols (without additive, with acetylacetone and with DEA) at (a) 600°C and (b) 800°C

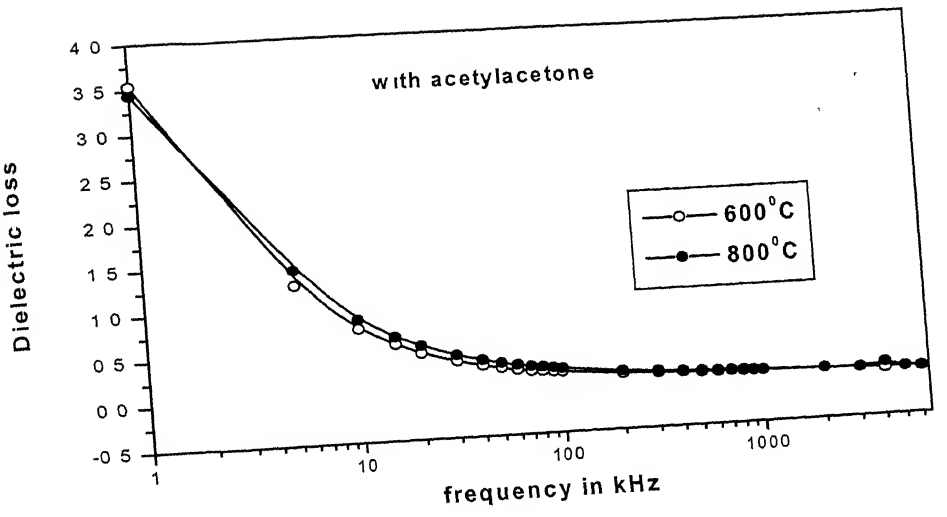

(a)

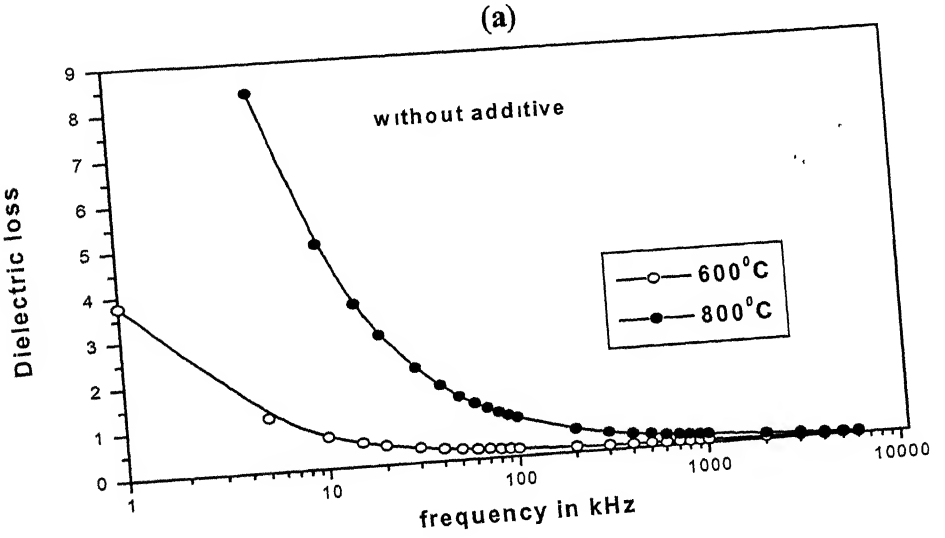

(b)

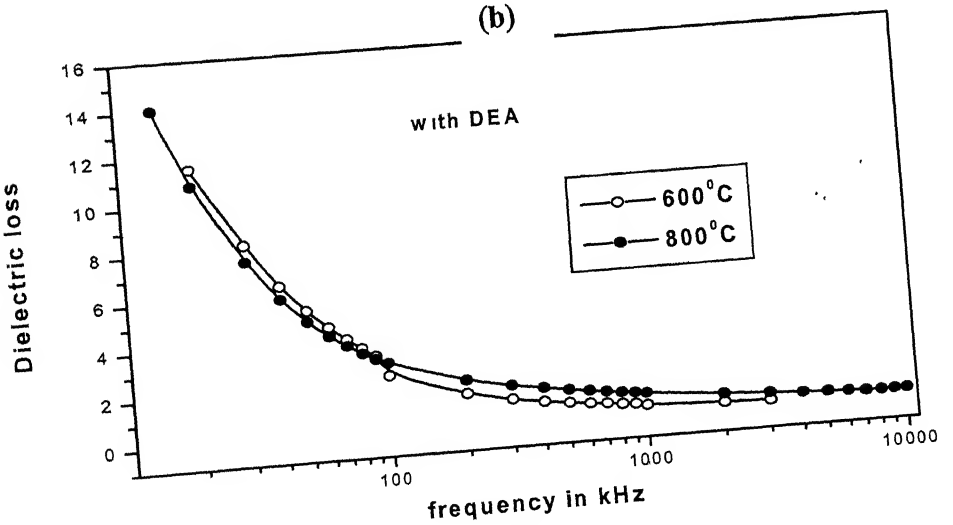

(c)

Fig. 3.30: Dielectric loss Vs frequency plot at two different temperatures (600^{0}C and 800^{0}C) for (a) with acetylacetone (b) without additive and (c) with DEA

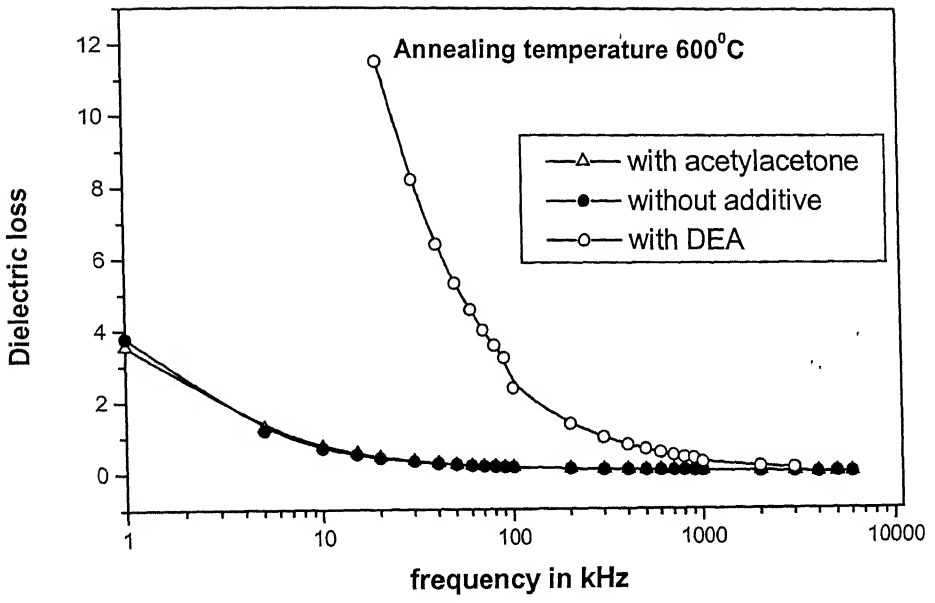

(a)

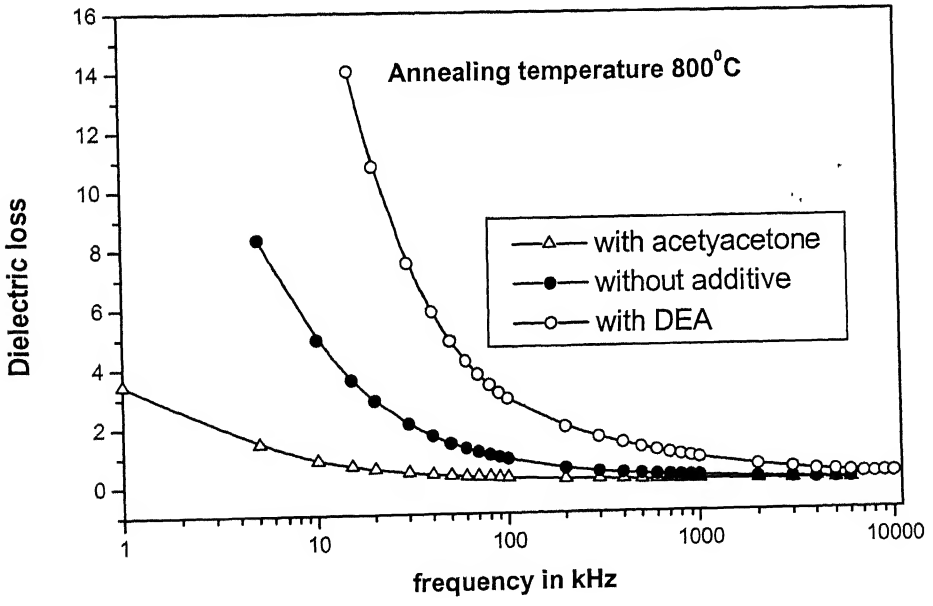

(b)

Fig. 3.31: Plot of average dielectric loss Vs frequency for three different sols (without additive, with acetylacetone and with DEA) at (a) 600^{0}C and (b) 800^{0}C

Chapter 4

Conclusions and recommendations

The two outcomes of the present work are as follows:

1. BST has a perovskite structure while the as deposited BST film is amorphous. The transformation to the perovskite phase occurs on heating the amorphous film to higher temperatures. During heating, the transformation amorphous to perovskite is known to proceed via some intermediate crystalline crystalline phases. The intermediate phases are carbonates or oxycarbonates. In the present work, while x-ray diffraction, is not able to unambiguously show the presence of such phases, the FT-IR data clearly shows that the intermediate phase with CO_3^- group forms when either no additive or DEA or ethylene glycol as additives are used in the sol. When acetylacetone is used as additive, no intermediate phase is found to form. However, the intermediate phase forms even with a sol containing acetyl acetone if the sol is aged for a few days before the film deposition.

   The reason for the formation of the intermediate (Ba, Sr) CO^-_3 phase is the exclusion of Ba^{-2} and Sr^{-2} ions from the Ti-O-Ti gel network and their subsequent segregation. This happens when the hydrolysis and the condensation reactions of the alkoxide are rapid. Use of acetylacetone slows down these reactions and allows Ba, Sr to be homogeneously incorporated in the gel network.

2. The films prepared by using the different additives have significant differences in their electrical properties i.e. dielectric constant and dielectric loss. However, in all cases the dielectric constants are much lower and the dielectric loss much

higher than those reported by others. The reason for this is not yet clear. One possibility in the peculiar microstructures of the films that show significant micro porosity

The other observation from the present work are summarized below

- As seen by TGA, the weight loss occurs in three distinct regions. It is seen that the organics may not be removed completely even upto 900^0C. For samples with acetylacetone combustion of organics between 225-400^0C occurs gradually.
- FT-IR data showed no carbonate peaks (1440-1450 cm^{-1}) for samples treated with acetylacetone. In all the other cases the CO_3^{-2} was detected indicating the formation of an intermediate carbonate phase.
- FT-IR spectra in case of acetylacetone showed a unique trend in shift of the peak ~1430 cm^{-1} towards the lower value when heated to higher temperatures indicating no intermediate carbonate phase formation.
- XRD results on the gel powders showed tetragonal structure. The broadening of the peak~ 45 ^{0} was the indication of tetragonality. A slow scan of the peak at 0.3^0/min was done. But the peak positions corresponding to (200) and (002) reflections could not be resolved due to enhanced noise level.
- XRD plots for the gel powder made without acetylacetone heated to different temperature showed a broad hump in the region of 20-30^0 but no distinct peaks of $BaCO_3$ (~24.68^0) or oxycarbonate phase (~27^0) were observed as detected by FT-IR except for the samples with DEA.
- Use of acetylacetone reduced the crystallization temperature of BST.

- Thin film samples also showed tetragonal structure. The data are matching with the reported values in the literature [29].
- Films were crack free in optical microscopic study even after annealing to high temperatures.
- SEM pictures showed a very different microstructure from the reported grainy microstructure in the literature. That may be due to presence of micropores in the film.
- Dielectric measurements show a very low (~25) value of dielectric constant and a high value of loss at low frequencies. These values are related to the porosity of the film and presence of residual organics in the film.
- The experiments performed to crystallize BST thin films with the use of microwave radiations were not successful. It is recommended to modify the existing set-up (radiations are to be guided or a suitable susceptors is to be used). The present set-up has an auto cut off circuit that also has to be removed to get continuous radiations for longer duration.
- Hydrothermal treatments on the films also did not lead to crystallization. A detailed and systematic study is recommended varying different conditions of the experiment.

References

1. S.Ezhilvalavan and T.Y.Tseng, "Progress in the developments of (Ba,Sr)TiO_3 (BST) thin films for Gigabit era DRAMs" *Materials Chemistry Physics* **65** (2000) 227
2. C.L.Chen, *Appl. Phys. Lett.* **75** (1999) 412
3. L.C.Sengupta and S.Sengupta, *IEEE Trans. Ultrason. Ferroelect. Freq. Contr.* **44** (1997) 792
4. S.B.Majumdar, M.Jain, A.Martinez, and R.S.Katiyar et al." Sol-gel derived grain oriented barium strontium titanate thin films for phase shifter applications" *J. Appl.Phys.* **90**, (2001) 896
5. Z.Huang, Z,Zhang, C.Jiang et al " Infrared optical properties of $Ba_{0.8}Sr_{0.2}TiO_3$ ferroelectric thin films" *Appl. Phys. Lett.* **77** (2000) 3651
6. Seema Agarwal, G.L.Sharma, R. Manchanda " Electrical conduction in (Ba,Sr)TiO_3 thin film MIS capacitor under humid conditions" *Solid State Communications* **119** (2001) 681
7. E.W.Avenear, *Appl. Phys. Lett.* **65** (1994) 1784
8. Bernard Jaffe and William R. Cook, Piezoelectric Ceramics, (Academic Press London and New York, 1971)pp 101
9. Tahan, Safari and Klein "Preparation and Characterization of $Ba_xSr_{1-x}TiO_3$ thin films by a sol gel technique" *J.Am. Ceram. Soc.* **79** (1996) 1593
10. Yongping Ding, Chengyu jin, Zhongyan Meng " The effects and mechanism of chemical additives on the pyrolysis evolution and microstructure of sol-gel derived Ba1-xSrxTiO3 thin films" *Thin Solid Films* **375** (2000) 196
11. Soo-Ik Jang, Hyun M. Jang "Leakage current characteristics of sol-gel derived $Ba_{1-x}Sr_xTiO_3$(BST) thin films" *Ceramic International* **26** (2000) 421
12. Lahiry, Gupta, Sreenivas, Mansingh "Dielectric properties of sol-gel derived $Ba_{0.4}Sr_{0.6}TiO_3$ thin films" *IEEE trans ultrasonics,ferroelectrics and frequency control* **47** (2000) 854

13. Tian, Luo, Pu and Ding "Synthesis and microstructure of the acetate based Sr-doped barium titanate thin films using a modified sol-gel technique" *Mater. Sc. Lett.* **19** (2000) 1211

14. S.Hoffmann and R.Waser "Control of the Morphology of CSD-prepared (Ba,Sr)TiO_3 Thin Films" *Journal of the European Ceramic Society* **19**(1999)1339

15. R.H. Horng*, D.S. Wuu, C.Y. Kung, J.C.Lin, C.C. Leu, T.Y. Haung, S.M.Sze "Ion-implanted treatment of (Ba,Sr)TiO_3 films for DRAM applications" *Journal of Non-Crystalline Solids* **280** (2001) 48

16. V.Craciun and R.K.Singh "Characteristics of the surface layer of barium strontium titanate thin films deposited by laser ablation"*Appl. Phys Lett.* **76** (2000)1932

17. S.-.Y Chen, H.-.W Wang and L.-C. Huang "Role of an intermediate phase $(Ba,Sr)_2Ti_2O_5CO_3$ in doped $(Ba_{0.7}Sr_{0.3})TiO_3$ thin films" *Materials Chemistry and Physics* **77**(2002) 632

18. Cheng, Meng, Tang, Guo, "Effects of individual layer thickness on the structure and electrical properties of sol-gel derived $Ba_{0.8}Sr_{0.2}TiO_3$ thin films" *J.Am. Ceram. Soc* **83** (2000) 2616

19. Liedtke, Hoffman, Waser "Recrytaiization of Oxygen Ion Implanted $Ba_{0.7}Sr_{0.3}TiO_3$ thin films" JACS 83 (2000) 436

20. F.Tcheliebou and S.Baik "Influence of the laser wavelength on the microstructure of laser ablated $Ba_{0.5}Sr_{0.5}TiO_3$ films" J. Appl. Phys. 80(1996) 7046

21. S.Yamamichi, H.Yabuta,T.Sakuma and Y. Miyasaka "(Ba+Sr)/Ti ratio dependence of the dielectric properties for $Ba_{0.5}Sr_{0.5}TiO_3$ thin films prepared by ion beam sputtering" Appl. Phys. Lett. 64(1994) 1644

22. D.Y.Noh, H.H.Lee, T.S.Kang, and J.H.Je "Crystallization of amorphous (Ba,Sr)TiO_3/ MgO(001) thin films" Appl. Phys. Lett. 72(1998) 2823

23. W.S.Cho et al J. Phys. Chem. Solids 59(1998) 659

24. T.Horikawa, N.Mikami, T.Makita et al "Dielectric Properties of (Ba,Sr)TiO_3Thin Films Deposited by RF Sputtering" Jpn. J. Appl. Phys.32(1993) 4126

25. San-Yuan Chen, Hong-Wen Wang and Li-Chi Huang " Electrical properties of Mg/La, Mg/Nb Co-Doped (Ba0.7Sr0.3)TiO3 thin films prepared by metallo-organic deposition method" Jpn J Appl. Phys Vol.40(2001)PP.4974-4978

26. N. Ichinose and T. Ogiwara "Preparation and Rapid Thermal Annealing Effect of (Ba,Sr)TiO_3 Thin Films" Jpn. J. Appl. Phys. 34(1995) 5198

27. S.-.I. Jang and H.M. Jang "Structure and electrical properties of boron-added (Ba,Sr)TiO_3 thin films fabricated by the sol-gel method" Thin Solid Films 330(1998) 89

28. J. R. MacDonald (ed.), "Impedance Spectroscopy", John Wiley & Sons, Vol. 1, 2 (1987)

29. F. M. Pontes, E. R. Leite, D. S. L. Pontes, and E. Longo "Ferroelectric and optical properties of $Ba_{0.8}Sr_{0.2}TiO_3$ thin films" J. Appl. Phys. 91(2002) 5972

30. Max diem "Infrared Spectroscopy" p-263

31. W. H. Sutton "Microwave Processing of Ceramic Materials" Ceram. Bull.68 (1989) 376

32. W. J. Dawson "Hydrothermal Synthesis of Advanced Ceramic Powders" Am. Ceram. Soc. Bull. 67(1988) 1673

33. S.-.I. Jang, B. C. Choi and H.M. Jang J. of Mater. Res. 12 (1997) 1327

34. Moulson and Herbert "Electroceramics" Chapman and Hill (1990) 81